

# Efficient Methodologies for Package/housing Effect on Active MMIC and Signal Integrity Problems

by

**Ashish Kalubhai Sarvaiya**

(200921005)

A Thesis Submitted in Partial Fulfilment of the Requirements for the Degree

of

**Doctor of Philosophy**

in

Information and Communication Technology

to

Dhirubhai Ambani Institute of Information and Communication Technology



August 2016

## Declaration

This is to certify that

1. the thesis comprises my original work towards the degree of Doctor of Philosophy in Information and Communication Technology at DA-IICT and has not been submitted elsewhere for a degree,
2. due acknowledgment has been made in the text to all other material used.

Signature of Student

## Certificate

This is to certify that the thesis work entitled “Efficient Methodologies for Package/housing Effect on Active MMIC and Signal Integrity Problems” has been carried out by Ashish Kalubhai Sarvaiya (200921005) for the degree of Doctor of Philosophy in Information and Communication Technology at this Institute under my supervision.

Thesis Supervisor

Prof. Sanjeev Gupta

## Acknowledgment

I express thank to the Almighty for providing me inspiration, strength, energy and patience to start and accomplish my goal with the support of all concerned, A few of them, I am trying to acknowledge.

I sincerely thank my guide Prof. Sanjeev Gupta, who has been the main source of inspiration, for guiding and motivating me. His sincerity, dedication, creativity and a very confident nature inspired me to work tirelessly for the entire duration of this work. Only because of him, my strengths and efforts were converging in one direction towards achievement of the goal.

I would like to thank Sci. Apurba Bhattacharya ( Head of Receiver Section, Space Application Center (SAC) - Indian Space Research Organization (ISRO), Ahmedabad) for providing all necessary details during this work.

I express my thank to all my friends who help me directly or indirectly in this research work in all possible ways. Finally, I express my thank to Mummy (Shreemati Vimlaben), Papa (Shree Kalubhai), wife Sangita, Bhai-Bhabhi, Dhruvil and dear son Aditya whose always kind support helps me to complete this work.

# Abstract

There has been a great demand in a Computer Aided Design (CAD) tool with a capability of design and analysis of gigahertz system having active Monolithic Microwave Integrated Circuit (MMIC)/Printed Circuit Boards (PCBs). For gigahertz system, previously neglected electromagnetic effects needs to be account into CAD tool for accurately predicating the performance of the system under test. The thesis proposes efficient methodologies for two major issues encounter in design and testing of gigahertz system having active MMICs/PCBs: package/housing effect and signal integrity problems.

The first part of the thesis discusses packaging/housing effect on active MMIC. When MMIC is mounted inside a test box or package/housing with a cavity, it may differ from its RF on-wafer (RFOW) and circuit simulation performance. The metallic side walls of the package/housing may support several resonant modes which induce surface currents on the walls of the package/housing. These unwanted currents may damage the devices under test. This undesirable effect is called package/housing effect. Hence it is need to be derive a systematic methodology for analysis and investigation of the package/housing effects on active MMIC.

Presently there is no CAD tool available that predict directly packaging/housing effect on active MMIC with a cavity in a single run. The thesis presents an EM field analysis of active MMIC and packaging/housing effect on active MMIC. An experimental test case is used here to investigate and analyze the package/housing effect. Low Noise Amplifier (LNA) MMIC is used as an experimental test case. In this dissertation, the theoretically cavity resonance problem is studied, the cavity resonance problem is investigated for the experimental test case using eigen mode solver and transient solver, and active non planar MMIC is modeled, simulated and analyzed the E/H field distribution due to the discontinuity presence in active MMIC. The pre mitigation technique - the selection of optimum test box dimensions is carried out and modified test box dimensions are proposed whose test box test results are matched with circuit simulation and RFOW results. When packages/housing test boxes are already fabricated and new design can not possible, the post design technique - the selection of RF absorber can be carried out. Here different RF absorbers are studied and appropriate RF absorber is proposed to mitigate the package/housing effect.

The second part of the dissertation deals transmission line effects at gigahertz frequency in MMICs/PCBs. When signal pass through transmission line at gigahertz frequency with a picoseconds rise/fall time, the wire/interconnect/transmission line at both MMIC/Chip and package/housing level are no longer ‘electrical transparent’ to the signals and signal integrity is affected by electromagnetics effects (or called transmission line effects) such as reflection, delay, jitter, attenuation and noise. It is called a signal integrity problem. To take into account these electromagnetics effects in a time domain analysis and to integrate these effects into circuit solver, the macromodel is to be derived. The black box representation that captures electromagnetics behavior at the input/ output ports is called a macromodel. Hence, the development of an efficient macromodel and a simple procedure of embedding this macromodel into circuit solvers become necessary for transient simulation of signal integrity in the distributed passive devices in MMIC/PCB.

The thesis proposes an efficient and simple approach to embed broadband frequency domain responses of passive and linear networks into circuit solver using the Vector Fitting Method (VFM) for signal integrity analysis. Tabulated frequency domain data in the form of the admittance matrix are obtained through Finite Integration Technique (FIT). Vector fitting method is used here to construct a macromodel from tabulated frequency domain data. Resulting pole residue macromodel is directly embedded into HSPICE or compatible circuit solvers. Single ended via connected with two microstrip line example show the validity of the proposed methodology. This example validates that proposed methodology is applicable for transient simulation of signal integrity problems, encounter in the design and testing of gigahertz system having MMIC/PCB.

# Contents

Certificate	ii
Abstract	iv
Contents	vii
List of Figures	viii
List of Tables	1
<b>1 Introduction</b>	<b>1</b>
1.1 Package/housing effect	1
1.2 Signal integrity problems	3
1.3 Motivation and objectives	4
1.4 Contributions of the thesis	5
1.5 Organization of the thesis	6
<b>2 Background</b>	<b>8</b>
2.1 Background of package/housing effect	8
2.1.1 Cavity resonance prediction from a model/circuit	9
2.1.2 Cavity resonance prediction using Method of Moment(MoM)	10
2.1.3 Cavity resonance prediction using FDTD	11
2.1.4 Crosstalk and EMI prediction	13
2.1.5 The package performance investigation	14
2.2 Background of signal integrity problem	15
2.2.1 High speed interconnect effects	18
2.2.2 High speed interconnect models and simulation issues	24
2.3 High speed interconnect simulation algorithms	26
2.3.1 Simulation technique based on transmission line macromodels	26
2.3.2 Model reduction based simulation algorithms	28
2.3.3 Full-Wave Models	29
2.4 Finite integration technique	30
2.4.1 Introduction	30
2.4.2 Types of solvers	31
2.5 Basics of 3D simulation	35
2.5.1 Modeling	35
2.5.2 Running a simulation	35
2.5.3 Accuracy issues and its solutions	37
2.6 Basics of on wafer RF characterization	45

---

2.7	MMIC fabrication technology . . . . .	46
<b>3</b>	<b>Package/housing effect with active MMIC</b>	<b>50</b>
3.1	An experimental test case . . . . .	50
3.2	A theoretical study . . . . .	53
3.3	Investigation on a test case . . . . .	55
3.3.1	Investigation using eigen mode solver . . . . .	55
3.3.2	Investigation using transient mode solver . . . . .	58
3.4	Modeling, simulation and analysis of active MMIC . . . . .	63
3.5	Mitigation techniques . . . . .	69
3.5.1	Selection of absorber . . . . .	69
3.5.2	Optimization of test box dimensions . . . . .	70
<b>4</b>	<b>An efficient methodology for transient simulation of signal integrity problems</b>	<b>73</b>
4.1	Introduction . . . . .	74
4.2	Admittance parameters extraction . . . . .	75
4.3	Vector fitting technique . . . . .	76
4.4	Inclusion of macromodel into circuit solver . . . . .	78
4.4.1	Foster pole residue representation . . . . .	78
4.5	Numerical results . . . . .	80
4.6	Conclusion and discussion . . . . .	80
<b>5</b>	<b>Conclusions and scope of further work</b>	<b>83</b>
5.1	Conclusions . . . . .	83
5.2	Scope of further work . . . . .	85

# List of Figures

2.1	Transmission line system and it's equivalent circuit . . . . .	16
2.2	Example of propagation delay: Network with lossless transmission line . .	19
2.3	Example of propagation delay: Transient response . . . . .	19
2.4	Example of attenuation and rise-time degradation: Network with lossy transmission line . . . . .	20
2.5	Example of attenuation and rise-time degradation: Transient response .	20
2.6	Example of undershoots, overshoots, and ringing in lossless interconnects.	21
2.7	Example of ringing in lossy interconnects . . . . .	22
2.8	Example of crosstalk. . . . .	23
2.9	Example of dominant poles . . . . .	28
2.10	(a) Discrete port: two wires with a source in the middle. (b) Face port: the source is distributed along the red line. . . . .	38
2.11	Port size rules of thumb for: (a) microstrip, (b) ungrounded, and (c) grounded coplanar line. . . . .	38
2.12	Absolute value of the electric field (represented in logarithmic scale) at a microstrip port. (a) Port size is too small; electric field has considerable magnitude at port's border and will negatively impact on the solution's accuracy. (b) Port size has been increased laterally and above the microstrip and fields are practically zero (green colour) at port's border. . . . .	39
2.13	Hexahedral and tetrahedral mesh for a piece of coaxial cable. (a) The staircase mesh provides a poor description of curved surfaces, unless a very fine mesh is used. (b) Conformal boundary approximation ensures the required geometric accuracy, with a minimum of mesh cells. (c) Tetrahedral mesh generators often require a segmentation of round structures, leading to a poor geometrical approximation. . . . .	40
2.14	Rules of thumb for meshing planar structures with hexahedral meshes (greymetal, dusky pink-substrate). (a) Discretization of a microstrip. (b) Discretization of gaps inside a metal sheet. . . . .	42
2.15	Time signal examples. (a) The output signal still oscillates with relatively high amplitude at the moment when the simulation was stopped. The frequency-domain results (e.g., S-parameters) are most likely inaccurate. (b) A time signal which is sufficiently decayed when the simulation is stopped will provide accurate frequency-domain results . . . . .	43
2.16	Final mesh after the adaptation process for a piece of coaxial cable. (a) Mesh adaptation without snapping on the true geometry. (b) Snapping onto the geometry during the adaptation process leads to a good approximation of the geometry and hence to more accurate results . . . . .	44



3.1	Layout of LNA MMIC chip . . . . .	51
3.2	Actual test box with LNA MMIC chip: Gold plated carrier plate is used to mount the complete assembly, Pre and post bias cards are placed in between MMIC Chip, six DC bias capacitors are mounted on bias cards, Gold ribbon wires are used to connect MMIC chip and bias cards . . . . .	51
3.3	Comparison of RF on wafer and test box test results. . . . .	52
3.4	A rectangular cavity resonator . . . . .	54
3.5	Case A: E/H fields for unassembled cavity structure . . . . .	57
3.6	Case B : Carrier plate layout and test box with carrier plate . . . . .	59
3.7	Case C : Model of test box with LNA MMIC. . . . .	60
3.8	S-parameters magnitude (dB) obtained using Agilent's ADS . . . . .	61
3.9	S-parameters magnitude (dB) obtained using CST MWS . . . . .	61
3.10	Box having CPML Boundary condition and Comparison of RFOV and measured results . . . . .	61
3.11	Comparison of results: validation of package/house effect by imposing different boundary conditions . . . . .	62
3.12	MMIC chip layouts are partitioned into 3 parts for debugging the problem, Parts are made in such a way that first two parts have one active device and last one has two active devices . . . . .	64
3.13	Single stage analysis includes only one active device: Comparison of 3D co-simulated transient field result and ADS circuit simulation result. . . . .	66
3.14	Two stage analysis includes two active devices: S-parameters and E-field distribution on partitioned chip . . . . .	67
3.15	Full chip analysis: Comparison with on wafer and measured results . . . . .	68
3.16	Selection of RF absorber: Comparison of results of package/housing effect (red line), without box (only chip, purple line) and box with absorber material (blue line). . . . .	71
3.17	Simulation results with proposed box height(a) CST result (b) ADS result; results validate that the proposed box dimensions can be used to mitigate the cavity resonance problem. . . . .	72
4.1	A complete proposed approach . . . . .	74
4.2	(a) Model of single ended via connecting with two microstrip lines (b) Schematic circuit diagram of the test model; Two-port network having source and load . . . . .	79
4.3	Y parameters of the single ended via simulated by FIT in CST MWS and Vector Fitting method. (a) Magnitude. (b) Phase . . . . .	81
4.4	Transient voltage waveforms: (a) at port 1 denoted as $V_{in}$ and at port 2 denoted as $V_{out}$ . . . . .	82

# List of Tables

3.1	Theoretical resonance modes for an experimental text box. . . . .	56
3.2	Eigen mode simulation results for different cases of cavity structures. . .	58
3.3	Result comparisons of few individual components of MMIC at 14 GHz . .	63

# Chapter 1

## Introduction

There has been a great demand in a Computer Aided Design (CAD) tool with a capability of design and analysis of gigahertz system having active Monolithic Microwave Integrated Circuit (MMIC)/Printed circuit boards (PCBs). For gigahertz system, previously neglected electromagnetic effects needs to be account into CAD tool for accurately predicating the performance of the system under test. The thesis proposes efficient methodologies for two major issues encounter in design and testing of gigahertz system having active MMICs/PCBs: package/housing effect and signal integrity problems.

### 1.1 Package/housing effect

When MMIC is put inside a test box with a cavity, it may differ from its on-wafer and circuit simulator performance. It is recommended that MMICs be tested in their package as well as subjected to the on-wafer RF characterization. Package/housing design requires prior adequate knowledge of RF field distribution inside the package housing. Package/housing performance degrades at high frequency mainly because of the ring resonance and cavity resonance. Ring resonances occur when stray electromagnetic fields couple to the ceramic frame of the package[1, 2]. Cavity resonances occur when the volume enclosed with the package behaves as a rectangular metal cavity [3]. Ring resonance can be eliminated as reported in [1, 2, 3]. In cavity resonance, the conductive surface of the enclosure supports several resonant modes which induce surface currents on the walls of the packages. These surface currents may result in catastrophic failure of the device. Hence comprehensive analysis and to derive a systematic methodology of the

package/housing effects are one of the prime requirements for stable MMIC design. As the Interaction between electromagnetic waves and active devices affects the system performance significantly, much attention has been focused on full wave analysis of package/housing effect with the presence of active MMIC. A properly designed package/housing should have only a small effect on the circuit. Resonant modes in the operating frequency band must be damped by lowering the associated Q of the package/housing and by suitably designing the circuit layout. A common technique for reducing the cavity resonance effect is to place a microwave absorber on the cover. A conventional microwave absorbers composed of materials with bulk resistive properties may be placed in the package, as have been done by Hallford and Bach [4]. Williams has suggested a dielectric substrate coated with a resistive film as an inexpensive alternative to the microwave absorber [5]. Armstrong and cooper experimentally investigate the use of microwave absorbing materials to suppress the coupling to resonant modes [6]. Jansen and Weiner have developed circuit's models for microstrip discontinuities in an enclosure, but their employment when a lossy material was present had not been verified [7]. John and Robert use the Moment of Method (MoM) formulation which model microstrip circuits in a lossy enclosure using rooftop currents [8]. They have investigated the coupling of power to a resonant mode as a function of circuit location in an enclosure. Robert uses the side wall images to compute the package effects in the MoM analysis of MMIC circuits [9]. Robert describes formulations to calculate a circuit's terminal characteristics, with and without a lateral enclosure[9].

To investigate and analyze the package/housing effect with the presence of active MMIC, full wave electromagnetic simulation must be carried out. These techniques are generally based on the Method of Moment (MoM), Finite Element Method (FEM), Finite Difference Time domain (FDTD) or Boundary Element Method (BEM). The behavior of packaged single and coupled MMIC via-hole grounds have been investigated using a graded mesh FDTD code[10]. Another full wave analysis of packaged microwave circuits with active and non linear devices using the FDTD technique is presented in [11]. With package and without the package analysis of circuit is carried out in [11]. Another approach is demonstrated by developing the CAD tool for designing the optimum package of MMIC[12]. It is shown that package effects could be isolated in the MPIE green's function [12]. The method for eliminating cavity resonance and equivalent circuits for

EMI prediction are discussed in [13, 14, 15]. In [16], modeling, analysis of the package and different mitigation techniques are used to make stable, resonance free microwave amplifier for a C-band space borne SAR payload. The electromagnetic simulation and characterization of the metal, ceramic package for packaging of high isolation switches is performed in [17].

## 1.2 Signal integrity problems

As the effective frequency bandwidth of operation of MMIC and high speed PCB extends to the microwave region, as rising and falling time of signal decrease to a few tens of picoseconds, the wire interconnects at both the MMIC/chip and the package/housing level are no longer ‘electrically transparent’ to signals. When signals pass through transmission lines, their signal integrity is affected by electromagnetic effects such as attenuation, reflection, noise, radiation, and delay. It is called signal integrity problems. To take into account these electromagnetics effects in a time domain analysis and to integrate these effects into circuit solver, the macromodel is to be derived. The black box representation that captures electromagnetics behavior at the input/output ports is called a macromodel. Hence, the development of an efficient macromodel and a simple procedure of embedding this macromodel into circuit solvers become necessary for transient simulation of signal integrity in the distributed passive devices in MMIC/PCB.

There has been a great demand for embedding the transmission line effects into CAD tools. CAD tools are either based on non-linear circuit simulators, which solve the Modified Nodal Analysis (MNA) matrix equations [18], or electromagnetic full wave simulators, which solve Maxwell’s equations [19]. Two major methodologies for embedding the transmission line effects into CAD tools have been discussed in [20], [21]. One methodology is to embed lumped and/or non-linear circuits into electromagnetic simulators based on the Finite-Difference Time-Domain (FDTD) method [22], Transmission Line Matrix(TLM) method [23], or Partial Element Equivalent Circuit (PEEC) method [24]. The other methodology is to embed the electromagnetic behavior of system under test at the ports into circuit simulators. This is called a macromodel. The macromodeling can be performed using two approaches. One approach is based on moments that are the characteristics of the circuit. In [25],[26],[27],[28],[29],[30],[31],[32],[33],[34], moment-matching using

Pade approximation have been discussed. The other approach construct the macromodel using least squares approximation [35],[36],[37],[38],[39], [40],[41], and vector fitting [42]. Here, we concentrate on the frequency-domain vector fitting (VF) process and suggest the way in which they can be applied to improve their ease of use.

## 1.3 Motivation and objectives

### Motivation

The list of challenges for solving package/housing effect with the presence of active MMIC operated at Ku band:

- There is no commercial tool available that directly predicting the active MMIC performance with the cavity in a single run.
- It is difficult to import layouts from one software platform to another software platform and to validate it.
- The best of our knowledge, this is the first attempt to investigate and analyze an EM field on active MMIC and package/housing effect on active MMIC.
- The best of our knowledge this is the first attempt to handle active MMIC chip with cavity with huge aspect ratio in size, hence biggest challenge is to optimize and reduce the number of cells and hence simulation time.
- An experimental test case contains active devices with a non- planar layout; hence to incorporate and model the layout into 3D full wave simulator is challenging task
- Simulation time for an experimental test case is high so it is difficult to debug frequently.

The list of challenges for the development of an accurate and efficient macromodeling technique and inclusion of macromodel into circuit solver:

- The mixed frequency/time domain problem [21]
- Computationally expensive [21]
- Strong knowledge of linear algebra

- Equivalent circuit representation or convolution technique can be used to club the macromodel into circuit solver, but these techniques are not efficient and simple[43],[44],[45].

### Objectives

Above listed challenges motivate to define objectives/problem definition into two major sections: For the first part of the dissertation, objectives are

- To study theoretical package/housing effect.
- To investigate the cavity resonance problem for the experimental test case using eigen mode solver and transient solver.
- To model active MMIC with package/housing assembly.
- To investigate and analyze an EM field on active MMIC using transient solver.
- To use pre-mitigation technique like optimization of box dimensions
- To study different types of RF absorber and propose a best suited RF absorber to match test box test data with RF on wafer and simulation results.

For the second part of the dissertation, the objective is “to propose an efficient and simple approach to embed broadband frequency domain responses of passive and linear multiport networks into circuit solver using the vector fitting method for signal integrity problems”.

## 1.4 Contributions of the thesis

The first part of the dissertation describes

- Theoretical study of package/housing effect having active MMIC.
- Investigation of the cavity resonance problem for experimental test case LNA with package/housing using eigen mode solver and transient solver.
- Modeling of active MMIC with package/housing assembly.
- Modeling and analysis of active non planar MMIC. The best of our knowledge this is the first attempt to analyze an E/H field distribution due to the discontinuity presence in active MMIC chip layout.

- Two mitigation techniques : (i) Optimization of test box dimensions (ii) Selection of absorber

The second part of the dissertation describes

- An efficient and simple approach to embed broadband frequency domain responses of passive and linear networks into circuit solver using the vector fitting method.
- A systematic macromodeling methodology and a simple procedure of embedding the macromodel into circuit solver.
- Single ended via connected with two microstrip line example, which shows the validity of the proposed methodology. This example validated that proposed methodology is efficient and simple for transient simulation of electromagnetic interference (EMI) and signal integrity in the design and testing of gigahertz system having MMIC/PCB.

## 1.5 Organization of the thesis

The thesis is organized as follows:

In chapter 2, previous work carried out in the area of package/housing problem and signal integrity problems are discussed. The Finite Integration Technique (FIT) is the core numerical method used to solve Maxwell's equation for analysis the computational domain. Basic introduction of FIT is described in the section 2.4. FIT is used in this thesis for analysis and investigation of the given problem definition. The basics of 3D simulation and things to be taken care while simulating any 3D full wave simulation is presented in section 2.5. The RF on wafer (RFOW) characterization is discussed in the section 2.6. At the end of the chapter, MMIC fabrication technology particularly, OMMIC ED02AH is discussed in 2.7.

In chapter 3, I address the problem of packaging/housing with active MMIC. In section 3.2, the theoretical cavity resonator is presented. I suggest different approaches for investigating the cavity resonance problems in packaging/housing having active MMIC. In order to validate the packaging/housing effect quickly, Eigen mode solver is discussed in the section 3.3.1. The transient mode solver is used for analysis of E/H field present



---

on active MMIC and validating the packaging/housing effect in the section 3.3 , 3.4, I further discuss the mitigation techniques in the section 3.5.

In chapter 4, I introduce an efficient and simple approach to embed broadband frequency domain responses of passive and linear networks into circuit solver using the vector fitting method. Tabulated frequency domain data in the form of the admittance matrix are obtained through finite integration technique in the section 4.2. The section 4.3 discuss the vector fitting method which used here to construct a macromodel from tabulated frequency domain data. Resulting pole residue macromodel is directly embedded into HSPICE/CST or compatible circuit solvers in the section 4.4.1. A numerical example discuss in the section 4.5, show the validity of the proposed methodology.

Finally, I summarize the work and conclude in chapter 5. I also discuss the future scope of research work.

# Chapter 2

## Background

In this chapter, previous work carried out in the area of package/housing problem and signal integrity problems are discussed. The Finite Integration Technique (FIT) is the core numerical method used to solve Maxwell's equation for analysis the computational domain. Basic introduction of FIT is described in the section 2.4. FIT is used in this thesis for analysis and investigation of the given problem definition. The basics of 3D simulation and things to be taken care while simulating any 3D full wave simulation is presented in section 2.5. The RF on wafer (RFOW) characterization is discussed in the section 2.6. At the end of the chapter, MMIC fabrication technology particularly, OMMIC ED02AH is discussed in 2.7.

### 2.1 Background of package/housing effect

Microwave sub system is generally consist of MMICs and active/passive devices having varieties of package/housing style. The housing is not only providing necessary physical support but also a way for heat transfer and protection against temperature ,humidity,vibration/shock,EMI/EMC etc. Further the cavity electric size increases at high frequency. The conductive surface of the enclosure supports several resonant modes and therefore produces the oscillating charges, which in turn induce surface currents on the conductive walls of the package. These surface currents may degrade performance of the active devices present in the system. These resonances are observed as large spikes in the insertion loss versus frequency characteristics of the packaged MMIC. There are different approaches used to mitigate the package/housing effects. Some major previous works

carried out are discussed below.

### 2.1.1 Cavity resonance prediction from a model/circuit

1. The cavity resonances are predicted from a model [3] that considers the package as rectangular metal cavity loaded with a H-plane dielectric slab. In this model, the length, width, and height of the cavity are represented as  $L, W$ , and  $H$  respectively. The dielectric slab is of thickness  $d$  and relative permittivity  $\epsilon_r$ . The cavity is excited by a microstrip line at the input and output ports. The resonance frequency  $f_r$  is approximately given by

$$f_r = f_c \sqrt{1 - \left(\frac{d}{H}\right) \left(\frac{\epsilon_r - 1}{\epsilon_r}\right)} \quad (2.1)$$

where  $f_c$  is the cut-off frequency of the  $TE_{101}$  mode in the empty cavity. As an example, if  $\epsilon_r=13, d=0.01016$  cm,  $L=0.4064$  cm,  $W=0.254$  cm, and  $H=0.04826$  cm, then  $f_c$  and  $f_r$  are 69.641 GHz and 62.508 GHz, respectively.

2. The effects of discontinuities and spurious propagation in enclosed microstrip have been studied using 10:1 scaled models by probing the vertical components of the electric field in the substrate and by measuring insertion loss [6]. A number of discontinuities were studied and results showed the higher-order modes excited in the enclosed microstrip to be perturbed versions of the LSM and LSE modes of inhomogeneous waveguide. A coefficient of coupling from discontinuity to each mode is defined and estimated by measuring the external Q of the enclosure. The coupling varies with the discontinuity and its position. Since these modes all have electric fields with components tangential to the air/substrate interface, they were suppressed by layers of resistive materials.
3. Millimeter wave discontinuity circuits have been developed on the basis of systematic full wave data generated by a rigorous numerical approach [7]. The applied physics related and topology sensitive modeling concept is used and extends previous quasi static descriptions into dynamic ones including parasitic wave coupling and package resonances. The dynamic model developed for open end, gap, step, bend, and T-junction are valid below and above cutoff of the dominant package

mode. They make it possible to predict package resonance and their effect on component behavior.

4. A full-wave parametric analysis of a straight-to-bent microstrip structure has been performed and an equivalent circuit of the structure has been proposed [15]. The circuit is composed of lumped elements modeling the reactive phenomena and the spurious emission caused by the excitation of the higher order modes at the microstrip discontinuity. The numerical results show that the coupling phenomena are strongly dependent on the frequency and on the geometrical parameters of the structure. Finally, low electromagnetic emission has been observed since the structure has been enclosed in a metallic box having small apertures.

### 2.1.2 Cavity resonance prediction using Method of Moment (MoM)

1. In [5], it has been shown that the resonant modes of a rectangular metal package may be damped by fixing a dielectric substrate coated with a thin resistive film to one of its walls, thus solving the reliability and machining problems associated with many conventional microwave absorbers. This is similar to the approach used in which resistive films supported by low dielectric substrates are placed at roughly quarter-wavelength intervals from a ground plane to suppress electromagnetic reflections. The technique discussed here differs, however, in that the substrates in this case may have a high dielectric constant, may be much thinner, and are designed to suppress resonant modes rather than propagating waves.
2. A moment method formulation is presented which models microstrip circuits in a lossy enclosure using rooftop currents [8]. A Green's function is developed that includes the effect of lossy material on the cover. The coupling of power to a resonant mode as a function of circuit location in an enclosure is investigated. The absorbing layer will be compared to the resistive film with respect to their effectiveness in reducing resonance effects. It is shown that the coupling of power to a resonant mode can be reduced further by repositioning certain circuit features within the enclosure.
3. A new method of applying the spectral domain moment method to enclosed mi-

crostrip circuits is presented in [9]. The mutual coupling between current elements on a circuit are first calculated as though the circuit were not laterally enclosed. A correction is then added representing the effect of the image currents which are introduced by the lateral enclosure. The first calculation involves a relatively lengthy spectral integration which results in impedances that are slowly varying with respect to frequency and thus can be interpolated using only a few evaluations in a band. The second calculation, the correction term, must be evaluated at many frequencies in a band depending on the number of enclosure resonances and their  $Q$ . The total method of moments matrix is formed by summing the two calculations. The method has the advantage of being able to add or remove the correction term in order to see the sidewall effects. It is also very intuitive. Its simplicity is based on the dominant effect that the TM, parallel plate mode has on enclosure coupling. It remains efficient for enclosures with high or low  $Q$  having any lateral size, but it is limited to structures with a top cover.

4. In most of the full-wave analysis of packaged (M)MICs, the packaging effects cannot easily be isolated from the original circuit response. Therefore, any changes in the packaging dimensions will require a complete repetition of the analysis procedure. A CAD tool is developed for designing optimum packaging of (M)MICs [12]. It is shown that the packaging effects can be isolated in the MPIE Green's function. In this case, the package effects appear as an additive term in the MoM impedance matrix. An optimum packaging design is therefore possible by iteratively computing this additive term for different box sizes.

### 2.1.3 Cavity resonance prediction using FDTD

Properly designed package should have only a small effect on the circuit. Resonant modes in the operating frequency band must be damped by lowering the associated  $Q$  of the package and by suitably designing the circuit layout. Conventional microwave absorbers or resistive films may be placed in the package to prevent package-circuit interaction. These damping elements must be put in properly selected locations in such ways to choke off the resonances without affecting the circuit behavior. To identify such locations, because of the complexity of the structures involved, only numerical methods can be used.

In addition to make the enclosure 'anechoic,' it is also necessary to carefully interconnect the package with the external feeding lines. This is obtained by a section of coaxial line with the outer conductor connected to the metal package and the inner conductor directly to the circuit. This feed-through structure should also be modeled by numerical methods. On the other hand, to properly design a package with reduced size, weight and cost, full-wave electromagnetic simulation design tools must be used. So far, the design of packages with state-of-the-art performance has usually been realized by expensive "cut and try" procedures. In this approach, the package and the circuit are studied separately and the simulations combined together. This procedure ignores the coupling between the package and the circuit. A significant effort to overcome this limitation has been done in recent years and several full-wave techniques have been developed to analyze MMIC circuits in an enclosure. These techniques are generally based on the Method of Moments (MOM) and its variants, including the Finite Element Method (FEM) and the Boundary Element Method (BEM). Although analytically oriented numerical methods, such as Mode Matching (MM) or Spectral Domain (SD) have a high efficiency, their applicability is nevertheless confined to a limited number of simple geometries. The FDTD has played an important role in the numerical simulation of the electrical behavior of simple packaged circuits. This technique, in fact, not only can take into consideration arbitrary 3-D geometries, but also provides time-domain data useful for the analysis of circuits containing nonlinear elements. Moreover, unlike spectral domain based methods, FDTD can also be used to properly model the interconnections of the package with the external feeding lines. In fact, at the moment, FDTD still requires excessive computer time and resources. Nonetheless, the current trend towards computers with increased number crunching performance makes this method quite appealing. In the near future, one way to achieve increased numerical performance will be the use of Massive Parallel Computers (MPC).

1. In [10], a FORTRAN 77 FDTD code has been developed running first on IBM workstation RISC 6000-365 then translated into the Digital FORTRAN 90 and exported to the Masspar machine DEC 12000 with 4 K processors. This code is used for several package simulations. Another way to improve the performance of the FDTD simulator is the use of a graded mesh, or, when necessary, a non-orthogonal mesh. A graded mesh feature has also been implemented in simulator. The behaviors of

the packaged single and coupled MMIC via-hole grounds are investigated using the FDTD technique. Theoretical simulations are compared with experimental measurements showing excellent agreement. Various possibilities to choke off package resonances have also been investigated. It is shown in particular that the common practice of inserting a damping layer just below the lid is often ineffective and the importance of placing damping layers also on the side wall is demonstrated.

2. In [11], comprehensive full-wave analysis of packaged nonlinear active microwave circuits by applying the extended Finite-difference time-domain (FDTD) method has been done. Based on the approach of using equivalent sources, the device-wave interaction is characterized and incorporated into the FDTD time-marching scheme. As a consequence, analysis of linear and nonlinear properties, including harmonic generation and intermodulation, can be accomplished by employing a large signal device circuit model. The implementation is first validated by comparing results of FDTD and HP MDS simulation of the circuit without the packaging structure. The analysis then goes beyond the capability of the circuit simulator to include the packaging effect. This analysis is useful in circuit design involving electromagnetic compatibility/electromagnetic interference (EMC/EMI) problems.

#### 2.1.4 Crosstalk and EMI prediction

The Multi Transmission Line (MTL) is a system consisting of  $N$  conductors and a conducting shield or common return conductor and serving to guide electromagnetic waves, which works under surroundings with much electromagnetic interference (EMI), such as the crosstalk from the natural coupling within the MTL, undesirable and sometimes very harmful. It can cause penetration of a signal excited in one simple transmission line (STL) into the near- and far-end load of another STL. Crosstalk may set limits to the dynamic range of circuits, to the frequency band of their application and to the scale of miniaturization. Therefore, the circuit design engineer has to deal with the crosstalk in order that there are the relatively pure signals flowing through the MTLs.

1. This paper [13] presents a new concept eliminating crosstalk that is composed of three methods, that is, terminating optimal impedances, mounting grounded guarding lines, and transforming the structure of microstrip lines to the layout of stripline.

Firstly, we extract the PUL parameters of microstrip transmission lines based the MoM. secondly, With the SPICE simulation software, we can simulate and optimize the structure of MTLs in order to obtain the ideal results of eliminating the crosstalk within MTLs. Finally, we obtain the excellent multi-path signals with simulation software, which show that the synthetic design of eliminating crosstalk is a practical operational and effective. For example, the concept of design can be applied to the power dividing networks for eliminating the signal crosstalk within MTLs.

2. The crosstalk between a single-ended line and a differential pair, and the crosstalk between differential pairs have been analyzed based on the telegrapher's equations for multi-conductor lines [14]. The obtained results can give guidelines for design the differential interconnects for minimizing the crosstalk. Several possible differential-line structures will be considered, including the co-planar lines, stacked-pair lines, diagonal-pair lines, to find a design of the interconnects that minimizes the crosstalk. Different structures may exhibit different crosstalk characteristics, and the crosstalk may be decreased by properly setting the differential pair. Furthermore, the effect of routing guard traces and ground tracks are also be examined.

### 2.1.5 The package performance investigation

1. In [17], performance degradation problems have investigated in a commercial rectangular metal ceramic package for packaging an SPDT MMIC working in 5-6 GHz frequency range. Electromagnetic simulations and experiments were carried out to study the effect of gaps between the feed thru edge and package edge. In addition, the effects of placement of ports on the cavity resonance and isolation between ports were also studied in an attempt to minimize insertion loss, maximize isolation between ports and to achieve an optimum VSWR (Voltage Standing Wave Ratio) on all ports. Effects of ground loops due to long inductive connections (bond wires) and gaps between different parts of the MMIC assembly on isolation, insertion loss and VSWR have been investigated. A new package structure was designed and fabricated to achieve the aforementioned objectives. It has been shown that by minimizing the ground loops by avoiding gaps between the elements in the as-



sembly, performance deterioration due to packaging can be minimized. Very high isolation of the order of 35-40 dB has been achieved in the SPDT switch MMIC packaged in the new package without any degradation of insertion loss.

2. This paper [16] describes modeling, analysis of the package and different mitigation techniques used to make stable, resonance free microwave amplifier for a C-band space borne SAR payload.
3. In this paper [46], electromagnetic (EM) leakage and spurious resonances in a K/Ka-Band (18-40 GHz frequency band ) MMIC hermetic package designed for a phase shifter chip are studied using the finite element method (FEM) and the numerical simulation results are compared with the measured data. In addition, the effect of adding a resistive coating to the inside surface of the package lid and also the use of dielectric packaging materials with very high loss tangent are studied in view of the suppression of the spurious resonances. Finally, design guidelines for the improved package are presented. Both the measured and calculated data indicate several spurious resonances in the 18-24 GHz frequency band/region and the origin of this phenomenon is identified by virtue of the modeling capability of the FEM. Moreover, the effect of dc bias lines, bond wires, shielding, and the asymmetry of the package on electrical performance are closely examined.

## 2.2 Background of signal integrity problem

As the performance requirements for modern computer and communications systems grow, the demand for high speed interconnects increases as well. Multi-gigabit speeds are supported by standard communication technologies, with the signal's rise times being as fast as 35 pico second. At these speeds, cables, connectors, vias and traces on printed circuit boards (PCBs) behave as distributed elements, or transmission lines. Moreover, reflections due to impedance mismatch, signal's rise time degradation due to the interconnect losses, and crosstalk due to coupling are typical signal integrity problems that system-level designers encounter in their work. Therefore, to accurately predict the propagation of the signals in their designs, engineers need to determine the electrical characteristics and to build reliable models of the interconnect structures.

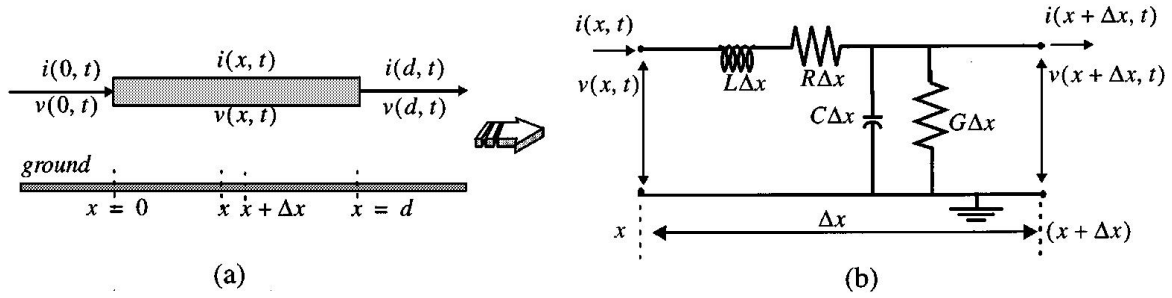


Figure 2.1: Transmission line system and its equivalent circuit

Interconnects can exist at various levels of design hierarchy such as on-chip, packaging structures, multichip modules, printed circuit boards, and backplanes. It is predicted that interconnects will be responsible for majority of signal degradation in high-speed systems. High-speed interconnect problems are not always handled appropriately by conventional circuit simulators, such as SPICE. If not considered during the design stage, these interconnect effects can cause logic glitches that render a fabricated digital circuit inoperable or they can distort an analog signal such that it fails to meet specifications. Since extra iterations in the design cycle are costly, accurate prediction of these effects is a necessity in high-speed designs. Hence, it becomes extremely important for designers to simulate the entire design along with interconnect sub circuits as efficiently as possible while retaining the accuracy of simulation. In order to understand important characteristics of interconnect structures, it is imperative to start from the general representation of the ideal transmission line model. The ideal transmission line does not exhibit losses associated with conductors and dielectrics of the mediums that carry such signals. Thus, an ideal transmission line can be described as a distributed parameter network consisting of capacitors and inductors to represent interactions due to electric and magnetic fields. A short sub-segment of the ideal transmission line can be modeled using a circuit shown in Figure 2.1. Circuit representation of the transmission line allows deriving partial differential equations which are generally called telegraphers equations. A solution of these equations in terms of propagating voltages and currents, allows deriving important characteristics of the ideal transmission line, such as characteristic impedance  $Z_0$  and time delay  $t_d$ .

For the single ideal conductor, the characteristic impedance is described by the following formula:  $Z_0 = \sqrt{\frac{L}{C}}$  where  $L$  and  $C$  are inductance and capacitance of the line per unit length respectively. It is important to note that increase in the inductance per unit

length leads to the increase of characteristic impedance, and the increase of the capacitance causes the decrease of the characteristic impedance. L and C values and their ratio can be controlled by the geometry and material properties of the interconnect. Time delay of the ideal transmission line can be expressed in terms of inductance and capacitance per unit length as:  $t_d = \sqrt{LC}$

Practical interconnects are fabricated using materials that exhibit losses. Different interconnects are coaxial cable, bond wire, microstrip line, stripline, power plane. The interconnect structures consist in general combinations of different types of interconnects, and each transition among them contribute to the reflections. Geometrical configurations and material properties of these structures affect the distribution of electric and magnetic (EM) fields. The EM field interactions in their turn completely govern electrical performance of the device which can be described mathematically by a set of so called Maxwell equations. Therefore, the choice of materials and geometry for interconnects is critical for minimizing signal integrity problems.

Speaking on a broader perspective, a "high-speed interconnect" is the one in which the time taken by the propagating signal to travel between its end points cannot be neglected. An obvious factor that influences this definition is the physical extent of the interconnect; the longer the interconnect, the more time the signal takes to travel between its end points. Smoothness of signal propagation suffers once the line becomes long enough for the signal's rise/fall times to roughly match its propagation time through the line. Then the interconnect electrically isolates the driver from the receivers, which no longer function directly as loads to the driver. Instead, within the time of the signal's transition between its high and low voltage levels, the impedance of interconnect becomes the load for the driver and also the input impedance to the receivers. This leads to various transmission line effects, such as reflections, overshoot, undershoot crosstalk, and modeling of these needs the blending of EM and circuit theory.

Alternatively, the term "high-speed" can be defined in terms of the frequency content of the signal. At low frequencies an ordinary wire, in other words, an interconnect; will effectively short two connected circuits. However, this is not the case at higher frequencies. The same wire, which is so effective at lower frequencies for connection purposes, has too much inductive/capacitive effects to function as a short at higher frequencies. Faster clock speeds and sharper slew rates tend to add more and more high-frequency contents.

An important criterion used for classifying interconnects is the electrical length of an interconnect. An interconnect is considered to be "electrically short" if, at the highest operating frequency of interest, the interconnect length is physically shorter than approximately one-tenth of the wavelength (i.e., length of the interconnect/ $\lambda$ ,  $\approx 0.1$ ,  $\lambda = v/f$ ). Otherwise, the interconnect is referred to as "electrically long". In most digital applications, the desired highest operating frequency (which corresponds to the minimum wavelength) of interest is governed by the rise/fall time of the propagating signal. For example, the energy spectrum of a trapezoidal pulse is spread over an infinite frequency range; however, most of the signal energy is concentrated near the low-frequency region and decreases rapidly with the increase in frequency. Hence, ignoring the high-frequency components of the spectrum above a maximum frequency,  $f_{max}$ , will not seriously alter the overall signal shape. Consequently, for all practical purposes, the width of the spectrum can be assumed to be finite. A practically used relationship between the desired  $f_{max}$  and the  $t_r$  (rise/fall time of the signal) can be expressed as :  $f_{max} \approx 0.35/t_r$ .

In summary, the primary factors that influence the decision "whether high-speed signal distortion effects should be considered" are interconnect length, cross-sectional dimensions, signal slew rate, and the clock-speed. Other factors that also should be considered are logic levels, dielectric material, and conductor resistance. Electrically short interconnects can be represented by lumped models whereas electrically long interconnects need distributed or full-wave models.

### 2.2.1 High speed interconnect effects

High-speed effects influencing a signal propagating on an interconnect could be multi-fold, such as delay, rise time degradation, attenuation, crosstalk, skin effect, overshoots, undershoots, ringing, and reflection. In this section, we give a detailed account of each of these high-speed effects (which are also known as transmission line effects).

1. Propagation Delay : A signal traversing from one end of a transmission line to the other end takes a finite amount of time; in other words, it experiences a certain amount of delay. Figure 2.2, 2.3 illustrates the case of an ideal delay line. In addition, the signal may encounter rise time degradation as shown in Fig. 2.4, where the rise time at the receiver end is larger than the rise time at the source end. Rise-

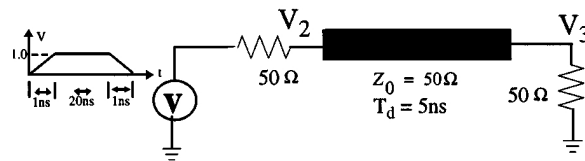


Figure 2.2: Example of propagation delay: Network with lossless transmission line

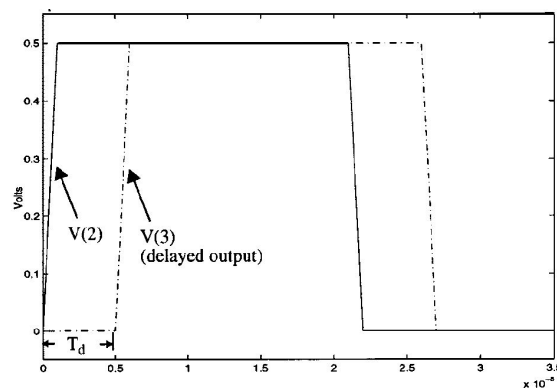


Figure 2.3: Example of propagation delay: Transient response

time degradation further adds to the overall delay experienced by the signal, as it influences the maximum and minimum attainable logic levels between the switching intervals.

2. **Attenuation** :The signal through an interconnect may suffer attenuation, due to ohmic or conductance losses. This is illustrated in Fig. 2.4,2.5. Ohmic losses are more pronounced at higher frequencies due to the uneven current distributions. Conductance losses are proportional to the dielectric loss factor of the dielectric material and are also a function of the frequency. If the losses are high, the signals may not retain the specified logic levels during the transit through an interconnect and may result in false switching of digital circuitry.
3. **Signal Reflection and Ringing** :

Signal reflection and the associated ringing can severely distort signal propagation at higher frequencies. The prime cause of reflection-related signal degradation is the discontinuity in characteristic impedance of the transmitting line. Such a discontinuity can be either distributed or lumped in nature. In the case of distributed discontinuity, the impedance variation on a line takes place over a certain length.

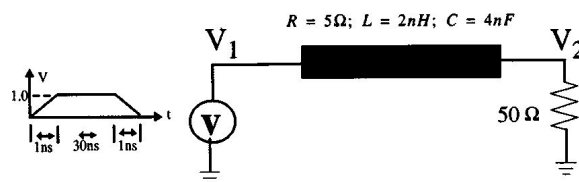


Figure 2.4: Example of attenuation and rise-time degradation: Network with lossy transmission line

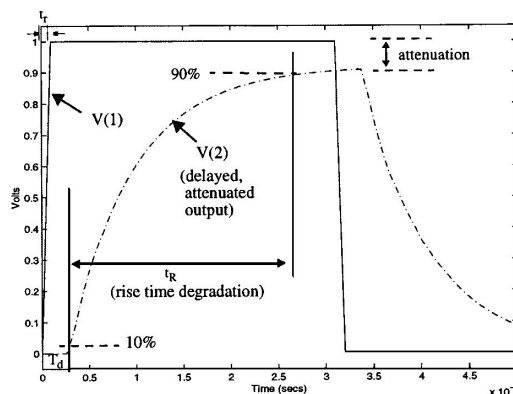


Figure 2.5: Example of attenuation and rise-time degradation: Transient response

For example, this can occur due to the change in the medium along the length of the signal trace, which may have to traverse several layers on a printed circuit board (impedance may not be well controlled from layer to layer). Following are some common causes of discontinuities: connectors between card-to-board, cable-to-card, leads between chip and chip carriers, or between card wiring and chip carriers, long vias, orthogonal wiring, flip-chip soldier balls, wire bonds, and redistribution lines, etc. Another major contributor to the reflection related signal degradation is the impedance mismatch between the line characteristic impedance and source/terminating impedances. Fig. 2.6 illustrates these effects for the case of a lossless line. Fig. 2.6(b) and 2.6(c) shows the undershoots for relatively small and large delay lines. In general, undershoots occur when the terminating impedance is less than the characteristic impedance of the interconnect. Fig. 2.6(d) and (e) shows the phenomenon of overshoots, which occur when the terminating impedance is larger than the characteristic impedance of the line. As seen, the undershoots, overshoots, and the ringing experienced by the signal increases with the delay of the interconnect. Fig. 2.7 illustrates the ringing associated with a lossy line, for

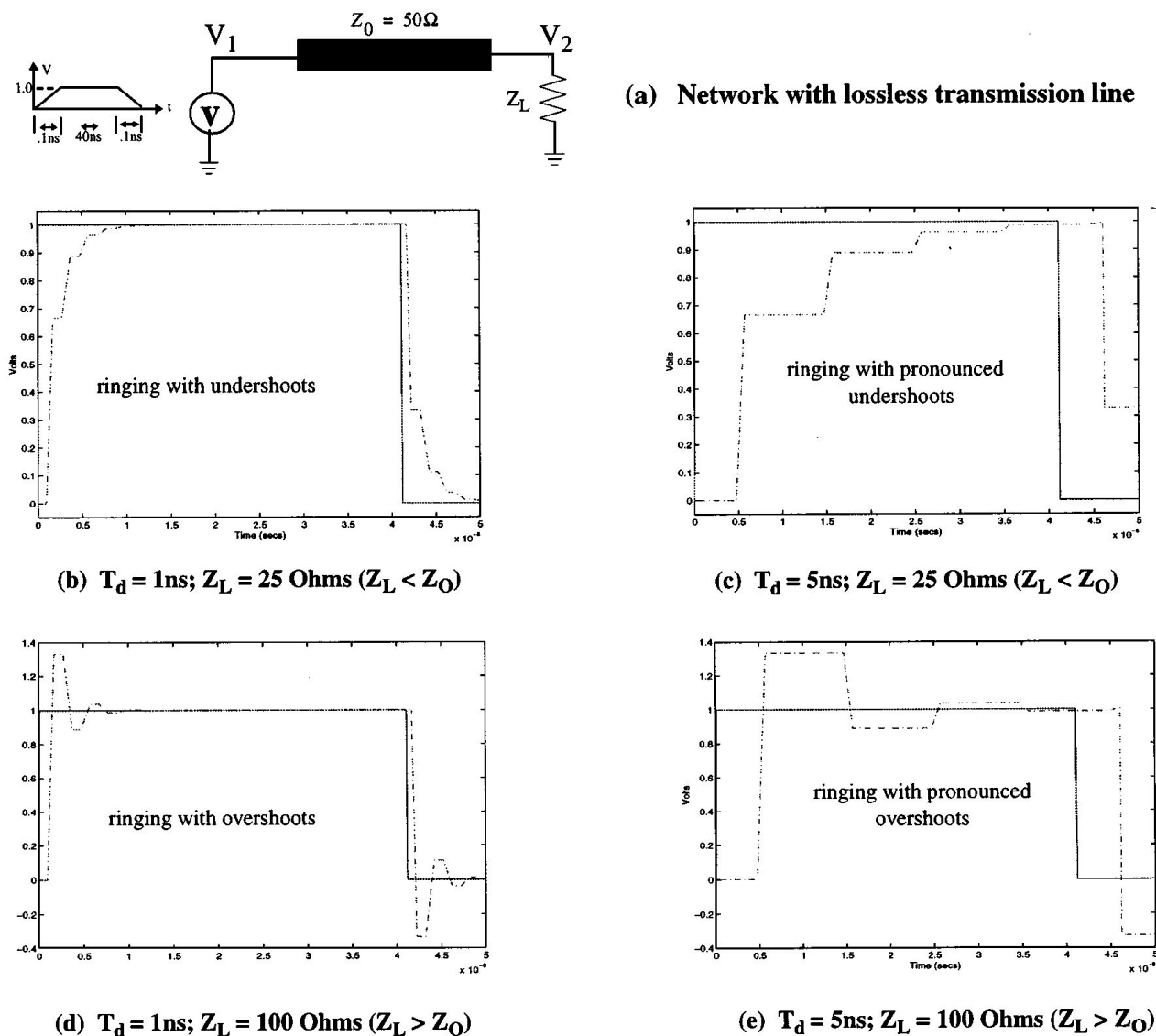
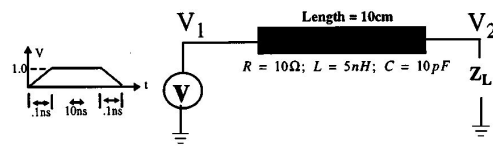


Figure 2.6: Example of undershoots, overshoots, and ringing in lossless interconnects.

various cases of terminations.

4. Crosstalk : Crosstalk refers to the interaction between signals that are propagating on various lines in the system. An analogy of crosstalk could be the "the interference from other lines while talking on the phone." Crosstalk is mainly due to the dense wiring required by compact and high-performance systems. High-density and closely laid interconnects result in electromagnetic coupling between signal lines. The active signal energy is coupled to the quiet line through both mutual capacitance and inductances, resulting in noise voltage-currents. This may lead to inadvertent switching and system malfunctioning. Crosstalk is a major constraint



(a) Network with lossy transmission line

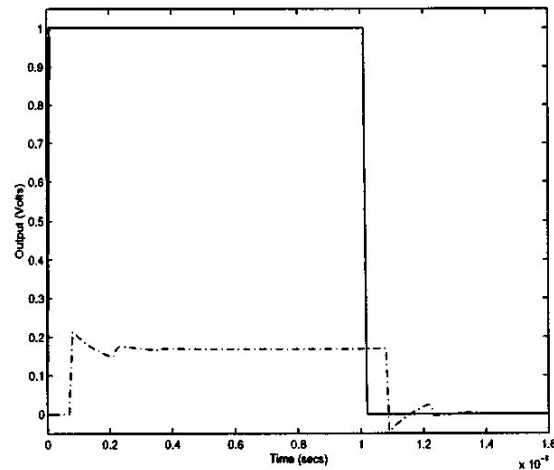
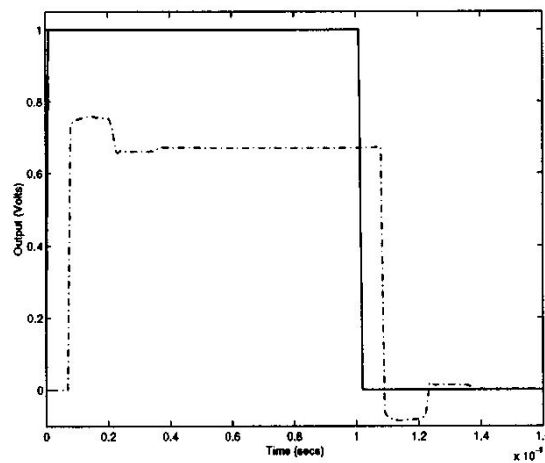
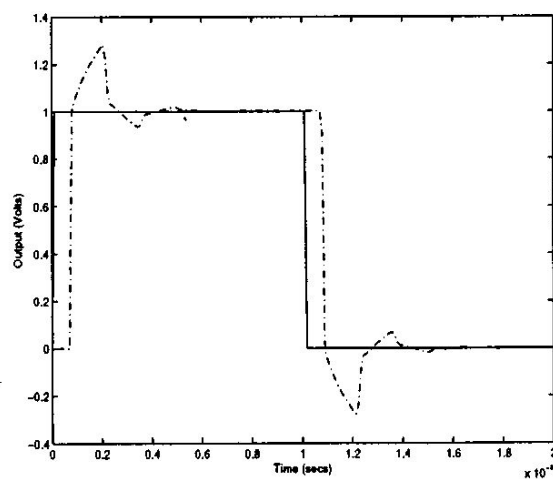
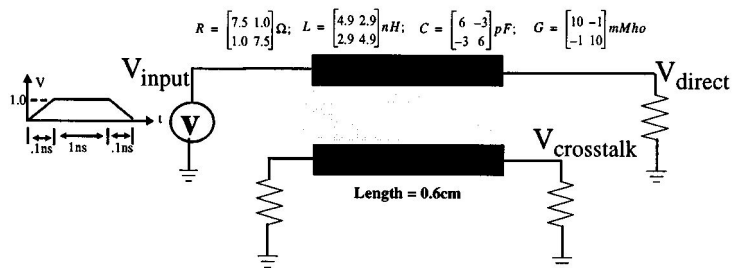
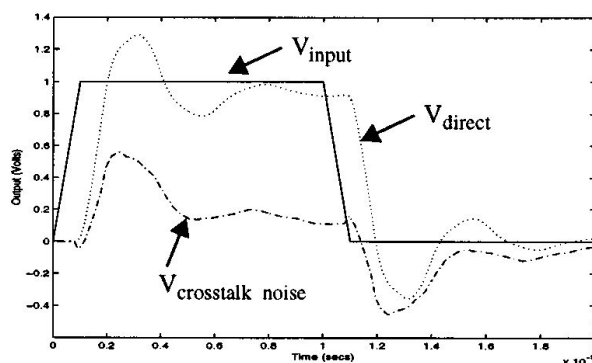
(b)  $Z_L = 20$  Ohms(c)  $Z_L = 200$  Ohms(d)  $Z_L = \text{open circuit}$ 

Figure 2.7: Example of ringing in lossy interconnects





(a) Network with multiconductor transmission line



(b) Time response

Figure 2.8: Example of crosstalk.

while routing in high-speed designs. An example of crosstalk is given in Fig. 2.8. By its very nature, crosstalk analysis involves systems of two or more conductors. Such systems are studied on the basis of dominant propagating modes. System behavior in response to any general excitation is then a linear combination of modal responses.

### 2.2.2 High speed interconnect models and simulation issues

Depending on the operating frequency, signal rise times, and nature of the structure, the interconnects can be modeled as lumped, distributed (frequency independent/dependent RLCG parameters, lossy, coupled), or full-wave models.

1. Lumped Models: At lower frequencies, the interconnect circuits could be modeled using lumped or circuit models. circuit responses are monotonic in nature. However, in order to account for ringing in signal waveforms, circuit models may be required. Usually lumped interconnect circuits extracted from layouts contain a large number of nodes that make the simulation highly CPU intensive.

2. Distributed Transmission Line Models: At relatively higher signal-speeds, electrical length of interconnects becomes a significant fraction of the operating wavelength, giving rise to signal distorting effects that do not exist at lower frequencies. Consequently, the conventional lumped impedance interconnect models become inadequate and transmission line models based on quasi-transverse electromagnetic mode (TEM) assumptions are needed. The TEM approximation represents the ideal case, where both E and H fields are perpendicular to the direction of propagation and it is valid under the condition that the line cross section is much smaller than the wavelength. However, the inhomogeneties in practical wiring configurations give rise to E or H fields in the direction of propagation. If the line cross section or the extent of these non uniformities remain a small fraction of the wavelength in the frequency range of interest, the solution to Maxwell's equations are given by the so-called quasi-TEM modes and are characterized by distributed R,L,C,G per unit length (p.u.l.) parameters. In practical situations, owing to complex interconnect geometries and varying cross-sectional areas, the interconnects may need to be modeled as nonuniform lines. In this case, the p.u.l. parameters are functions of the distance, along the length of the transmission line.
3. Distributed Models with Frequency-Dependent Parameters: At low frequencies, the current in a conductor is distributed uniformly throughout its cross section. However, as the operating frequency increases, the current distribution gets uneven and starts getting concentrated more and more near the surface or edges of the conductor. This phenomenon can be categorized as follows: skin, edge, and proximity effects. The skin effect causes the current to concentrate in a thin layer near the conductor surface and this reduces the effective cross section available for signal propagation. This leads to an increase in the resistance to signal propagation and other related effects. The edge effect causes the current to concentrate near the sharp edges of the conductor. The proximity effect causes the current to concentrate in the sections of ground plane that are close to the signal conductor. To account for these effects, modeling based on frequency-dependent p.u.l. parameters may be necessary.
4. PEEC and rPEEC Models: As switching speeds extend into the gigahertz range,

two-dimensional (2-D) transmission line models become inadequate due to the spatial EM effects of three-dimensional structures. The modeling of these structures has been successfully accomplished using partial element equivalent circuit (PEEC) models. PEEC models are RLC circuits where individual resistances and capacitances are extracted from the geometry using a quasi-static (nonretarded) solution of Maxwell's equations. The rPEEC models include the retardation and provide full-wave solution. Simulation of these models is relatively CPU intensive as they involve large resultant networks.

Interconnect Simulation Issues : Simulation of large interconnect networks is associated with two major bottlenecks: mixed frequency/time problem and CPU expense.

- **Mixed Frequency/Time Problem:** The major difficulty in simulating high frequency models such as distributed transmission lines is due to the fact that, while described in terms of partial differential equations, they are best represented in the frequency-domain. As seen, they do not have a direct representation in the time-domain. On the other hand, nonlinear devices can only be described in the time-domain. These simultaneous formulations are difficult to handle using a traditional ordinary differential equation solver such as SPICE.
- **CPU Expense:** Frequency-domain simulation of large linear networks is conventionally done at each frequency point using LU decomposition and forward-backward substitution. For time-domain simulation, integration techniques are used to convert a set of time-domain differential equations into a set of difference equations which leads to a nonlinear set of difference equation. To solve these at each time point, Newton iterations are required, which may need several LU decompositions. This causes the CPU cost of a time-domain analysis to be expensive (note that matrices for interconnect networks are usually very large).

## 2.3 High speed interconnect simulation algorithms

The objectives of interconnect simulation algorithms are to address both mixed frequency/time problem as well as to handle large linear circuits without too much of CPU

expense. There have been several algorithms proposed for this purpose, which are broadly classified into two main categories, as follows.:

1. Approaches based on macromodeling each individual transmission line set. Techniques such as "method of characteristics" are grouped in this category and are discussed in Section 2.3.1.
2. Approaches based on model-order reduction (such as AWE, CFH, PRIMA) of the entire linear subnetwork containing lumped as well as distributed subnetworks. It is to be noted that the second approach can also be used in conjunction with the first approach.

### 2.3.1 Simulation technique based on transmission line macromodels

In this approach, transmission-line networks described by telegrapher's equations (partial differential equations) are translated into a set of ordinary differential equations (known as the macromodel), through some kind of discretization.

The conventional approach for discrete modeling of distributed interconnects is to divide the line into segments of length  $\Delta x$ , chosen to be small fraction of the wavelength. If each of these segments (assume that the line discretized into "M" segments) is electrically small at the frequencies of interest, then each segment can be replaced by lumped models. Generally the lumped structures used to discretize transmission lines contain the series elements and  $L \Delta x$ , and  $R \Delta x$  and shunt elements,  $G \Delta x$  and  $C \Delta x$ . The parameters (L,R,G,C are the p.u.l.inductance, resistance, conductance, and capacitance of the line, respectively).

Distributed versus Lumped: Number of Lumped Segments Required: It is often of practical interest to know how many lumped segments are required to reasonably approximate a distributed model. For illustration, consider LC segments, which can be viewed as low-pass filters. For a reasonable approximation, this filter must pass at least some multiples of the highest frequency  $f_{max}$  of the propagating signal (say ten times,  $f_0 \geq 10f_{max}$ ). In order to relate these parameters, we make use of the 3-dB passband frequency of the LC filter given by  $f_0 = \frac{1}{\pi\sqrt{LCd}} = \frac{1}{\pi\tau d}$ , where  $d$  is the length of the line and  $\tau$  represents the delay p.u.l. From  $f_{max} \approx 0.35/t_r$ , and  $f_0 = \frac{1}{\pi\tau d}$ , we can express the relation in terms

of the delay of the line and the rise time as,  $t_r \geq 3.5(\pi\tau d) \approx 10\pi d$ . In other words, the delay allowed per segment is approximately  $tr/10$ . Hence, the total number of segments (N) needed to accurately represent a total delay of  $\tau d$  is given by  $N = \frac{\tau d}{t_r/10}$ .

Example: Consider a digital signal with rise time of 0.2 ns propagating on a lossless wire of length 10 cm, with a Per Unit Length ( P.U.L.) delay of 70.7 ps (this can be represented by a distributed model with P.U.L. parameters of  $L=5$  nH/cm and  $C=1$  pF/cm). If the same circuit were to be represented by lumped segments, one needs  $N \approx 35$  sections. It is to be noted that using more sections does not clean up ripples completely but helps to reduce the first overshoot (Gibb's phenomenon). Ripples can be reduced when losses are properly taken into account. One of the major drawbacks of the above conventional discretization is that it requires a large number of sections, especially for circuits with high operating speeds and sharper rise times. This leads to large circuit sizes and the simulation becomes CPU inefficient. In order to overcome these difficulties, several techniques for efficient discretization are listed below. These methods can be broadly classified, based on the passivity property as follows.

1. Macromodels with no guarantee of passivity:
  - (a) Method of characteristics,
  - (b) Transfer function approximation and
  - (c) Chebyshev polynomial-based approximation
2. Macromodels with guaranteed passivity by construction of macromodels
  - (a) Compact finite differences,
  - (b) Integrated congruent transform and
  - (c) Exponential Pad-based matrix-rational approximation

### 2.3.2 Model reduction based simulation algorithms

Interconnect networks generally tend to have a large number of poles, spread over a wide-frequency range. Even though the majority of these poles would normally have very little effect on simulation results, however, they make the simulation to be CPU extensive by forcing the simulator to take smaller step sizes.

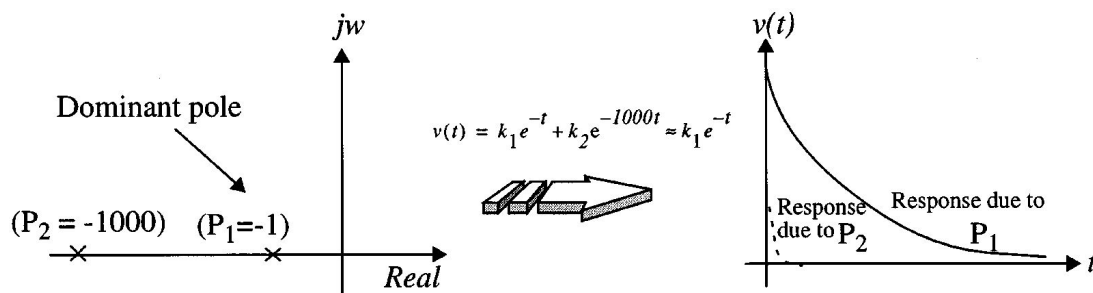


Figure 2.9: Example of dominant poles

**Dominant Poles:** Dominant poles are those that are close to the imaginary axis and significantly influence the time as well as the frequency characteristics of the system. The moment-matching techniques (MMTs) capitalize on the fact that irrespective of the presence of a large number of poles in a system, only the dominant poles are sufficient to accurately characterize a given system. This effect is demonstrated in Fig. 2.9, where it is clear that pole will have little effect on the final transient result.

It has been shown that the moments provide an estimation of delay and rise times. Elmore delay, which approximates the midpoint of the monotonic step response waveform by the mean of the impulse response, essentially matches the first moment of the response. This can be considered as one of the basic forms of approximation. However, in order to get accurate prediction of interconnect effects, it is essential that the reduced-order model must match (or preserve) as many moments as possible. Several algorithms can be found in the literature for reduction of large interconnect subnetworks. They can be broadly classified into two categories:

1. Approaches based on explicitly matching the moments to a reduced-order model- AWE and
2. Approaches based on implicitly matching the moments - PVL, PRIMA, which are based on Krylov subspace formulation

### 2.3.3 Full-Wave Models

At further subnanosecond rise times, the line cross section dimensions become a significant fraction of the wavelength and field components in the direction of propagation can no longer be neglected. Consequently, full-wave models that take into account all possible field components and satisfy all boundary conditions are required to accurately

estimate high-frequency effects. However, circuit simulation of full-wave models is highly involved. The information that is obtained through a full-wave analysis is in terms of electromagnetic field parameters such as propagation constant, characteristic impedance, etc. However, a circuit simulator requires the information in terms of currents, voltages, and circuit impedances. This demands a generalized method to combine modal results into circuit simulators in terms of a full-wave stamps.

1. Measured Data: In practice, it may not be possible to obtain accurate analytical models for interconnects because of the geometric inhomogeneity and associated discontinuities. In general, the behavior of high-speed interconnects can easily be represented by measured frequency-dependent scattering parameters or time-domain terminal measurements. However, handling measured data in circuit simulation is a tedious and a computationally expensive process.
2. EMI Subnetworks: Electrically long interconnects function as spurious antennas to pick up emissions from other nearby electronic systems. This makes susceptibility to emissions a major concern to current system designers of high-frequency product. Hence, the availability of interconnect simulation tools including the effect of incident fields is becoming an important design requirement.
3. Sensitivity Analysis: Sensitivity analysis involving large interconnect sub networks can be highly CPU intensive. Model-reduction-based approaches provide an efficient means for this purpose.
4. Minimum Realization of Reduced-Order Models: It is evident that the size of the reduced-order model increases with the increase in the number of ports. In such cases, it may become essential to realize the macromodels with a minimum possible number of states, so as to achieve fast transient simulations. Also, it is observed that Krylov-subspace-based reduced models require high order to capture high-frequency effects such as skin effect. This can make the transient simulation expensive as the reduced model becomes expensive to evaluate and post-processing of macromodels to further reduce the order may become necessary.

## 2.4 Finite integration technique

All numerical approaches to solve Maxwell's equations partition space into sub domains, where solutions can be found more easily. When discussing the properties of the different methods, it is necessary to classify them. A major point of difference is the domain they are working in, which is either time domain or frequency domain. Concentrating on the methods that most relevant commercially, we find on the time domain the finite integration technique (FIT), finite difference time domain (FDTD) in its explicit or implicit variants; and the transmission line matrix (TLM) method. The frequency domain is represented by the finite element method; FIT; and the MoM. All methods are volume discretization methods, except for the MoM, which is a surface discretization method.

The Finite Integration Technique (FIT) is the core numerical method used to solve Maxwell's equation for analysis the computational domain. Basic introduction of FIT is described in the preceding section. FIT is used in this thesis for analysis and investigation of the given problem definition.

### 2.4.1 Introduction

The Finite Integration Technique (FIT) is used as a core numerical technique in Commercial 3D fullwave electromagnetic software-CST STUDIO SUITE. It provides universal spatial discretization technique which can be used to solve various electromagnetics problems from dc to high frequency applications in time and frequency and time domain. FIT uses following discrete set of Maxwell's Grid Equations (MGEs):

$$Ce = -\frac{d}{dt}b, \quad \tilde{C}h = -\frac{d}{dt}d + j, \quad \tilde{S}d = q, \quad Sb = 0, \quad (2.2)$$

Where topological matrix  $C$  and  $\tilde{C}$  as the discrete equivalent of the analytical curl operator and discrete divergence operators  $S$  and  $\tilde{S}$ . The properties of continuous gradient, curl and divergence operators are maintained in FIT grid space. Even the set of maxwelle's grid equation maintain charge and energy conservation.

$$\mathbf{S}C = \tilde{\mathbf{S}}\tilde{\mathbf{C}} = 0 \Leftrightarrow \mathit{divrot} \equiv 0, \quad \mathbf{C}\tilde{\mathbf{S}}^T = \tilde{\mathbf{C}}\mathbf{S}^T = 0 \Leftrightarrow \mathit{rotgrad} \equiv 0, \quad (2.3)$$



FIT supports not only orthogonal hexahedral grids but topologically irregular grids (sub grids) and tetrahedral grids. The classical FDTD methods are limited to staircase approximations of complex boundaries. In contrast, the Perfect Boundary Approximation (PBA) technique applied to the FIT algorithm maintains all the advantages of structured Cartesian grids while allowing accurate modeling of curved structures. The FIT method can be even further enhanced by the Thin Sheet Technique (TST) which improves the modeling of thin perfectly electric conducting sheets.

### 2.4.2 Types of solvers

Transient, frequency domain and eigenmode solver are available concerning high frequency electromagnetic field problems. The following section is to provide basic information about the solvers and to present the corresponding fundamental equations.

#### Transient solver

All time domain methods: FIT, FDTD and TLM- feature a Cartesian (or cuboid hexahedral or circular cylindrical coordinate) grid and an explicit time integration scheme. These two facts are closely related. The coordinate grid implicates a simple band structures of the system matrix on which the leap frog algorithm can be applied. The fields are propagated through the structure by matrix vector multiplications with a specific time step. The larger the time step, the shorter the simulation time. The maximum possible time step is determined by the Courant-Friedrich-Lewy (CFL) - criteria. It is basically the time required for the light to pass the smallest mesh cell in the calculation domain. It might be more illustrative to think of the CFL-criteria as a way to force information from a mesh cell to touch every neighboured mesh cell in every mesh time steps. The memory requirements and the simulation time increase linearly with the number of mesh points. Because of these properties, time domain simulators are well suited to solve electrically large and detail rich structures.

There are other time domain approaches that use non orthogonal grids and/or implicit time integration scheme. An implicit algorithm always has to solve a system of equation for very time step, but then the time step size may be chosen somewhat larger. It is possible to derive frequency domain data by applying Fourier transformation to the time domain

signals, steady-state 3-D EM fields can also very easily be extracted from the transient broadband simulation run. Since the excitation signal is broadband, it is possible to obtain fields for various frequencies in one simulation run. Time domain naturally offers the possibility to study the transient behaviour of EM structures. Arbitrary signals can be fed into the simulator. Not only the signals, but also fields can be studied in time domain: e.g., transient farfields become increasingly important in UWB applications. In multiport devices, every port can be excited individually with a different time signal, and the fields can be monitored accordingly.

In traditional FDTD and TLM methods, every hexahedral mesh cell is filled entirely with one material. This leads to the so-called staircase approximation of the geometry. Obviously, such a discretization can make the accurate geometrical representation of many practical devices very difficult, since most components contain rounded features. In order to increase the accuracy in such cases, very fine meshing needs to be applied. Conformal methods, such as the Perfect Boundary Approximation (PBA), can improve the geometry description without compromising the memory efficiency of standard FDTD. The performance increase through such a method is remarkable. PBA, for example can also be used to model finite-thickness metallization within one mesh cell. This would result in tiny mesh cells in traditional FDTD and vice versa to a very small time steps and very long simulation times. In TLM, however even more advanced compact models can be found, fine structured elements like slots, vents, or cables are replaced by the specific micro model in order to avoid the sampling of all details by the grid. This approach has been proven particularly useful in EMC applications.

This standard FDTD grid is structured. This means that every mesh line starts on one side of the calculation domain and ends on the other side. In order to avoid the increase of mesh cells in the outer regions, sub gridding algorithms have been introduced, which allow locally smaller mesh cells. The mesh cells need only to be small in regions where small details are present. Additional accelerations of the simulation can be achieved by using different time steps at different mesh levels. Although many different sub gridding algorithms have been proposed, many of them exhibit the so-called long time instability.

The transient solver is based on the solution of the discretized set of Maxwell's Grid Equations. Substituting the time derivatives by central differences yields explicit update

formulation for the loss-free case.

$$\begin{aligned}\mathbf{e}^{n+\frac{1}{2}} &= \mathbf{e}^{n-\frac{1}{2}} + \Delta t \mathbf{M}_\epsilon^{-1} \left[ \tilde{\mathbf{C}} \mathbf{M}_\mu^{-1} + \mathbf{j}_s^n \right] \\ \mathbf{b}^{n+\frac{1}{2}} &= \mathbf{b}^n + \Delta t C \mathbf{e}^{n+\frac{1}{2}}\end{aligned}\tag{2.4}$$

In the FIT, unknown calculation variables are given by electric voltages and magnetic fluxes which are located alternatively in time by leap frog scheme. This explicit time integration schemes are conditionally stable. The stability limit for the time step is given by the Courant-Friedrichs-Levy (CFL) criterion.

$$\Delta t \leq \frac{\sqrt{\mu\epsilon}}{\sqrt{\left(\frac{1}{\Delta \mathbf{x}}\right)^2 + \left(\frac{1}{\Delta \mathbf{y}}\right)^2 + \left(\frac{1}{\Delta \mathbf{z}}\right)^2}}\tag{2.5}$$

### Frequency domain solver

A characteristic of frequency domain solvers is the implicitness of this approach; the resulting system is typically a large linear system of equations. Thus a matrix inversion is needed in order to obtain the solution for one frequency, no matter whether the grid is structured or not. In commercial applications, FEM or tetrahedral grids is the therefore the most popular general purpose numerical method. Tetrahedrons are the simplest volume entities, and their flexibility in approximating arbitrary geometries has many benefits. However tetrahedron quality is crucial: very flat tetrahedrons may compromise solution speed and accuracy as they make it more difficult for the algebraic solution method to solve the system.

There are two distinct methods of solving the linear systems of equations resulting from FEM discretization: direct and iterative solvers. A direct solver works directly on the system of equations derived from the discretization. Its key advantage is that it can solve for several port excitations at the same time in parallel. On the other, the memory requirements are quite high. Typically, the memory requirements increase quadratically with the numbers of tetrahedrons. Iterative solvers transfer the original system of equations into another one that can be solved by repeated application of operations according to the specific algorithm. The iterative algorithm has to be executed for each excitation individually. In compensation, the memory requirements are much less compared to a di-

rect solver. Similarly to the time domain methods, where small time steps lead to many steps to be simulated, the overall computing time of a frequency domain method also depends, for both types of solvers, on the sampling granularity of the frequency range of interest.

Frequency domain solvers are well suited to solve infinite periodic problems, such as phased array, frequency selective surfaces(FSS), photonic band gap structure(PBG), etc. Periodic boundaries can be set up either with a phased difference between them or, more practically, with certain scan angle. A Floquet mode port is a useful addition to this capability. It enables the usage of plane waves to monitor polarization or RCS, as well as the determination of main and grating lobes of a phased array.

The frequency domain solver is based on Maxwell's Grid Equations in the time harmonic case. The general-purpose frequency domain solver can be used together with hexahedral or tetrahedral grids.

$$(\text{curl}\mu^{-1}\text{curl} - \omega^2\epsilon)\vec{E} = -i\omega\vec{J} \Rightarrow (\tilde{C}\mathbf{M}_\mu^{-1}C - \omega^2\mathbf{M}_\epsilon)\mathbf{e} = -i\omega\mathbf{j} \quad (2.6)$$

### Eigen mode solver

The eigen mode solver allows computation of the structure's eigenmodes and the corresponding eigenvalues. The eigenmode solver is based on the eigenvalue equation for non-driven and loss-free time harmonic problems. The solution is obtained in the loss-free case via the Krylov-Subspace or Jacobi-Davidson method:

$$\text{curl}\mu^{-1}\text{curl}\vec{E} = \omega^2\epsilon\vec{E} \Rightarrow \tilde{C}\mathbf{M}_\mu^{-1}\mathbf{C}\mathbf{e} = \omega^2\mathbf{M}_\epsilon\mathbf{e} \quad (2.7)$$

## 2.5 Basics of 3D simulation

### 2.5.1 Modeling

In setting up a computer model for a real device, there are several steps, which are common to all discussed simulation methods. All of them are bear risks to introduce errors into the simulation, i.e., discrepancies between simulation results and measurements. First of all, a geometrical model needs to be created. This can be either done by using a modeller built into the simulation software or by importing the geometrical data from

a mechanical CAD tool. Importing from CAD tools is not as easy as it sounds, and the quality of import filters varies significantly; if comparing to an existing device, the exact same dimensions have to be used. Sounds simple? Besides obvious errors, there are always tolerances, and sometimes details are neglected, which are relevant at microwave frequency and radiofrequency (RF).

The knowledge of the exact material properties is essential for an accurate simulation, but this normally not available. The computational effort for volume-based methods depends also on the volume size, and the size of the simulation model must always be finite, even if in reality the component is placed in an infinite surrounding. In order to reduce surrounding space, boundary conditions need to be introduced that represents, for example, electric walls, free space, symmetry, or periodicity. For our connector, this is not relevant, because we can simply assume that the space surrounding it is a perfect conductor, as we know that there will be virtually no field penetrating the conductor shielding.

Finally, we have to define ports in the model to excite the structure and to monitor simulation results such as transmission and reflection. Ideally, these ports should not an impact on simulation results.

## 2.5.2 Running a simulation

Having set up our geometric representation of the real structure in the software environment, we can now start the steps towards the final results. The first step is the actual space discretization- the mesh setup- which is automated to a large extent in modern commercial software. Despite the high degree of automation, the proposed mesh might need to be checked or influenced manually in order to obtain accurate results. In a second step, the software creates the system matrices based on the geometrical information from this grid and method chosen for approximating Maxwell's equations. After all the required matrices are created and assembled, the third steps starts; namely the solution of the finite algebraic system. Here for example, we want to calculate the S-parameters, since they are the most often requested results for passive component characterization.

- In the frequency domain, this process is straight forward : one simulation delivers the S-parameters at one frequency point. However, the behaviour is usually rele-

vant in a specified frequency range, so looking at a single frequency is not sufficient. Therefore, a number of simulations in the frequency band of interest have to be performed. Special algorithms are used to minimize the number of simulation required to achieve a predefined accuracy by interpolating the S-parameters in between the simulated frequency points.

- In time domain, the approach is quite different. The user specifies the frequency range of interest. A Gaussian signal  $X(f)$  covering this frequency range is defined. This spectrum is then transformed into time domain by using an inverse Fourier transformation, resulting in a time signal  $x(t)$  with a Gaussian envelope. The mode pattern at the input port is then excited with this time pattern and propagated through the structure. Reflected and transmitted time signals, denoted generically by  $y(t)$ , are monitored and after the simulation is ready, a Fourier transform is applied to yield the respective spectral  $y(f)$ . These spectra are eventually divided by the excitation spectrum: the S-parameters for the entire frequency range in one single go!

The accuracy of simulation, namely the accordance of simulation results and the behaviour in reality, is usually limited due to simplifications in the simulation model. Having the simulation results in front of us, we may wonder whether there are the true S-parameters of our device. All numerical methods promise that the simulation results will eventually converge against the actual solution, if only the mesh is fine enough and all details and effects are represented in the numerical model. If the results of interest do not change significantly anymore after several mesh refinement steps, the converged simulation has been reached. Cross verification of the results by applying two different numerical approaches to the same problem gives even more confidence, e.g., by comparing the time domain solution and frequency domain solutions. This reassurance is even more convenient to reach, if the simulation software offers the possibility to switch between numerical approaches without changing the interface. There is just another constraint, which has not yet been considered- simulation performance. It is defined by the time required for a simulator to reach a predefined accuracy.

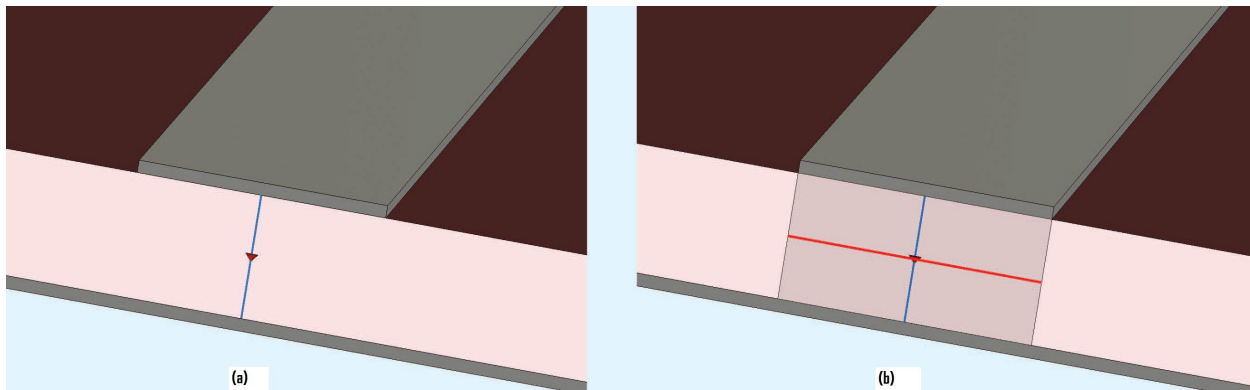


Figure 2.10: (a) Discrete port: two wires with a source in the middle. (b) Face port: the source is distributed along the red line.

### 2.5.3 Accuracy issues and its solutions

To obtain an accurate solution after the simulation, there are quite a few points:

- Model the reality correctly
- Ensure that the mesh is fine enough
- Ensure that the solution of the discretized system of equations is numerically accurate.

#### Modeling the Reality

1. Excitations : For exciting the desired modes in the device, ports need to be defined at the locations at which, in reality, the sources will be connected. This is usually at some point along a transmission line (waveguide, microstrip, etc.). A discrete port is simply a lumped voltage or current source, possibly with nonzero internal impedance/admittance. The source is connected by perfectly conducting wires to two points of the device [Figure 2.10].

Long connection wires may strongly influence the solution. This is because of the wire inductance, which grows linearly with the wire length. To reduce the parasitic inductance of the discrete port, the so-called face port (or delta-gap port) has been proposed. Here, the voltage source is distributed along a small gap in a metallic face [Figure 2.10(b)]. The face port has a much smaller self inductance (imagine it as a parallel connection of many wire inductances).

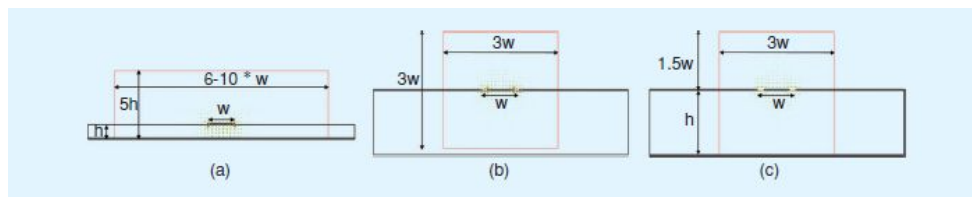


Figure 2.11: Port size rules of thumb for: (a) microstrip, (b) ungrounded, and (c) grounded coplanar line.

The discrete or face ports will always introduce a small perturbation of the numerically calculated field at the location where they are placed in the model. To completely eliminate this perturbation, one can imagine extending the excited transmission line to infinity, thus preventing any reflections from appearing. Of course, no infinite structure can ever be modeled numerically, so a special type of port, the so-called waveguide port was introduced as a means of truncating the infinite line, without introducing any perturbations.

A waveguide port is a surface perpendicular to a transmission line on which the modes that can propagate along the transmission line are calculated. The field patterns corresponding to these modes are then used as excitation during the simulation. To ensure accurate mode calculation for arbitrary line configurations, the modes are typically calculated by solving a two-dimension eigenmode problem on the port's surface.

The size of the waveguide port is of utmost importance for the accuracy of the solution. Whereas for a hollow or coaxial waveguide the port size is clear-it should be as large as the waveguide's cross section-for other types of transmission lines (microstrip, strip line, etc.), the user might often have difficulty in guessing just how large the waveguide port should be. These transmission lines allow the propagation of static-type TEM or quasi- TEM modes, whose fields become zero, theoretically, at infinity. A few rules of thumb are given in Figure 2.11.

It is recommended, however, to make a few tests with the port size before starting the longer-lasting 3-D simulation. Just let the program calculate the port modes and have a look at the fields at the port, especially at the port's boundary. You should see no fields at the boundary. If there are fields at the boundary, the port size needs to be increased (Figure 2.12). The first golden rule of an accurate simulation:



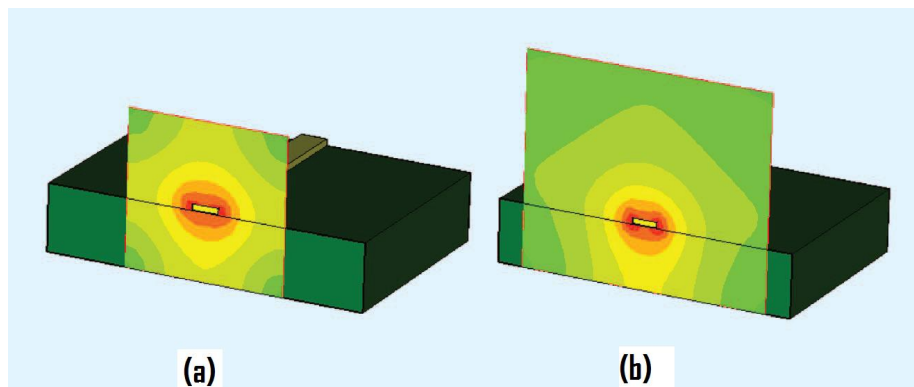


Figure 2.12: Absolute value of the electric field (represented in logarithmic scale) at a microstrip port. (a) Port size is too small; electric field has considerable magnitude at port's border and will negatively impact on the solution's accuracy. (b) Port size has been increased laterally and above the microstrip and fields are practically zero (green colour) at port's border.

2. Boundary Conditions: As already mentioned, the simulation domain, infinite in reality, has to be truncated for the purpose of simulating it on a computer. At the boundary, special boundary conditions need to be imposed, depending on the real operating conditions of the device. For example, if the device that needs to be simulated is in reality placed within a metallic box, then electric boundary conditions (which impose zero tangential electric field, just as for a perfect metallic object) can be used on all sides of the boundary. An infinitely extended ground plane can be modeled by an electric boundary condition as well.

If the structure is placed in open space, such as an antenna, then a so-called radiation or absorbing boundary condition is the right one. It simulates the unperturbed propagation of EM waves through this boundary. When choosing the domain's truncation, do not forget to leave some free space around the antenna! A perfectly matched layer (PML) boundary requires just a fraction of a wavelength of additional space, whereas other absorbing boundary conditions often need more than one wavelength. Absorbing boundary conditions should be used only when necessary since they typically require more computing resources than, e.g., the electric ones. For infinite periodic structures, the periodic boundary conditions are available. Whenever both the simulated structure and the excitation are symmetric, the usage of symmetry conditions can reduce the number of unknowns by half for each symmetry plane and therefore shorten the simulation time.

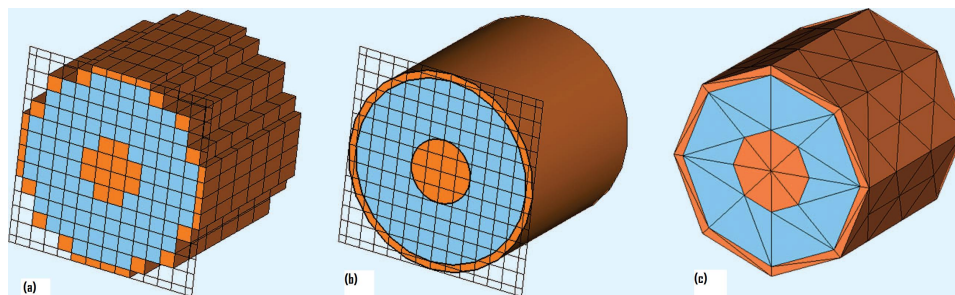


Figure 2.13: Hexahedral and tetrahedral mesh for a piece of coaxial cable. (a) The staircase mesh provides a poor description of curved surfaces, unless a very fine mesh is used. (b) Conformal boundary approximation ensures the required geometric accuracy, with a minimum of mesh cells. (c) Tetrahedral mesh generators often require a segmentation of round structures, leading to a poor geometrical approximation.

The permittivity, permeability, and conductivity values for all materials present in the model naturally play an important role in the solution's accuracy. Often, these values are frequency-dependent (dispersive materials), and the more accurately this frequency dependence is known, the more accurate the solution can be. Frequency-domain solvers, as well as the advanced time domain simulators, can take this frequency dependence easily into account. Please do not forget that the often used constant tangent delta material model is actually fiction. No material can have a constant loss tangent from dc to several GHz. Even the most common materials, such as Flame Retardant 4 (FR4), exhibit a more complicated dispersion-in the case of FR4 the first order Debye model appears to be sufficiently accurate.

### Meshing the Structure

How fine does the mesh need to be? First, it should be fine enough to correctly represent the geometry. Second, it should be fine enough to represent the possibly sharp field variations within the device.

With most time-domain simulators, the used hexahedral mesh leads to a staircase representation of the boundaries, so the mesh needs to be made quite fine just to obtain a good representation of the geometry [Figure 2.13(a)]. The advanced conformal meshing eliminates this drawback by using the memory-efficient hexahedral mesh almost everywhere in the model and special algorithms conforming to the curved boundaries at material interfaces [Figure 2.13(b)].

This way, a considerable saving in terms of mesh cells can be achieved. Although

tetrahedral meshes can, in principle, offer a good geometry approximation, this is only true if the real structure is meshed; some meshers require the segmentation of round structures and finally lead to polygonal approximation of curvatures [Figure 2.13(c)]. Representing the field variations in the mesh is an even more complicated issue.

The first rule of thumb that can be applied a-priori, before any simulation is started, is that in a time-domain simulation with hexahedral mesh, the size of a mesh cell should never be larger than  $\lambda/8$ , where  $\lambda$  is the wavelength corresponding to the upper limit of the interesting frequency range. Mesh cell sizes of  $\lambda/10$  or  $\lambda/15$  are often successfully used in practice.

For frequency domain FEM solvers based on second-order finite elements,  $\lambda/4$  is a good value to start with. Of course, a model is typically made of several materials. Since the wavelength is dependent on the material properties, the size of every individual mesh cell depends on the material it is filled with. That is why programs that only allow a uniform mesh (the same mesh cell size everywhere) may lead to an unnecessarily large number of mesh cells. For lossy materials, the rule of thumb is to ensure two to three mesh lines within the skin depth. This can prove disadvantageous for good conductors at high frequencies since the tiny skin depth would lead to tiny mesh cells and considerably increase the simulation time.

Advanced simulators apply special surface impedance models for metals during the simulation process and eliminate completely the need to mesh the skin depth. How about sharp field variations-field singularities- due to geometrical features, such as edges, corners, etc.? There are two ways to represent them in the mesh. The a-priori solution used by some field simulation programs is to automatically detect these features and to use advanced edge/corner correction algorithms during the simulation. A second way is increasing the mesh density a-posteriori by the so-called adaptive meshing, which will be discussed later. These approaches are applicable in both time and frequency domain.

All this seems very complicated, and it appears almost impossible for a normal user to achieve a mesh of good quality. But any advanced simulation program should be able to do all these steps : generate an initial mesh according to a minimal user input (e.g., number of steps per wavelength), taking into account geometry, material properties, and sharp corners and edges and refine the mesh through an automatic adaptive meshing, until convergence is reached.

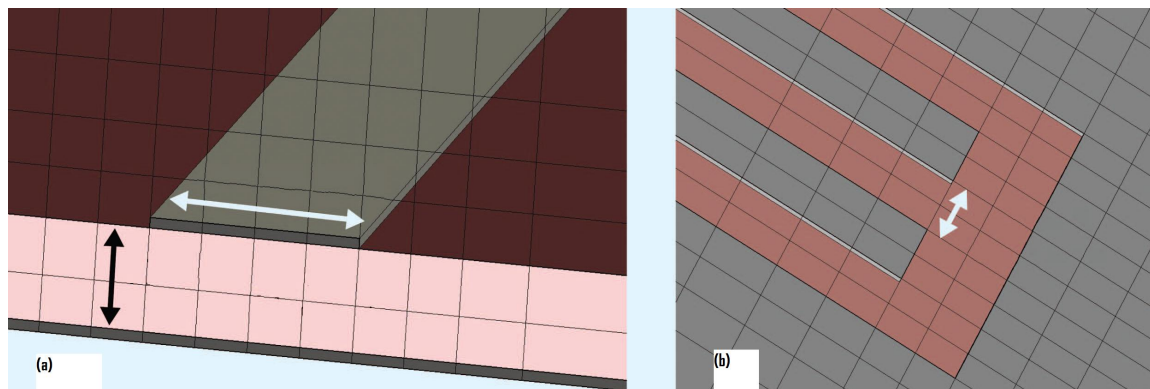


Figure 2.14: Rules of thumb for meshing planar structures with hexahedral meshes (greymetal, dusky pink-substrate). (a) Discretization of a microstrip. (b) Discretization of gaps inside a metal sheet.

With a minimum of user input however, the size of the final mesh can be optimized and thus reduce the overall computing time. For instance, we should ensure that there are at least two mesh cells within the substrate thickness, two to four mesh cells across a strip, and two mesh lines in a radiating gap (Figure 2.14). The mesh cells should be smaller close to metallic edges to sample the fringing fields. The height of the microstrip only has to be discretized if the used software does not support finite thickness metallization.

### Accuracy

**Accurate Numerical Solution** In frequency domain simulations, a linear system of equations needs to be solved at each frequency point. If the condition number of the system matrix is large, for example, because some tetrahedral in the mesh are excessively flat, the solution may be quite inaccurate. When using an iterative solver, a large number of iterations may be necessary. In a time-domain simulation there is no system to solve. Issues like matrix conditioning number are irrelevant here. The main accuracy issue in the time domain simulation is related to the inverse Fourier transformation of the time signals, in order to obtain frequency domain parameters. Namely, all signals should start at zero and end at zero in order to ensure accurate frequency-domain values. Especially for high-Q structures, the output time signals continue to oscillate a long time even after the excitation has been turned off (Fig. 2.15). A good time-domain simulator will however provide the user automatically with a criterion on when to stop the simulation. The position of a resonance will settle quite quickly and will be quite accurate even if the simulation is stopped too soon. The amplitude of the S parameters however will only

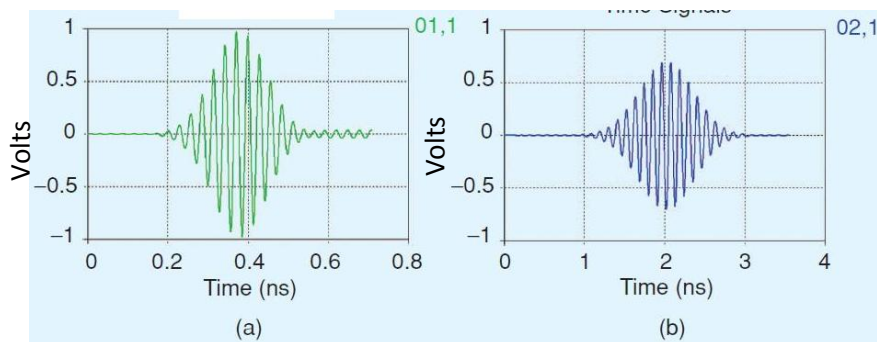


Figure 2.15: Time signal examples. (a) The output signal still oscillates with relatively high amplitude at the moment when the simulation was stopped. The frequency-domain results (e.g., S-parameters) are most likely inaccurate. (b) A time signal which is sufficiently decayed when the simulation is stopped will provide accurate frequency-domain results

be accurate if the time signals have sufficiently decayed. To predict the correct amplitude, algorithms such as an autoregressive filter can be applied on non-decayed signals and considerably save simulation time.

- Mesh adaptation and convergence : The accuracy of a simulation result has to be tested by performing a convergence study. In a convergence study the number of mesh cells is continuously increased until the results of interest, usually S-parameters do not change anymore, at least not significantly. A convergence study is thus an essential part of any simulation project. Many software tools feature automatic mesh adaptation schemes. Typically fields are evaluated after a simulation run. Wherever strong field variations occur, the mesh is refined and the simulation is restarted. This process is repeated until the results do not change significantly anymore.

Although convergence study and mesh adaptation appear to be very similar approaches to guarantee accurate results, in practice they are different. For a convergence study, we assume that the geometry approximation of the structure as well as the results in the entire frequency range of interest is improved continuously with the refined mesh.

Frequency domain solvers perform the mesh adaptation typically only for one frequency, per default usually the highest frequency in the band of interest. The highest frequency is, for example for filters, not necessarily the one that is relevant

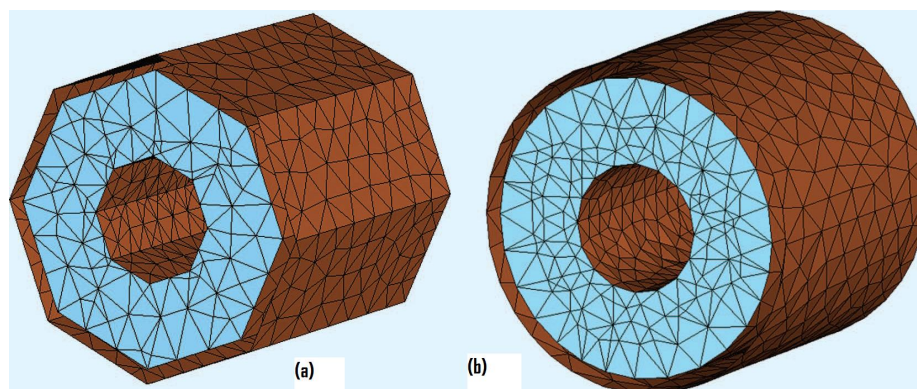


Figure 2.16: Final mesh after the adaptation process for a piece of coaxial cable. (a) Mesh adaptation without snapping on the true geometry. (b) Snapping onto the geometry during the adaptation process leads to a good approximation of the geometry and hence to more accurate results

for the device functionality. A relevant frequency has to be chosen for mesh adaptation. This information is reliably available only a posteriori. In addition, the field distribution might change significantly with frequency, e.g., for multiplexers or multiband antennas. One single adaptation frequency is not sufficient in such cases. Either the simulation has to be split up into several separate frequency bands, or several adaptations frequencies have to be used in one simulation over the entire band. In order to derive accurate simulation results, the geometry representation on the grid has to be as good as possible.

Particularly tetrahedral grid based frequency domain solvers do often not improve the geometry approximation during mesh adaptation. In the mesh adaptation process the initial tetrahedrons are simply subdivided in order to improve the field sampling (Figure 2.16). Therefore we see a convergence of results, though not for the input model but for the initially approximated geometry. This effect is even more critical if shapes are segmented before simulation.

In contrast to frequency domain, the time domain approaches can perform the mesh adaptation broadband. Moreover, every refinement also entails a better geometry approximation, since the entire meshing process is restarted at every mesh adaptation step.

Finally it should be mentioned that, unlike a tetrahedral mesh, a structured time domain grid can be easily controlled by the user, by manipulating mesh lines or meshing densities. Thus the final mesh of an adaptation is nearly reproducible by

the user without rerunning the adaptation.

- How much accuracy do I need?

The answer to this question depends on the purpose of the simulation, as well as on the phase in the design process. In the beginning, it is recommended that set up the simulation with a coarse mesh and stop the simulation quite early. Towards the end of the design process, when it is close to the design goal, it is worth investing more resources in a more accurate solution: make the mesh finer and allow the time signals to fully decay towards zero (in a time-domain simulation) or set the error criterion for the linear equation system to a lower value (in a frequency domain simulation). The verification of measurements or analytic results requires the highest accuracy settings.

## 2.6 Basics of on wafer RF characterization

There are several reasons for the need of the on wafer RF characterization. The first reason is that MIC designer always wants the true performance of the device. It is highly recommended that results must not include the device plus package effect at early stage of the design. De-embedding technique has been developed prior to on wafer RF characterization but it is not used because it introduces additional errors and uncertainties. As we know that RF packages can be very expensive and die yield can be low hence the second reason is that designer wants to determine 'known good die' to reduce packaging cost and increase yields. The third reason is that designer wants to automate the measurements because it can be cost effective and fast.

A typical on wafer characterization setup may consist of vector network analyzer, cables, RF probes, probe positioners, probe station, contact substrate, calibration substrate, calibration software, and bias supply. One of the important component of this setup is microwave/RF probe. RF probe is used to measure the response of very small devices like MMICs without harming them.

**Microwave/RF Probes:** In order to probe a circuit, it is needed to launch a signal into it with some type of transmission line, usually 50 ohm. This requires at least two conductor, the "signal" conductors and the "ground" conductor. Basic three types of

the probes are

1. GSG- Ground Signal Ground
2. GS- Ground Signal
3. SG- Signal Ground

GSG is the most common type of the RF Probe. This is similar to coplanar waveguide. GS probes would be needed if RF circuit has only one ground pad. Most RF Probes are 50 ohm impedance because almost all microwave test equipments operates at 50 ohm impedance. However , sometimes high-impedance probes are used in order to sniff out the performance of a circuit without loading it down. Commercial RF probes are air co-planar transition, ACP series probe, Infinity series probe, Infinity waveguide port, cascade RF Probe etc. RF probe is selected and used depending upon the application, frequency range and types of layout of Device Under Test (DUT).

## 2.7 MMIC fabrication technology

In this section, I have discussed the OMMMIC ED02AH process because it is used here for fabricating the MMIC. The OMMMIC ED02AH process is developed specifically for microwave applications up to the millimeter wave, and for high rate digital circuits for optical links [47].

- E : Enhancement mode transistor
- D : Depletion mode transistor
- 02 : "0.2" m gate length (in fact, 0.18m)
- A : "A" type OMMMIC process
- H : Pseudomorphic HEMT Layer

The main features of this technology are summarized below:

- Hetero-epitaxy with a pseudomorphic (GaInAs) active layer
- Depletion and enhancement mode recessed transistors:  $V_t=0.225V$  or  $-0.9V$



- 2 types of diodes (0.18m "GM" and 3m "BE") for mixing, level shifting, or varactors.
- Resistors, using the GaAs active layer, non etched.
- Resistors, using a thin film metal layer (NiCr)
- Full  $Si_3N_4$  protection ensuring high reliability
- 2 types of MIM capacitors, using the  $Si_3N_4$  layer and the  $Si_3N_4 + SiO_2$  layer.
- $SiO_2/Si_3N_4$  + air bridge isolation between layers to reduce the parasitic capacitances.
- High yield 1.25m thick gold metallisation for interconnections and spiral inductors. Possibility of multi metal lines to reduce series resistances.
- Via holes through the 100m substrate to reduce parasitic inductances to ground.
- For digital circuits such 40Gb/s multiplexors or demultiplexors, availability of 0.13m gates instead of the 0.18m gates (ED01AH option). This increases the  $F_{text}$  value up to around 75GHz or more. The effect is taken into account in the models via the  $L_{gate}$  parameter.

### Front side ED02AH process description

- Active layer: The active components are based on a (Ga,Al)As - (Ga,In)As - GaAs heterostructure obtained by Metalorganic Vapour Phase Epitaxy (MOVPE), using an industrial multiwafer system.
- Isolation (Mask LI): Isolation between active components (P-HEMTS, diodes, resistors) is obtained by a boron implantation of the required zones while a resist layer protects the active areas defined by the LI mask. A small mesa is also etched for alignment of the subsequent masks.
- Ohmic contacts (Mask OH): Ohmic contact metal consists in a AuGeNi layer, which is deposited on the contact regions using a lift-off technique, and then alloyed under reducing atmosphere.

- NiCr resistor Metal Deposition (Mask MD - NiCr resistor option only) : A thin 40 Ohms square NiCr layer is selectively deposited onto the substrate by a lift off process to define the high precision resistors.
- MIM capacitor Bottom Electrode and 3m diodes (Mask BE): A TiPtAu metal layer is patterned with a lift off technique to form the MIM capacitor Bottom Electrodes and the first interconnection metal. This layer is also used for the 3m diodes, using a proper recess before BE metallization. The total BE metal thickness is 650nm.
- Channel recess and Gate Metallization (Masks LE and GM): The 0.18m gates are written using an Electron Beam equipment. The definition of the Noff P-Hemts is then obtained by an etching of the required zones while a resist protects the remaining areas of the wafer. The channel is then recessed, and the gate metal is deposited using a lift off technique. The total gate thickness is 360nm. In the case of the ED01AH option, the gates are written 0.13m long, and the GM metal thickness in 250nm.
- Silicon nitride deposition :A 150nm  $Si_3N_4$  layer is deposited on the wafer to protect the active areas and to form the MIM Capacitor dielectric.  $Si_3N_4$  is used because of its high dielectric constant, suitable for MIM capacitors, and for its ability to prevent the formation of unstable Ga and As oxides at the surface of the wafer. Deposition is made using a Plasma Enhanced Chemical Vapor Deposition (PECVD) technique which ensures the components created are of a high standard of reliability.
- $Si_3N_4$  layer etching (Mask CG): Vias through the  $Si_3N_4$  layer are opened with the CG mask to enable contact with the previously deposited metals. Streets for dicing are also opened.
- MIM Capacitor top electrodes (Mask TE):A metal is evaporated and defined using a lift-off technique to form the MIM capacitor top electrodes This layer is also used as a protection between the TiAl gates and the Au lines for a high reliability and as a contact layer for the NiCr resistors. The total TE metal thickness is 560nm.
- Dielectric deposition and contact opening (Mask CO): A 800nm thick Silicon oxide is then deposited on the wafer. Windows are opened to interconnect the second

interconnection metal with the OH, BE and TE metals. The streets for dicing are also opened.

- Air Bridge (Mask AB): A 1 $\mu$ m thick photoresist pad is defined. After second interconnection metal evaporation, this photoresist pad is removed leading to a 1 $\mu$ m air bridge.
- Second interconnection metal (Mask IN) : A 1.25 $\mu$ m thick TiPtAu layer is evaporated. The second interconnection layer is then defined by lift-off.
- Final protection :A second 150nm Silicon Nitride layer is deposited on the wafer. The PECVD technique ensures the total encapsulation of the circuit.
- Pad opening (Mask CB): The contact areas are then opened for bonding, as well as the streets for dicing.
- Stabilization bake : A final high temperature bake stabilizes the technology and ensures a long term reliability.

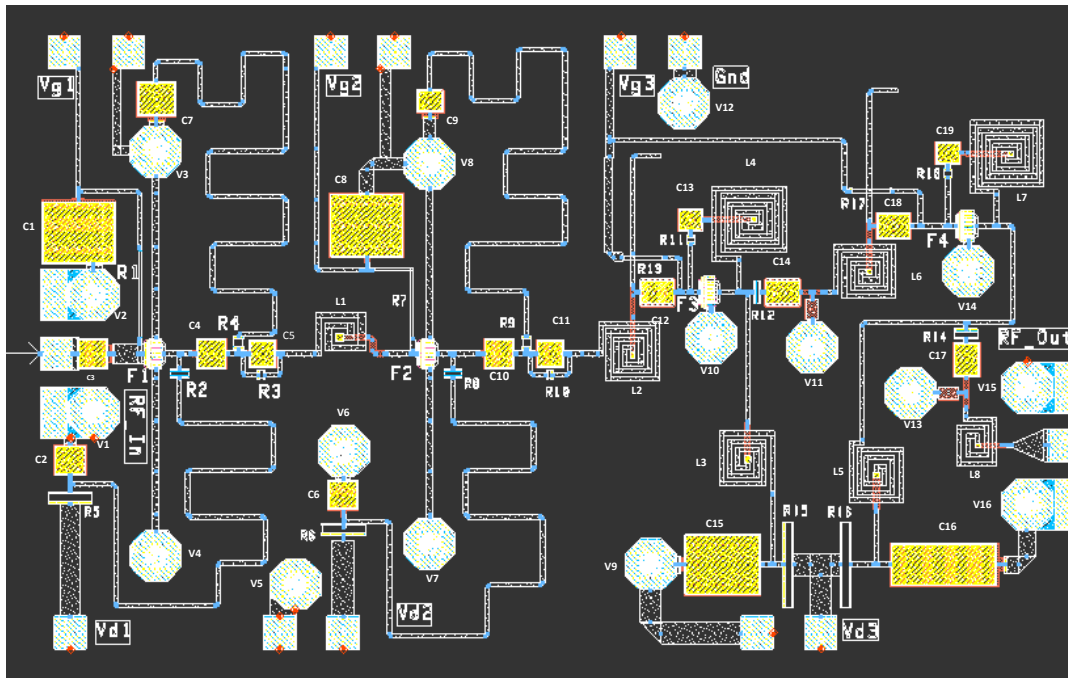
# Chapter 3

## Package/housing effect with active MMIC

The first part of the thesis discusses packaging/housing effect on active MMIC. When MMIC is mounted inside a test box or package/housing with a cavity, it may differ from its RF on-wafer (RFOW) and circuit simulation performance. The metallic side walls of the package/housing may support several resonant modes which induce surface currents on the walls of the package/housing. These unwanted currents may damage the devices under test. This undesirable effect is called package/housing effect. Hence in this chapter, we have presented systematic methodology for analysis and investigation of the package/housing effects on active MMIC.

### 3.1 An experimental test case

Presently there is no CAD tool available to predict active MMIC performance in a cavity. To investigate the cavity resonance problem, Low Noise Amplifier (LNA) MMIC chip is used here as an experimental test case chip which is operated in Ku band having greater than 30 dB gain. LNA MMIC chips are designed and simulated at Space Application Centre (SAC), Indian Space Research Organization (ISRO)-Ahmedabad, India. LNA MMICs are fabricated with the help of OMMIC fabrication lab, France. The 2.5D electromagnetic analysis of LNA is carried out using ADS circuit simulator software. The actual layout of LNA MMIC chip is as shown in Fig.3.1. High frequency wafer probe station and network analyzer are used for the on wafer RF measurements on the empty package and MMIC



Low Noise Amplifier MMIC Chip details: Active devices:F1,F2,F3 and F4, Resistors: R1 to R18, Inductors: L1 to L7, Capacitors: C1 to C19, Gate supply pads: Vg1, Vg2 and Vg3, Drain supply pads: Vd1, Vd2 and Vd3, Vias: v1 to v16

Figure 3.1: Layout of LNA MMIC chip

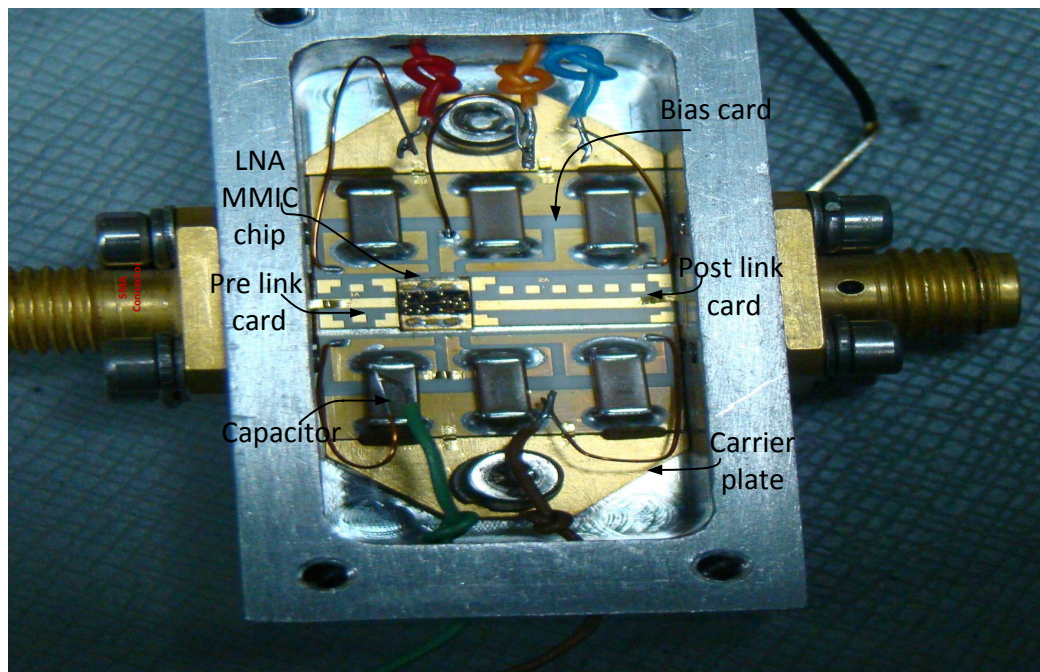


Figure 3.2: Actual test box with LNA MMIC chip: Gold plated carrier plate is used to mount the complete assembly, Pre and post bias cards are placed in between MMIC Chip, six DC bias capacitors are mounted on bias cards, Gold ribbon wires are used to connect MMIC chip and bias cards

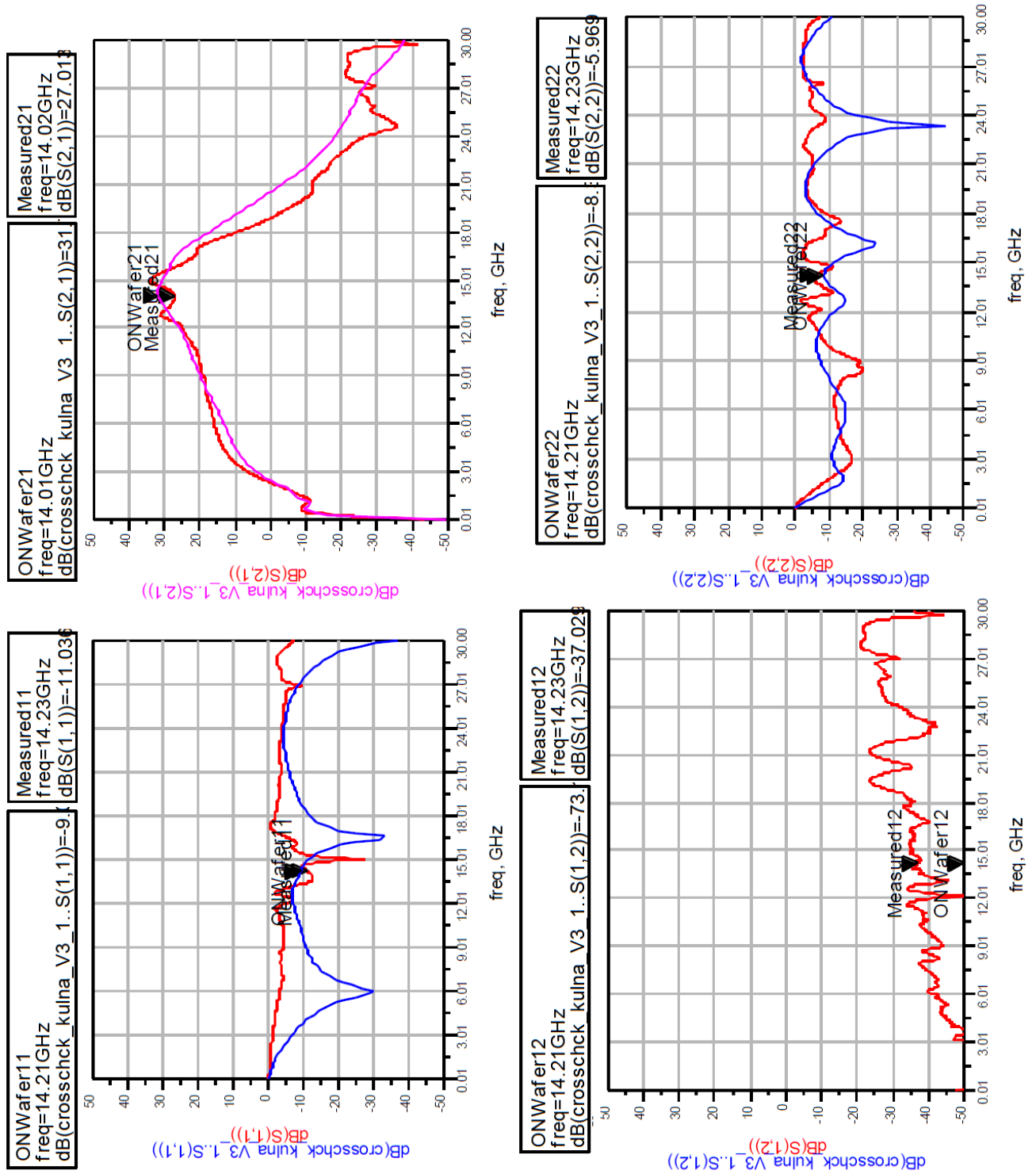


Figure 3.3: Comparison of RF on wafer and test box test results.

chips in wafer form. A 2-port network analyzer is used to perform measurements of the packaged/housed LNA MMIC Circuit. An actual Test box used for experimental test case, having LNA chip and other circuits is as shown in Fig. 3.2. RFOW measurement and in test box test data of MMIC have compared in Fig. 3.3. As shown in Fig. 3.3, RFOW measurement results and test box test data differed considerably. This is studied theoretically in Section 3.2. The Section 3.3 describes the investigation of the cavity resonance problem using eigen mode solver and transient solver. The section 3.4 presents modeling, simulation and simulation of active non planar MMIC with package/housing. Different mitigation techniques used to make stable, resonance free microwave low noise amplifier for a Ku-band are discussed in section 3.5.

To analyze the effect of package/housing on and inside active MMIC, ADS circuit simulator can't blend the EM field theory and circuit theory, hence full wave simulation of active MMIC with package/housing is mandatory. Presently Commercial full wave simulator can do this simulation of passive structures only. To embed the active MMIC models in the circuit simulator is a difficult task. In Section 3.3, active non planar MMIC is modeled, simulated and analyzed the E/H field distribution due to the discontinuity presence in chip layout. A computational electromagnetic technique, especially Finite Integration Technique (FIT- core method used by CST Microwave Studio-3D EM Software) is used here for full wave analysis.

## 3.2 A theoretical study

One of the way to construct the microwave resonators is to use closed sections of waveguide. Because radiation loss from an open-ended waveguide can be significant, waveguide resonators are usually short circuited at both ends, thus forming a closed box, or cavity. Electric and magnetic energy is stored within the cavity enclosure, and power is dissipated in the metallic walls of the cavity as well as in the dielectric material that may fill the cavity. Coupling to a cavity resonator may be by a small aperture, or a small probe or loop. There are many possible resonant modes for a cavity resonator, corresponding to field variations along the three dimensions of the structure[48]. The geometry of a rectangular cavity is shown in Figure 3.4. It consists of a length,  $d$ , of rectangular waveguide shorted at both ends ( $z = 0, d$ ). For finding the resonant frequencies of this cavity under

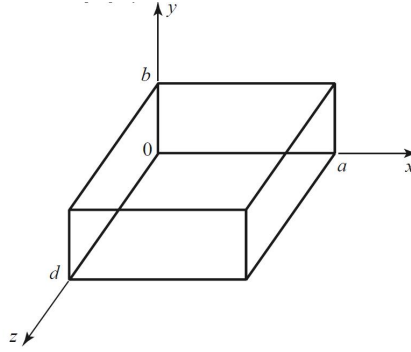


Figure 3.4: A rectangular cavity resonator

the assumption that the cavity is lossless, it is easier to start with the fields of the TE or TM waveguide modes since these already satisfy the necessary boundary conditions on the side walls ( $x = 0, a$  and  $y = 0, b$ ) of the cavity. Then it is only necessary to enforce the boundary conditions that  $E_x = E_y = 0$  on the end walls at  $z = 0, d$ .

The transverse electric fields ( $E_x, E_y$ ) of the  $TE_{mn}$  or  $TM_{mn}$  rectangular waveguide mode can be written as

$$\bar{E}_t(x, y, z) = \bar{e}(x, y) (A^+ e^{-j\beta_{mn}z} + A^- e^{j\beta_{mn}z}), \quad (3.1)$$

where  $\bar{e}(x, y)$  is the transverse variation of the mode, and  $A^+, A^-$  are arbitrary amplitudes of the forward and backward traveling waves. The propagation constant of the  $m, n^{\text{th}}$  TE or TM mode is

$$\beta_{mn} = \sqrt{k^2 - \left(\frac{m\pi}{a}\right)^2 - \left(\frac{n\pi}{b}\right)^2}, \quad (3.2)$$

where  $k = \omega\sqrt{\mu\epsilon}$  and  $\mu$  and  $\epsilon$  are the permeability and permittivity of the material filling the cavity. Applying the condition that  $\bar{E}_t = 0$  at  $z = 0$  to 3.1 implies that  $A^+ = -A^-$  (as we should expect for reflection from a perfectly conducting wall). Then the condition that  $\bar{E}_t = 0$  at  $z = d$  leads to the equation

$$\bar{E}_t(x, y, d) = -\bar{e}(x, y) A^+ 2j \sin\beta_{mn}d = 0. \quad (3.3)$$

The only nontrivial ( $A^+ \neq 0$ ) solution occurs for

$$\beta_{mn}d = l\pi, \quad l = 1, 2, 3, \dots, \quad (3.4)$$



which implies that the cavity must be an integer multiple of a half-guide wavelength long at the resonant frequency. No nontrivial solutions are possible for other lengths, or for frequencies other than the resonant frequencies.

A resonance wave number for the rectangular cavity can be defined as

$$k_{mnl} = \sqrt{\left(\frac{m\pi}{a}\right)^2 + \left(\frac{n\pi}{b}\right)^2 + \left(\frac{l\pi}{d}\right)^2}. \quad (3.5)$$

Then we can refer to the  $TE_{mnl}$  or  $TM_{mnl}$  resonant mode of the cavity, where the indices  $m, n, l$  indicate the number of variations in the standing wave pattern in the  $x, y, z$  directions, respectively. The resonant frequency of the  $TE_{mnl}$  or  $TM_{mnl}$  mode is given by

$$f_{mnl} = \frac{c}{2\pi\sqrt{\mu_r\epsilon_r}} \sqrt{\left(\frac{m\pi}{a}\right)^2 + \left(\frac{n\pi}{b}\right)^2 + \left(\frac{l\pi}{d}\right)^2}. \quad (3.6)$$

If  $b < a < d$ , the dominant resonant mode (lowest resonant frequency) will be the  $TE_{101}$  mode, corresponding to the  $TE_{10}$  dominant waveguide mode in a shorted guide of length  $\lambda_g/2$ , and is similar to the short-circuited  $\lambda/2$  transmission line resonator. The dominant TM resonant mode is the  $TM_{110}$  mode.

The theoretical resonance frequency calculation is carried out for the given package using 3.6, with a width of 13.9 mm, height of 8.4 mm and a length of 35.1 mm in the MATLAB software. The results are as shown in Table 3.1.

## 3.3 Investigation on a test case

### 3.3.1 Investigation using eigen mode solver

To investigate the cavity resonance issue for a given experimental test case, one of the prompt approaches is to use the eigen mode solver in CST MWS software. The eigen mode solver has capability to solve the computational domain with high accuracy. The eigen mode solver gives the eigen frequency presence in the computational domain. Here the eigen frequencies are the resonance frequencies of the package/housing. For the ease of debugging, problem is divided into three cases. Three cavity profiles as mentioned below are modeled for investigation purpose.

Table 3.1: Theoretical resonance modes for an experimental text box.

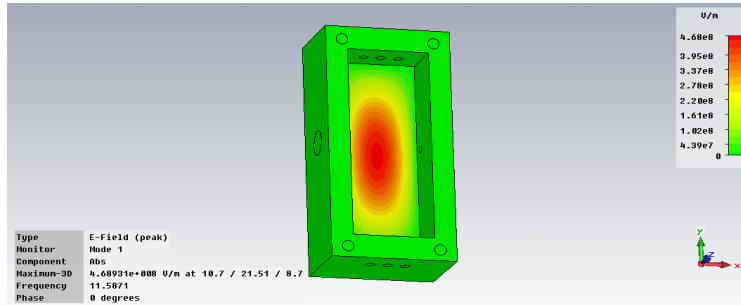
Different mode	Theoretical resonance frequency (GHz)
Mode 1	11.60
Mode 2	13.76
Mode 3	17.85
Mode 4	18.36
Mode 5	19.79

- Case A): Unassembled cavity structure
- Case B): Package/housing with carrier plate only (without LNA Chip and assembly components)
- Case C): Package/housing with LNA chip and all other components

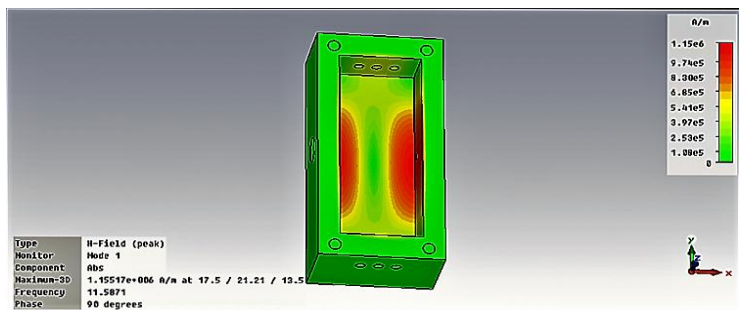
The eigen mode analysis is carried out for three cases. For unassembled cavity (Fig.3.5)(Case A), the resonance frequencies obtained by eigen solver is identical with theoretical resonance frequencies as shown in table 3.2. It is also found that unassembled cavity structure is not free of resonance up to 18 GHz, with the lowest mode occurring at 11.60 GHz. By incorporating the carrier plate into the cavity, eigen mode analysis is performed (Case B). The carrier plate is made of kovar material and it's layout is as shown in Fig. 3.6. The simulation results show an early onset of resonance with the addition of other structures. Next, Package/housing with LNA chip's eigen mode analysis is performed (Case C). As shown in table 3.2, mode 2 and mode 3 having a resonance frequency of 11.45 GHz and 14.6 GHz respectively can adverse the electrical performance of the LNA MMIC chips. These results validate that cavity resonance effect deviates the RF on wafer and test box test results; hence we conclude that the faced problem is because of the package/housing effect. Using eigen mode solver, it is also possible to predict the E/H field inside the cavity structure. Here for unassembled cavity structure, E and H field are observed as shown in Fig.3.5.

### Discussion and conclusion

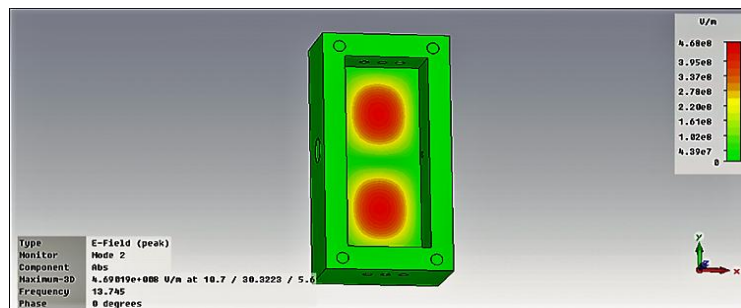
Eigen model solver technique is a simple to apply and effective technique to find out the resonance presence in the enclosed cavity structure. As shown in table 3.1 and 3.2, it has been investigated that circuit simulation results, RF on wafer measurement results and test box test data results are not matching because of the package/housing effect.



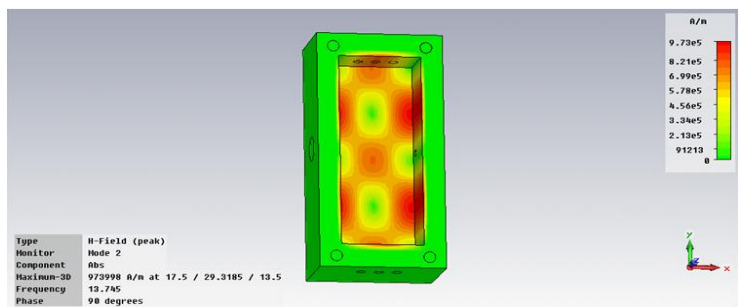
(a) Absolute E-field Mode 1 at 11.5871 GHz frequency



(b) Absolute H-field Mode 1 at 11.5871 GHz frequency



(c) Absolute E-field Mode 2 at 13.745 GHz frequency



(d) Absolute H-field Mode 2 at 13.745 GHz frequency

Figure 3.5: Case A: E/H fields for unassembled cavity structure

Table 3.2: Eigen mode simulation results for different cases of cavity structures.

Cavity profile cases	Case A	Case B	Case C
Mode 1	11.58	11.31	8.15
Mode 2	13.74	12.96	11.45
Mode 3	16.71	15.48	14.60
Mode 4	18.32	18.87	17.10
Mode 5	19.75	20.39	20.22

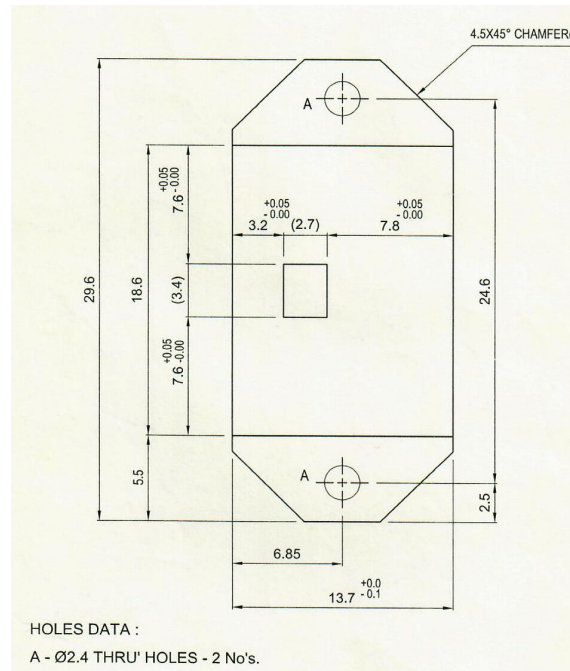
Package/housing effect degrades the performance of the LNA MMIC chip and shows the gain dip at different location in the desired band. E field and H field distribution are also analyzed using eigen mode analysis for unassembled cavity structure.

### 3.3.2 Investigation using transient mode solver

In this section, an investigation is performed using CST-MWS transient solver. The CST-MWS transient solver allows the simulation of a structure's behavior in a wide frequency range in just a single computation run. Consequently, this is an efficient solver for most driven problems. In this section, for investigating the cavity resonance problem for a given test box, active MMIC chip is replaced by its equivalent scattering parameters(S-parameters) and transient analysis are performed.

Test box which is used to model consist of an LNA MMIC chip having GaAs substrate, pre link card and post link card, biasing cards, carrier plate, package/housing, single and multilayer capacitors and gold ribbon wires. SAC,Ahmedabad have provided complete assembly details of the package/housing, carrier plate, bias cards, pre and post link cards for modeling in computational domain. Multilayer capacitor's three dimensional geometrical details or the equivalent S-parameters of the capacitors are not available, hence they are not modeled but used as lumped elements in the simulation. Model of the actual test box with a LNA MMIC chip is as shown in Fig.3.7. The Hexahedral meshing technique is used to perform the transient simulation. For investigating effects, below mentioned boundary conditions are imposed in transient simulations and transient simulations are carried out.

Nature of effect to be validate	Imposed boundary conditions on lid
Package/housing effect	PEC boundary conditions
RFOW measurement effect	CPML boundary conditions



Carrier Plate (CP) details (all dimensions are in mm)

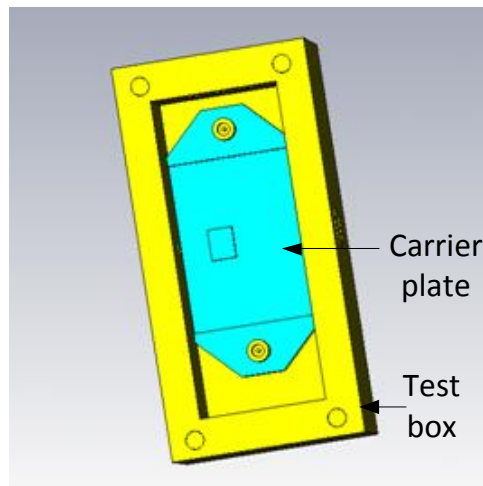


Figure 3.6: Case B : Carrier plate layout and test box with carrier plate

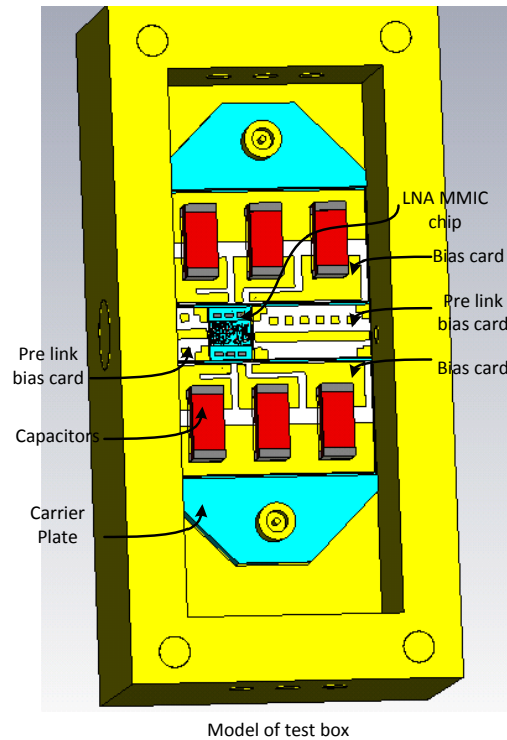


Figure 3.7: Case C : Model of test box with LNA MMIC.

### Comment on Simulation Results

The S-parameters of LNA MMIC obtained using circuit simulation is as shown in Fig. 3.8. Magnitude curve do not have glitches or dips which manifest the absence of cavity resonance effect. When PEC boundary condition is applied on the lid, results are as shown in Fig 3.9. The gain curve is having dips at many frequencies which manifest the cavity resonance effect. When Convolution Perfect Matched Layer (CPML) boundary condition is applied on the lid, results are as shown in Fig 3.10. The gain curves do not have large numbers of dips which manifest the diluting or absence of cavity resonance effect. Figure 3.11 shows the comparison of three different results; Circuit simulation results, CPML boundary conditions results and PEC boundary condition results are compared in Fig. 3.11. CPML boundary conditions results can be consider as RF on wafer measurement results which is matching with circuit simulation results. PEC boundary condition results validate the package/housing effect in an experimental test case.

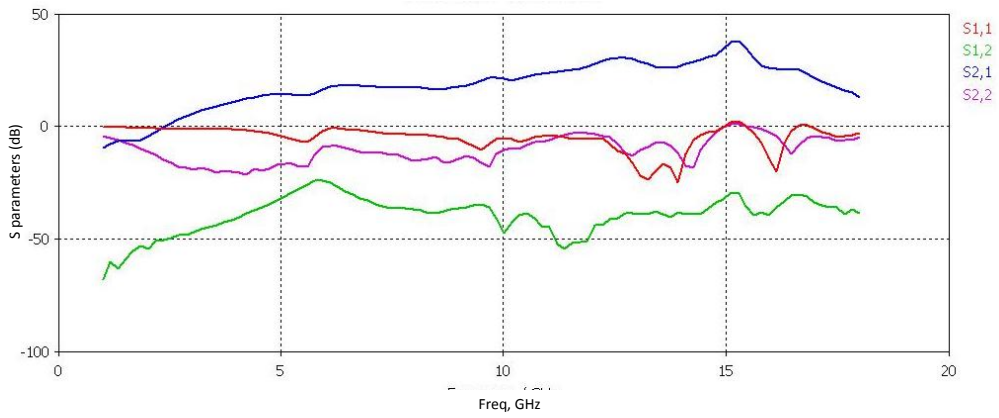


Figure 3.8: S-parameters magnitude (dB) obtained using Agilent's ADS

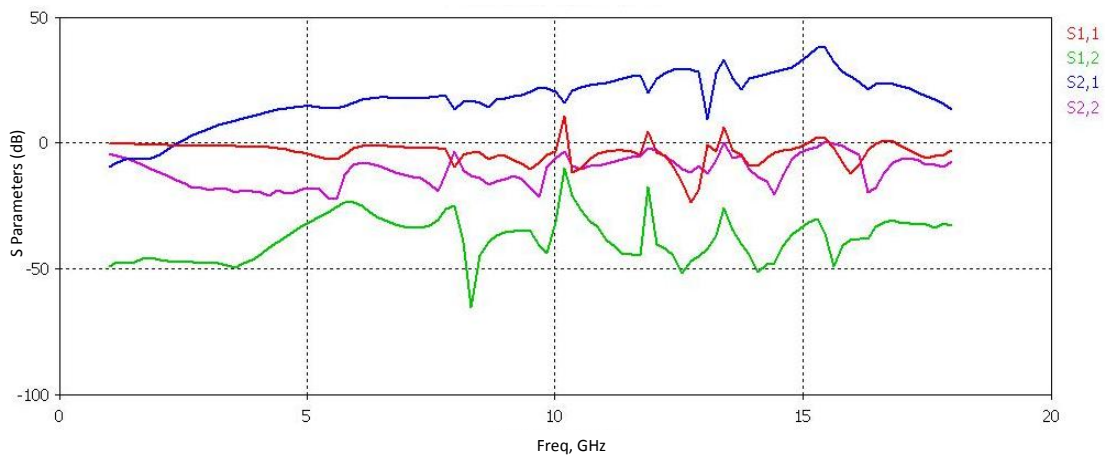


Figure 3.9: S-parameters magnitude (dB) obtained using CST MWS

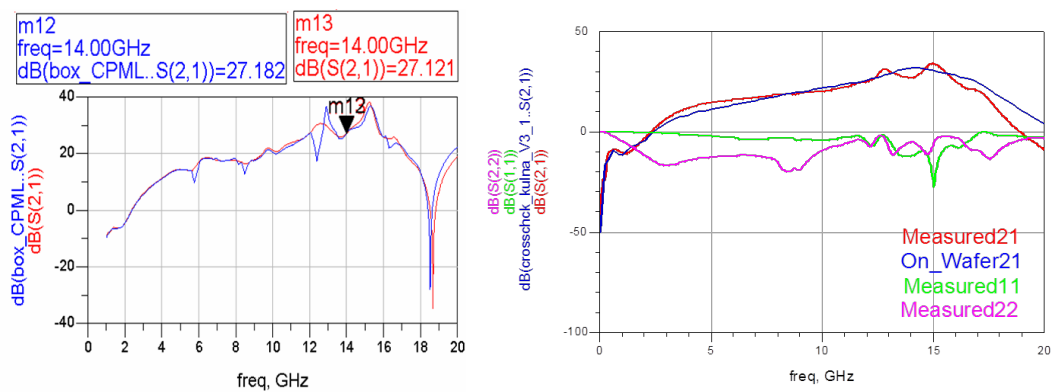


Figure 3.10: Box having CPML Boundary condition and Comparison of RFOW and measured results

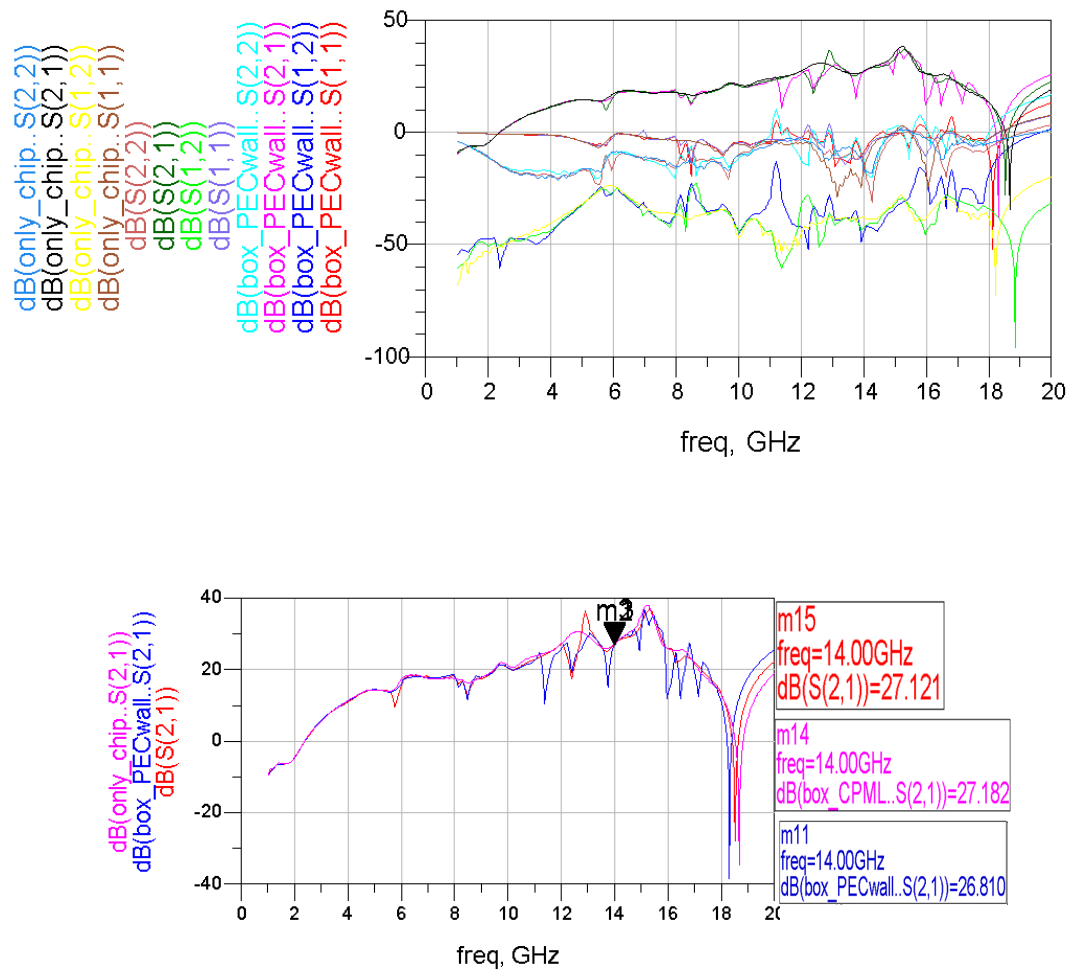


Figure 3.11: Comparison of results: validation of package/house effect by imposing different boundary conditions



Component	$S_{11}$ in ADS (dB)	$S_{11}$ in CST (dB)	$S_{21}$ in ADS (dB)	$S_{21}$ in CST (dB)
10 uF Capacitor	-16.55	-18.51	-0.09	-0.06
2 pF Capacitor	-20.13	-20.04	-0.05	-0.05
1.11 nH Inductor	-3.80	-4.44	-2.63	-2.33
1.9 nH Inductor	-1.53	-1.23	-5.75	-7.94
0.93 nH Inductor	-4.84	-5.75	-1.97	-1.64

Table 3.3: Result comparisons of few individual components of MMIC at 14 GHz

### 3.4 Modeling, simulation and analysis of active MMIC

In previous section, for investing the cavity resonance problem for a given test box, active MMIC chip is replaced by its equivalent scattering parameters (S-parameters) and transient analysis has performed. In this section, full LNA MMIC chip is modeled in 3D full wave software-CST MWS with active devices inside chip are replaced with S-parameters. Finally, transient analysis is carried out using transient solver.

An experimental test case's circuit simulation is performed in Advanced Design Software(ADS) software; layout is generated from circuit simulation. For modeling the non planner MMIC chip, CST- MWS software is used. Initially actual layout data from ADS software has been imported into CST MWS software as shown in Fig. 3.12. Different layers details, material properties, frequency range and external ports are imported, but some of the layer's details are absent in the imported layout which are also important hence the absent layers details are searched and manually healing has been done. As resistors and active devices can not simulate into CST MWS, equivalent S-parameters are used to replace them. The chip contained 18 numbers of resistors and 4 active devices, hence total no's of ports become 46 for transient simulation. Due to this, 3D layout becomes dense and complex. Transient simulation is performed for this case but the obtained full wave simulation results are not same as the circuit simulation results. For resolving this issue, as shown in Fig. 3.12, full layout have been partitioned into 3 parts which reduce no of mesh cells and hence save the simulation time. In this debugging approach, simulation time reduces but obtained results are not same as the circuit simulation results.

It may be possible that some of the layers are boolean merged while directly importing the layout into CST MWS hence GDS-II option have been selected. GDS II is a database file format which is the de facto industry standard for data exchange of integrated circuit

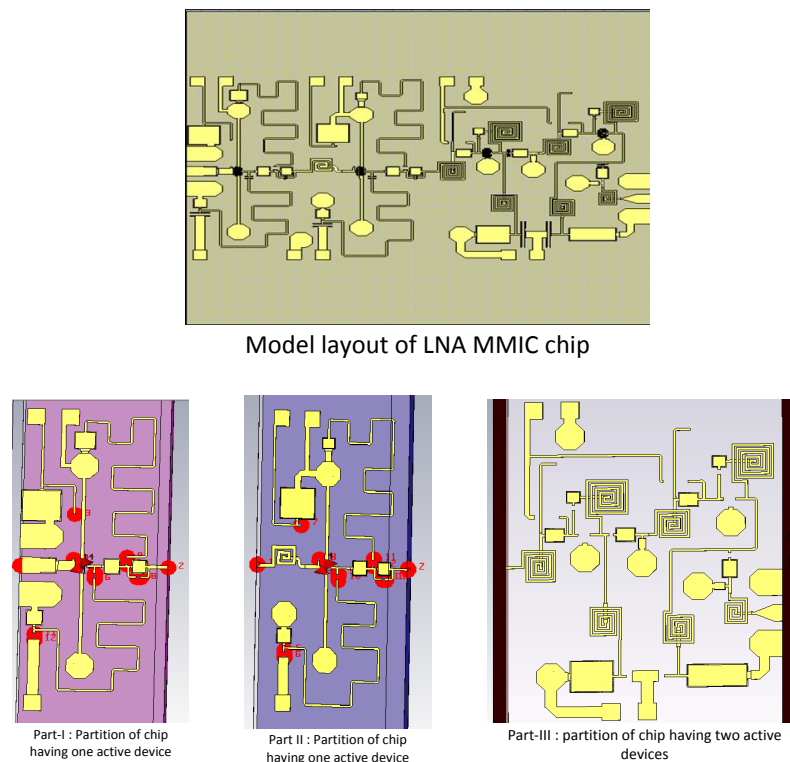


Figure 3.12: MMIC chip layouts are partitioned into 3 parts for debugging the problem, Parts are made in such a way that first two parts have one active device and last one has two active devices

or IC layout artwork. It is a binary file format representing planar geometric shapes, text labels, and other information about the layout in hierarchical form. The data can be used to reconstruct all or part of the artwork to be used in sharing layouts, transferring artwork between different tools, or creating photo masks. Using GDS-II file format, ADS generated MMIC layout has been imported in to the CST MWS, but GDS-II is a two-dimension file format so there is no lateral (height) information available in imported layout. For non planar MMIC, height of the each layer is very crucial information hence manual height information is provided by understanding the MMIC fabrication process. With this input, layout is prepared and transient simulation is performed. Due to the complex artwork of MMIC chip and manual errors, still obtained results are not matched with circuit simulation.

Now, I conclude that modeling of non planar active MMIC requires exhaustive background of MMIC fabrication process. Hence, it is mandatory to study the MMIC fabrication process and its layout. ADS software works closely with different commercial foundries to offer high-frequency Process Design Kits (PDKs) in Si, SiGe, GaAs, InP

and GaN processes. Hence, for a given experimental test case, MMIC fabrication process and its layout is studied thoroughly and decided to model the chip manually stage by stage. To model active non planar MMIC and to validate the imported layout in 3D electromagnetic are the most challenging tasks in this thesis.

In manual modeling option, initially, individual components of MMIC are modeled, simulated and compared with results obtained using ADS software. The results almost match as shown in table 3.3. Then, once again partitioned layouts have been prepared and intermediate stage results are compared. The obtained results match with ADS results as shown in Fig 3.13 and 3.14. After getting the expected results, the full LNA chip is modeled and simulated without package/housing. Results approximately match with ADS results as shown in Fig. 3.15. Deviation in result is because of the limitation of assigning mesh cells more than 1 million in CST MWS. E-Field distribution on partitioned MMIC is observed as shown in Fig. 3.14.

### Discussion and conclusion

In this section, modeling of active non planner MMIC and transient analysis of active MMIC with discontinuity in the layout is performed. For modeling the MMIC, directly ADS software to CST MWS imports option is used but due to some missing layers, this option does not work. Then Full layout has been partitioned into 3 parts for reducing the mesh cells and hence the simulation time. In this debugging approach also simulation time reduces but results are not matched with circuit simulation results. GDS-II file format option is also used but results are matched with circuit simulation results.

At last then studying the layer details of MMIC chip, individual components of MMIC are modeled, simulated and compared with results obtained using ADS. The results almost matched. And so, once again partition layout has been prepared and intermediate stage results are compared which matched with ADS results. After becoming confident with these results, the full LNA chip is modeled and simulated without package/housing. Results approximately matched with ADS. Deviation in result is because of the limitation of assigning mesh cells more than 1 million in CST MWS. E-Field, H-Field, Surface current, power density and power loss of the MMIC are studied. The simulation time is about 15 days in the CST Microwave Studio. Thus, parallel processors or special processing cards can be applied to reduce simulation time.

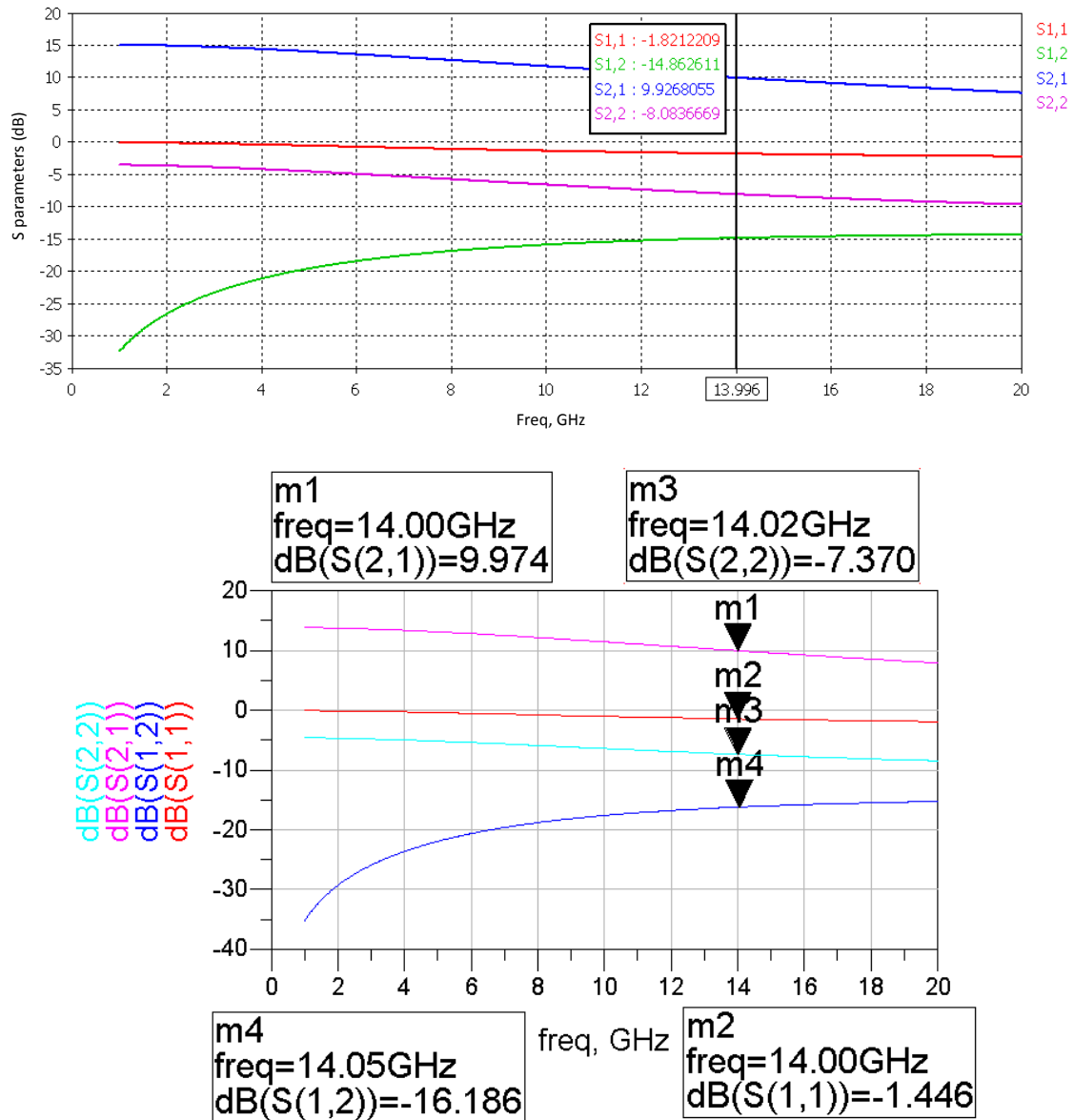


Figure 3.13: Single stage analysis includes only one active device: Comparison of 3D co-simulated transient field result and ADS circuit simulation result.

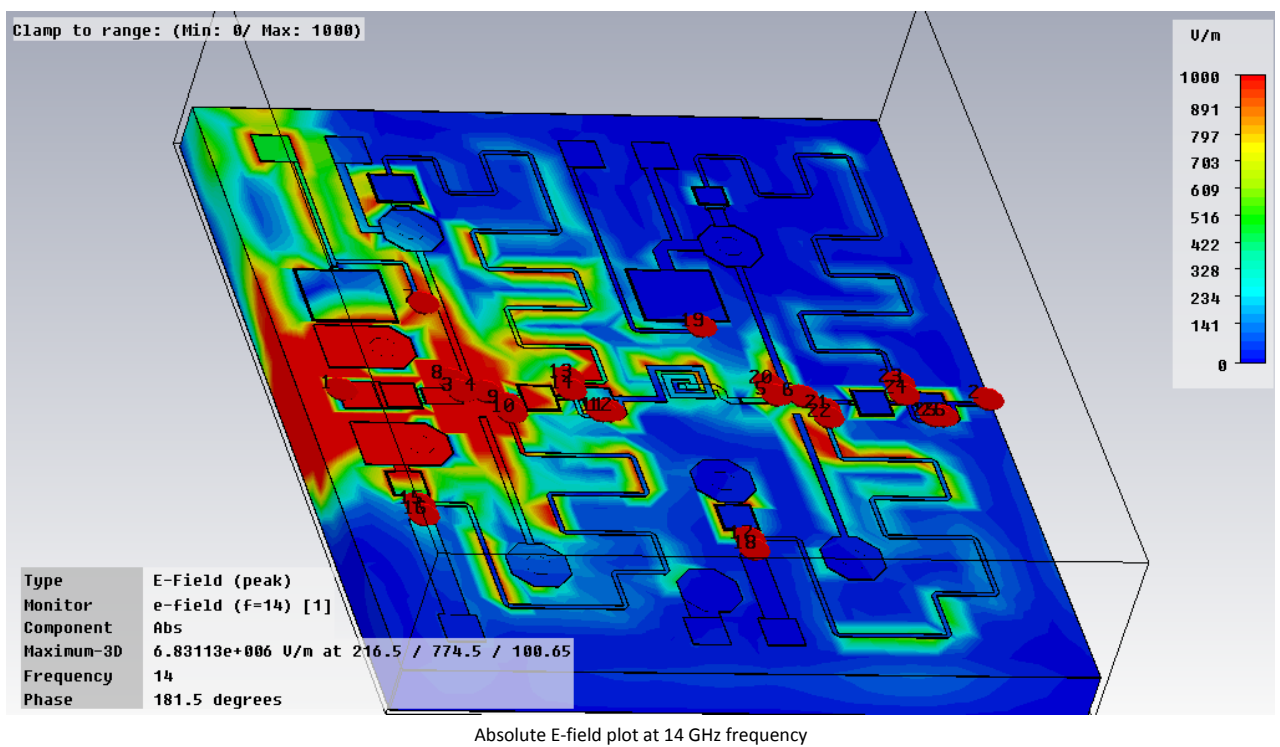
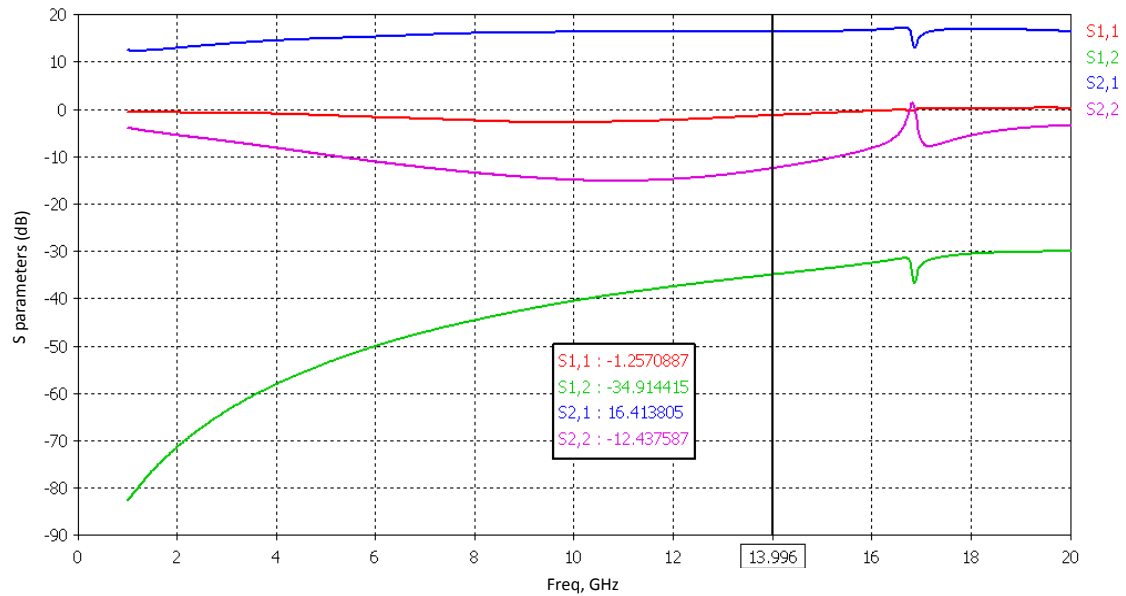


Figure 3.14: Two stage analysis includes two active devices: S-parameters and E-field distribution on partitioned chip

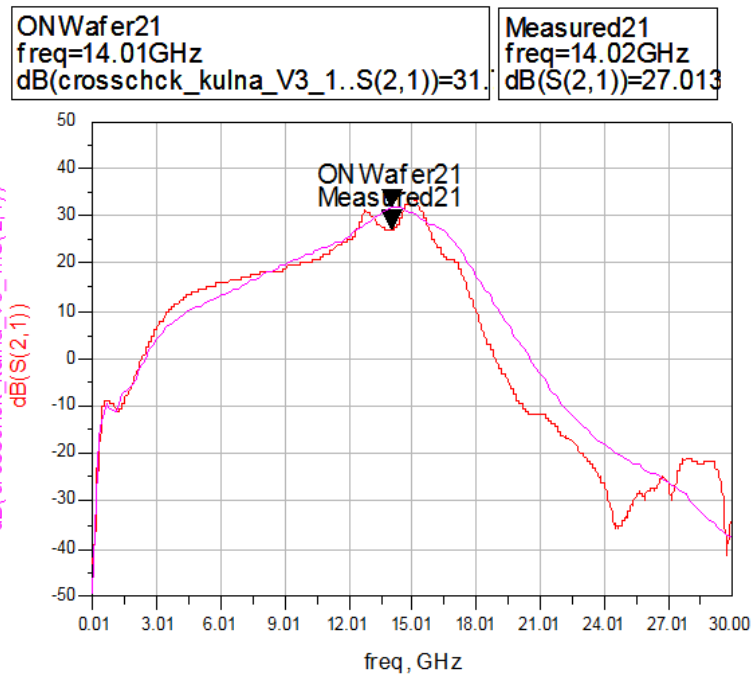
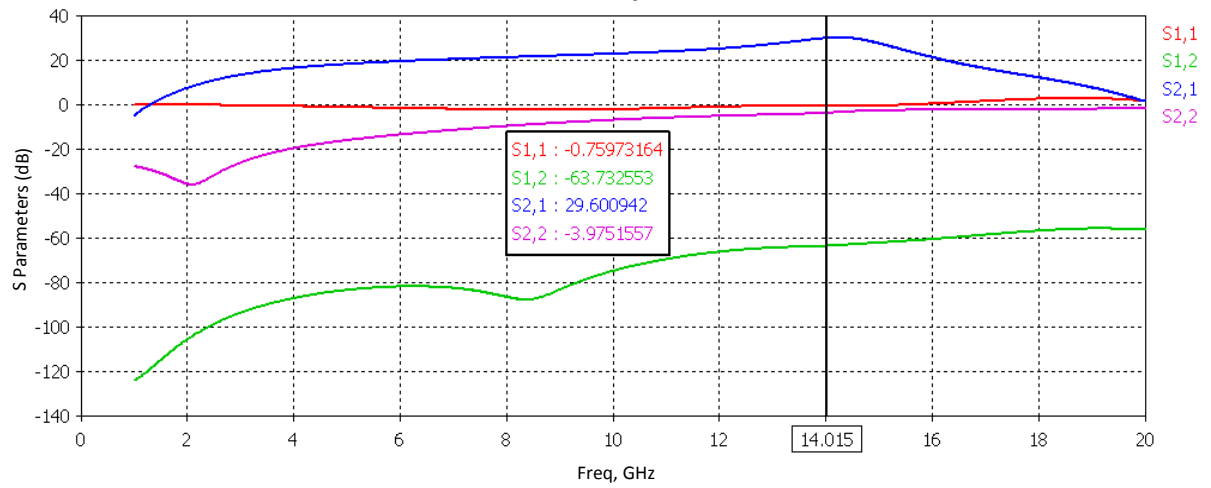


Figure 3.15: Full chip analysis: Comparison with on wafer and measured results

It was finally concluded that for this kind of huge aspect ratio problem either dedicated workstation or special GPU cards are needed to cut back the simulation time. True transient co-simulation type method which is supported by CST MWS can be used to handle active devices with MMIC chip and cavity. It is likewise necessary to note down before performing true transient co-simulation, the active device model which is used in MMIC must be available in commercial 3D software like CST Microwave Studio. It is also concluded that to reproduce the accurate layout from one tool to another tool is also the most challenging part of this thesis; hence it is recommended that software package must have both circuit simulation and 3D simulation facility in a single package.

## 3.5 Mitigation techniques

When package/housing test boxes are in design phase and not actually fabricated, various pre mitigation techniques for cavity resonance problem can be used. Pre mitigation techniques are selection of material of test box and selection of optimum test box dimensions. The selection of optimum test box dimensions is discussed in this thesis. When packages/housing test boxes are already fabricated and new design is not possible, post mitigation technique like the selection of absorber can be used. The selection of absorber technique is discussed in this thesis.

### 3.5.1 Selection of absorber

There are different types of microwave absorbers available in market. Virtually all types of the absorbers will absorb energy and solve the problem of cavity resonance. The selection of most appropriate, feasible and cost effective absorber for the problem is slightly tricky. The range of frequency which is going to be suppressed, thickness of absorber, narrowband or wideband problem, indoor or outdoor problem, types of adhesive are some of the criteria for choosing the absorber. Usually for a cavity resonance problem, a magnetically loaded absorber is recommended due to the fact that the E field goes to zero at the cavity walls while the H field is at a maximum giving a material with high magnetic loss the best absorption characteristics. In addition, the low conductivity of magnetically loaded elastomers will prevent shorting out of components if they come in contact with the absorber. Their relatively thin thickness also makes them optimal for eliminating cavity

resonances. Often, inserting a high permeability or permittivity material in the cavity will modify the characteristics of the VSWR pattern such that the EM energy being emitted by the device no longer excites the cavity. The broadband magnetically loaded microwave absorbers made of silicon can be used to convert electromagnetic energy into heat through magnetic reorientation of iron particles. These absorbers have a high magnetic loss tangent and not suitable for the wide band amplifier, as it can dampen the signal at frequency of interest. These materials have impedance equal to free space and do not reflect radiation at a normal incidence angle.

A thin, flexible, magnetically loaded, high-loss silicone rubber material that is electrically non-conductive can be placed within a cavity. It is very effective at dampening resonances due to its high permittivity and permeability. Other applications include preventing the flow of microwave currents on a metal surface. Thus, it can be applied to antenna elements, microwave dishes, the inner or outer surfaces of waveguides for isolation, attenuation or modification of radiation patterns. It will also greatly reduce the reflectivity of metal objects due to surface current flow.

Here for the given problem, commercial narrowband RF absorber- ECCOSROB SF 11-18 GHz is used for mitigating the cavity resonance problem. ECCOSROB SF 11-18 GHz is a series of thin, free space, resonant absorbers that are magnetically loaded and can reflect 1 percentage or less of normally incident energy (at least 20 dB down) at design frequencies when intimately backed to a metal surface. This type is ideally suited to applications where a thinner material is essential and broadband performance is not required. Applications include lining radar nacelles (particularly where high power is present), lining of cavity backed and shrouded telecommunication antennas, lining metal surfaces to attenuate surface currents, and for lining magnetron housings to prevent detuning. This type of absorber is placed on the cover as shown in Fig. 3.16 and simulation has been carried out. Results are as shown in Fig. 3.16. Results show that by selecting the appropriate RF absorber, packaging/housing effects can be diluted or mitigated.



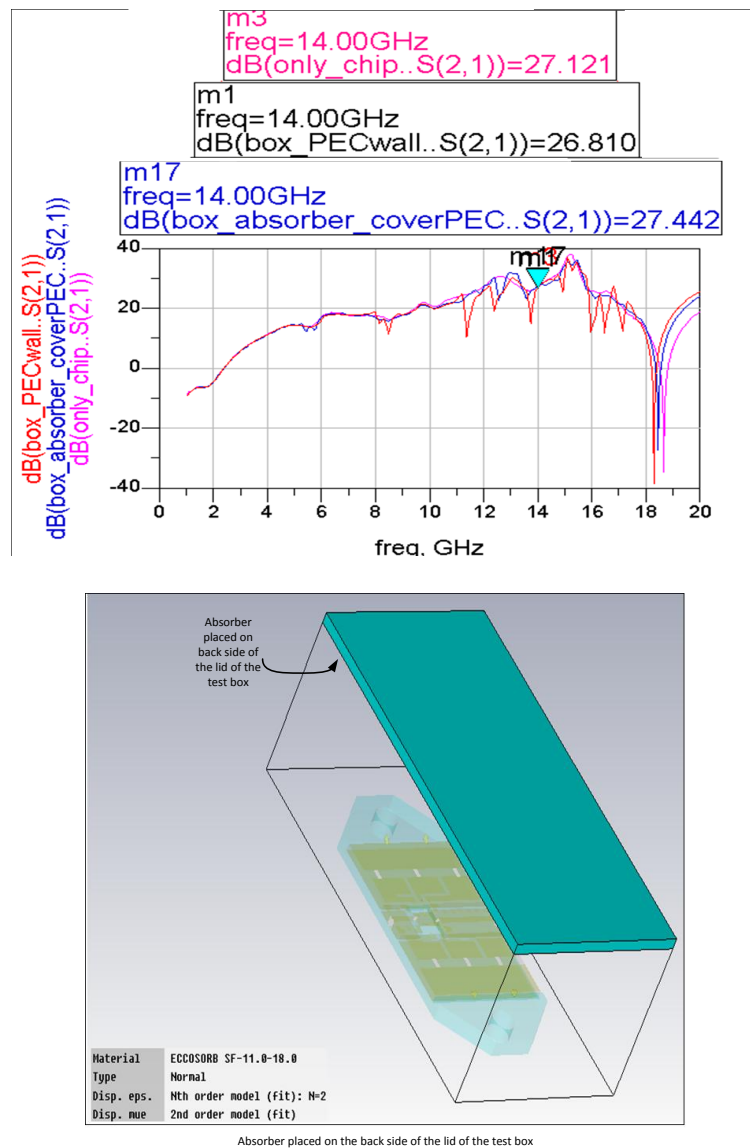


Figure 3.16: Selection of RF absorber: Comparison of results of package/housing effect (red line), without box (only chip, purple line) and box with absorber material (blue line).

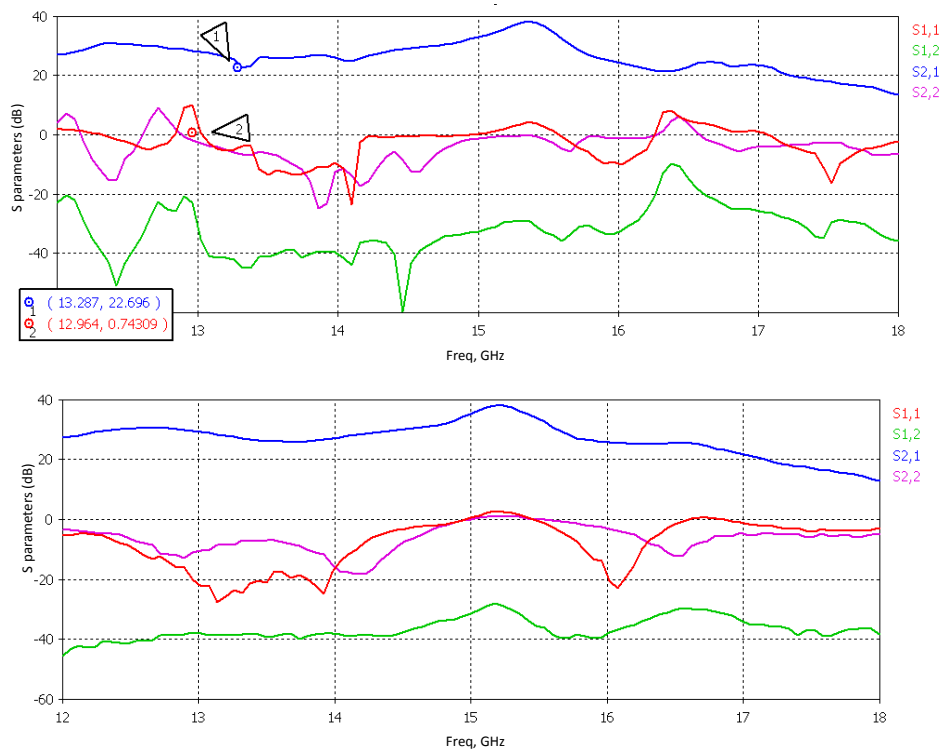


Figure 3.17: Simulation results with proposed box height(a) CST result (b) ADS result; results validate that the proposed box dimensions can be used to mitigate the cavity resonance problem.

### 3.5.2 Optimization of test box dimensions

it is evident that increase in length and width of the cavity, reduces the frequency of the cavity resonance modes. The resulting coupling effect in the desired frequency range can be eliminated by either reducing the length of the cavity or changing the excitation at the frequency region, where no resonance modes occur. As we know that the height of the cover also makes a difference in simulation and actual measurement results, hence using parametric sweep of height in simulation with an optimization goal in CST, the new height of the box is also suggested in below table. Results obtained in this simulation show almost identical with ADS simulated results Fig. 3.17.

Box dimension (present)	20x 15x9.22 mm
Box dimension (proposed)	20x15 x14.35 mm

## Chapter 4

# An efficient methodology for transient simulation of signal integrity problems

The second part of the dissertation deals transmission line effects at RF frequency (1GHz to 300GHz) in MMICs/PCBs. When signal pass through transmission line at gigahertz frequency (1GHz to 300GHz) with a picoseconds rise/fall time, the wire/interconnect/transmission line at both MMIC/Chip and package/housing level are no longer ‘electrical transparent’ to the signals and signal integrity is affected by electromagnetics effects (or called transmission line effects) such as reflection, delay, jitter, attenuation and noise. It is called a signal integrity problem. To take into account these electromagnetics effects in a time domain analysis and to integrate these effects into circuit solver, the macromodel is to be derived. The black box representation that captures electromagnetics behavior at the input/ output ports is called a macromodel. Hence, the development of an efficient macromodel and a simple procedure of embedding this macromodel into circuit solvers become necessary for transient simulation of signal integrity in the distributed passive devices in MMIC/PCB.

Any transmission line is best represented by frequency domain, but for transient simulation and to do an analysis of signal integrity problems, it is mandatory to have a time domain model which can be directly connected with transient solver, hence either from measurement or using the full wave simulator, Y parameters of giving under test

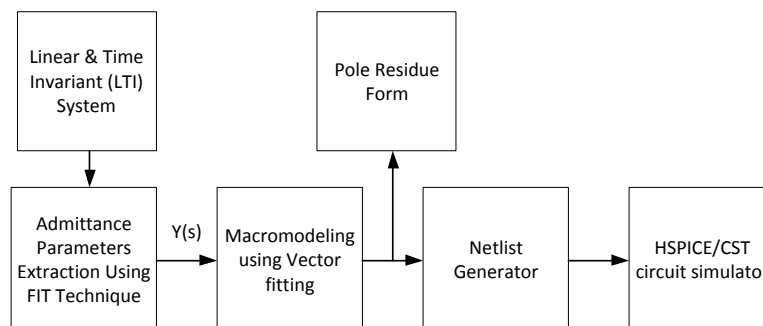


Figure 4.1: A complete proposed approach

network should be extracted. In section 4.2, FIT technique is used to extract the Y parameters of given networks. Once the admittance matrix is available, pole residue form is obtained using the vector fitting technique. In section 4.4.1, we have discussed how to embed pole residue form into circuit solver for transient simulation and analysis. In this chapter, we propose an efficient and simple approach to embed broadband frequency domain responses of passive and linear multiport networks into circuit solver using the vector fitting method for signal integrity analysis.

## 4.1 Introduction

For signal integrity analysis at high frequency, it is mandatory to develop an efficient macromodel of given broadband frequency domain response of any passive and linear multiport network and to club it into circuit solver in a simple and efficient way. There are two major issues in it. One difficulty is the mixed frequency/time domain problem and the other is the computationally expensive [21]. A traditional ordinary differential equation solver such as a SPICE-like circuit simulator cannot efficiently handle this mixed domain problem. The multi port frequency dependent networks equivalent circuit representation is highly desirable for circuit solvers [49]. In spite of the CPU expenses and convergence issues of full wave method, the full wave method can be used to extract the network property, such as its Y-parameters, Z-parameters, or S-parameters [50]. Thereafter, the macromodeling techniques [21, 42] can be used to construct macromodel from the given tabulated frequency domain data characterizing the network property of the system. A vector fitting method is a robust technique used in this dissertation for constructing

multiport macromodel from tabulated frequency domain data [42].

Y-parameter based macromodel can be used to club with Electromagnetic Transients Program (EMTP) -type circuit solvers via either an equivalent circuit [43] or convolution method [44]. Because of the accuracy problem in equivalent circuit option [45], Norton equivalent and convolution methods may be used for interfacing macro model with electromagnetic transient's simulators for multiport Y-, Z- and S-parameter-based models [51]. The disadvantage of these techniques is that they require a prior knowledge of source code of the circuit solver. As most solvers do not have a facility to club the user defined models directly, S-parameters, data have to convert into Y- parameters prior to model extraction. This approach is used in this dissertation. Tabulated frequency domain data in the form of the admittance matrix are obtained through Finite Integration Technique (FIT) which is discussed in section 4.2.

In this proposed method, prior knowledge of source code of the circuit solver is not required. Hence the proposed method is simple. Once the pole residue form is created via vector fitting, automatic net list is generated in a foster pole residue form which is then directly embedded into HSPICE or compatible circuit solvers. Equivalent circuit representation or convolution methods are not used here so the proposed method has not suffered from accuracy problem even when the circuit is having complicated interconnecting systems. Hence it is also more efficient than previous work. A complete proposed approach is as shown in Fig. 4.1. A practical example of single ended via connected with two microstrip lines is discussed which shows the validity of the proposed approach.

## 4.2 Admittance parameters extraction

The tabulated frequency domain data in the form of the admittance matrix are obtained through Finite Integration Technique (FIT). The Finite Integration Technique (FIT) provides a dual grid discretization scheme applicable to various electromagnetic problems. FIT uses following discrete set of Maxwell's Grid Equations (MGEs):

$$Ce = -\frac{d}{dt}b, \tilde{C}h = -\frac{d}{dt}d + j, \tilde{S}d = q, Sb = 0, \quad (4.1)$$

Where topological matrix  $C$  and  $\tilde{C}$  as the discrete equivalent of the analytical curl operator and discrete divergence operators  $S$  and  $\tilde{S}$ .

A method for the calculation of admittance matrix where the admittance matrix  $Y(s)$  can alternatively be transformed from its scattering  $S$ -parameters is efficient and used in this thesis. The  $S$ -parameters can also be obtained through measurement e.g. vector network analyzer.  $Y$ -parameter matrix of  $N_p$ -port subnetwork can be shown as following:

$$\begin{bmatrix} Y_{11}(\omega_k) & \cdots & Y_{1n}(\omega_k) \\ \vdots & \ddots & \vdots \\ Y_{n1}(\omega_k) & \cdots & Y_{nn}(\omega_k) \end{bmatrix} \quad (4.2)$$

where  $\omega_k = 2\pi f_k, k = 1, 2, \dots, K$  are discrete frequency points within the desired band.

### 4.3 Vector fitting technique

In the Vector Fitting Method, the objective is to identify a rational approximation of the each element of 4.2 that approximates a given broadband frequency response  $Y_{ij}(s)$  as closely as possible.

$$Y_{ij}(s) = \sum_{n=1}^N \frac{r_{n_{ij}}}{s - q_n} + d_{ij} + se_{ij} \quad (4.3)$$

denote,  $r_{n_{ij}}$  and  $q_n$  respectively, the residues and poles, both of which are complex, in general and while the terms  $d_{ij}$  and  $e_{ij}$  are real constants,  $i, j = 1, 2, \dots, N_p$ .

Vector fitting is an iterative procedure for solving 4.3. Each iteration consists of a pole identification step followed by a residue identification step with known pole. An iterative process is used to enhance accuracy, and  $Y_{ij}(s)$  converges to an optimized rational function fit.

The pole identification step requires in each iteration to solve in the least squares (LS) sense equation

$$W(s) = \sigma(s) \cdot Y_{ij}(s) = \sum_{n=1}^N \frac{\hat{r}_{n_{i,j}}}{s - \hat{q}_n} + \hat{d}_{i,j} + s\hat{e}_{i,j} \quad (4.4)$$

where

$$\sigma(s) = 1 + \sum_{n=1}^N \frac{\tilde{r}_{n_{i,j}}}{s - \tilde{q}_n} \quad (4.5)$$

Substituting 4.5 into 4.4 and for a given sample points  $M_f$ , following linear equation in

compact form can be derived:

$$\mathbf{A}_f \cdot \mathbf{u} = \mathbf{b}_f \quad (4.6)$$

where

$$\mathbf{A}_f = \begin{bmatrix} \Omega_f & & & \Omega_{f,1} \\ & \Omega_f & & \Omega_{f,2} \\ & & \ddots & \vdots \\ & & & \Omega_f & \Omega_{f,K} \end{bmatrix}$$

$$\Omega_f = \begin{bmatrix} \frac{1}{S_1 - \tilde{q}_1} & \cdots & \frac{1}{S_1 - \tilde{q}_n} & 1 & S_1 \\ \vdots & \ddots & \vdots & \vdots & \vdots \\ \frac{1}{S_{M_f} - \tilde{q}_1} & \cdots & \frac{1}{S_{M_f} - \tilde{q}_n} & 1 & S_{M_f} \end{bmatrix}$$

$$\Omega_{f,k} = \begin{bmatrix} \frac{-H_k(S_1)}{S_1 - \tilde{q}_1} & \cdots & \frac{-H_k(S_1)}{S_1 - \tilde{q}_n} \\ \vdots & \ddots & \vdots \\ \frac{-H_k(S_{M_f})}{S_{M_f} - \tilde{q}_1} & \cdots & \frac{-H_k(S_{M_f})}{S_{M_f} - \tilde{q}_n} \end{bmatrix}$$

$$\mathbf{u} = \left[ u_1^T \cdots u_k^T \tilde{u}^T \right]^T$$

$$\mathbf{u}_k = \left[ \hat{r}_{1,k} \cdots \hat{r}_{N,k} d_k e_k \right]^T$$

$$\tilde{u} = \left[ \tilde{r}_1 \cdots \tilde{r}_N \right]^T$$

$$\tilde{\mathbf{b}}_f = \left[ \tilde{b}_{f,1}^T \cdots \tilde{b}_{f,k}^T \right]^T$$

$$\tilde{b}_{f,k} = \left[ H_k(S_1) \cdots H_k(S_{M_f}) \right]^T$$

where  $k=1,2,\dots,K$ .

Solving the least squares problem of 4.6, the coefficients of  $\sigma(s)$  and product of  $\sigma(s) \cdot Y_{ij}(s)$  are obtained.  $Y_{ij}(s)$  can be expressed as  $Y_{ij}(s) = \frac{W(s)}{\sigma(s)}$ , which shows that poles of  $Y_{ij}(s)$  coincides with the zeros of  $\sigma(s)$ . The zeros of  $\sigma(s)$  are calculated from  $\mathbf{u}$ , which are calculated as the eigenvalues of the matrix

$$\mathbf{H} = \mathbf{A} - \mathbf{b} \tilde{u}^T \quad (4.7)$$

where  $\mathbf{A}$  is a diagonal  $\sigma(s)$  matrix containing the starting poles,  $\mathbf{b}$  is a column vector of ones and  $\tilde{u}^T$  is a row-vector containing the residues for  $\sigma(s)$ .

The second step is the calculation of the residues of  $Y_{ij}(s)$ . In principle, it can be directly obtained from 4.6; instead, equation 4.3 is solved with the obtained zeros of  $\sigma(s)$ , which again constitutes a least squares problem to improve accuracy, and the residues of  $Y_{ij}(s)$  are computed. An iterative process is used to enhance accuracy, and  $Y_{ij}(s)$  converges to an optimized rational function fit.

## 4.4 Inclusion of macromodel into circuit solver

There are basically two ways to incorporate the macromodel of distributed interconnect structures into circuit simulators (1) synthesize the equivalent circuit using basic circuit elements of the circuit simulator, or (2) use recursive convolution. In this chapter, we present the application of (1) techniques for interfacing rational function approximations of the Y parameter with SPICE.

### 4.4.1 Foster pole residue representation

Once the macro model of the given network is created as described in the preceding section, for embedding macromodel into HSPICE or compatible circuit solvers, following syntaxes in Foster Pole-Residue form is used [52]. Transconductance  $G(s)$  form:

$$G_{xxx} \ n + \ n - FOSTER \ in + \ in - k_0 \ k_1 + (ReA_1, ImA_1)/(Rep_1, Imp_1) \\ + (ReA_2, ImA_2)/(Rep_2, Imp_2) + (ReA_3, ImA_3)/(Rep_3, Imp_3) \dots \dots \quad (4.8)$$

A pole-residue pair is represented by four numbers - real and imaginary part of the residue, then real and imaginary part of the pole. We must make sure that  $Re[p_i] < 0$ ; otherwise, the simulations will certainly diverge. For example, to represent  $G(s)$  in the



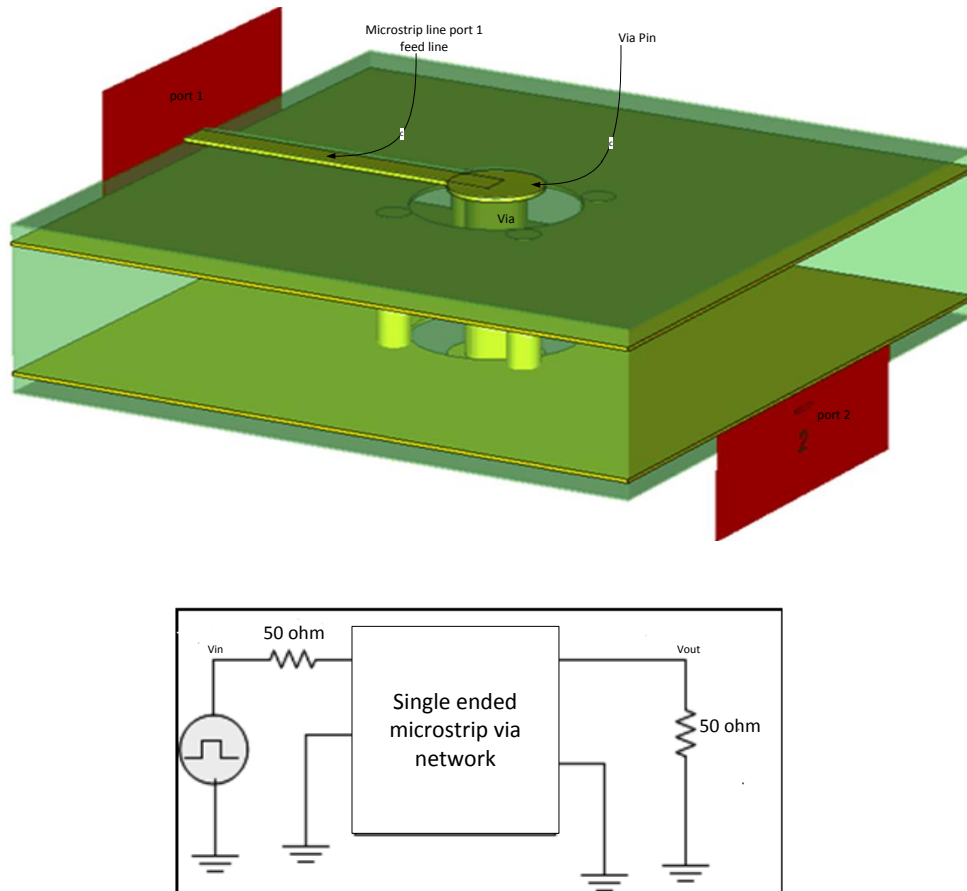


Figure 4.2: (a) Model of single ended via connecting with two microstrip lines (b) Schematic circuit diagram of the test model; Two-port network having source and load

forms of equation 4.9,

$$G(s) = 0.001 + 1 \times 10^{-12}s + \frac{0.0008}{s + 1 \times 10^{10}} + \frac{0.001 - j0.006}{s - (-1 \times 10^8 + j1.8 \times 10^{10})} + \frac{0.001 + j0.006}{s - (-1 \times 10^8 - j1.8 \times 10^{10})} \quad (4.9)$$

We will input in the net list file as: G1 1 0 FOSTER 2 0 0.001 1e-12+ (0.0004, 0)/ (-1e10, 0) (0.001, -0.006)/ (-1e8, 1.8e10).

The netlist file can be prepared as per above form for each elements of 4.2. This net list file can be well inserted into HSPICE or its compatible circuit solvers for transient simulation.

## 4.5 Numerical results

The Printed Circuit Boards (PCBs) may hold large numbers of discontinuities, and their presence causes signal distortion problems. For this reason, an accurate modeling of discontinuities at PCB level is essential for signal integrity (SI) analysis. A suggested methodology is validated for a simple via hole connecting with microstripes in multilayer PCB. A single ended via connected with two microstrip lines is shown in Fig. 4.2.  $Y$ -parameter matrix of this network is extracted by Finite Integration Technique (FIT) using CST Microwave Studio (MWS). The example network is having input and output port, port 1 and port 2 respectively. In FIT, for transient simulation, Gaussian pulse source and ABC boundary condition are applied. Each element of the  $Y$ -parameter matrix is approximated with the vector fitting method. 50 poles, including 10 real and 40 complex conjugate poles are drawn out to meet the parameters of the test network up to 6 GHz. Good agreements can be observed in Fig. 4.3 between the FIT simulated  $Y$ -parameters and the macromodel  $Y$ -parameters based on the vector fitting method. For embedding the macromodel into circuit solvers, netlist file which is the equivalent sub circuit in time domain, is automatically created and inserted into HSPICE or equivalent circuit simulator by the proposed approach in this thesis. Obtained time domain model is employed to perform the transient analysis of simple via hole in multilayer PCBs. The conventional circuit is having 50 ohm source and 50 ohm load impedance at port 1 and 2 respectively as shown in Fig. 4.2. The circuit is excited at port 1 by a pulse having a rise/fall time of 0.02 ns and a pulse width of 4 ns and transient simulation is performed. Transient simulation results are shown in Fig.4.4. The result indicates that the line is ringing with overshoots.

## 4.6 Conclusion and discussion

The second piece of dissertation proposes an efficient and uncomplicated access to embed broadband frequency domain responses of passive and linear networks into circuit solver using the vector fitting method. In this thesis, systematic methodology is discussed and details of embedding the macromodel into circuit solver are described. Single ended via connected with two microstrip lines test case is presented which validate that the

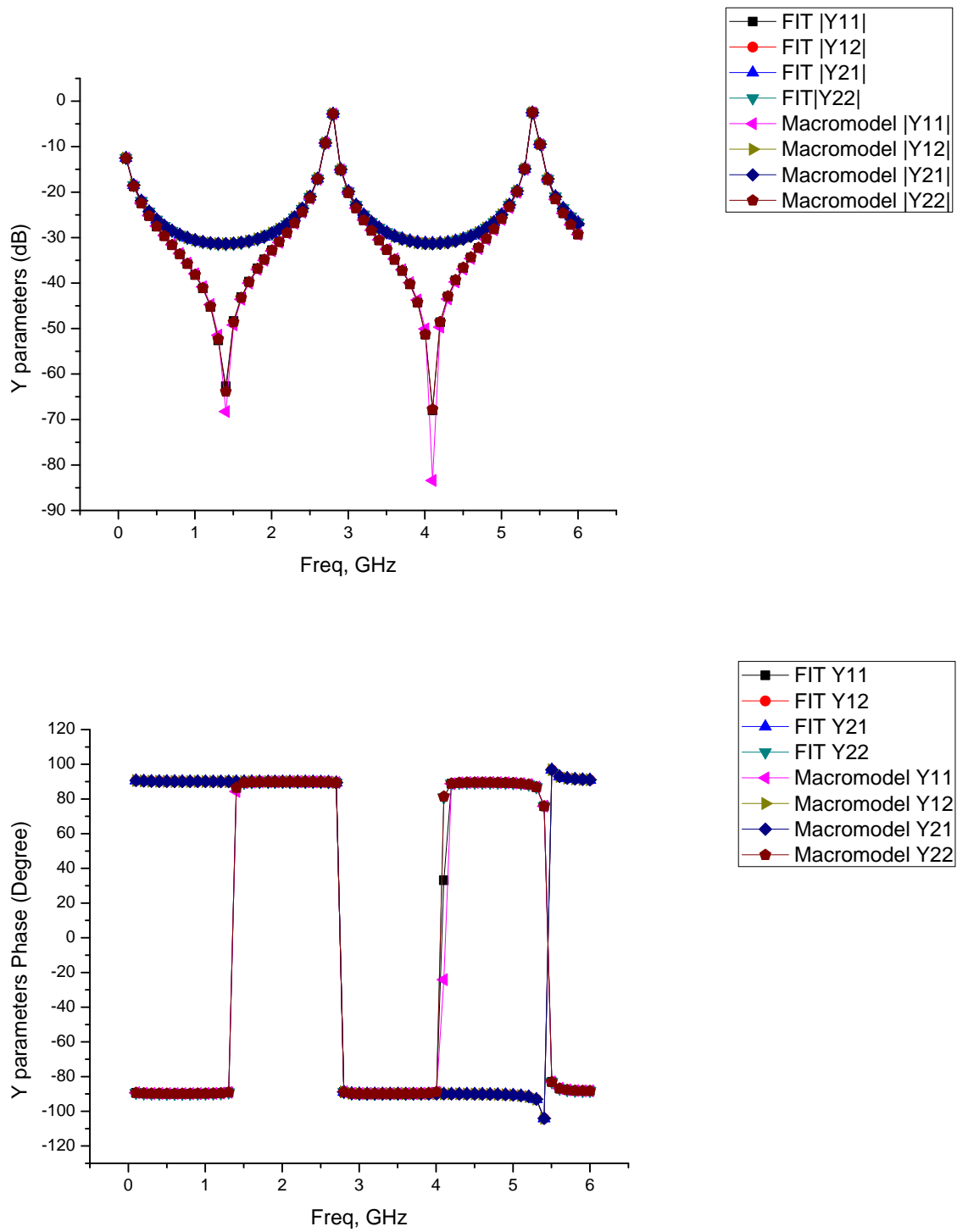


Figure 4.3: Y parameters of the single ended via simulated by FIT in CST MWS and Vector Fitting method. (a) Magnitude. (b) Phase

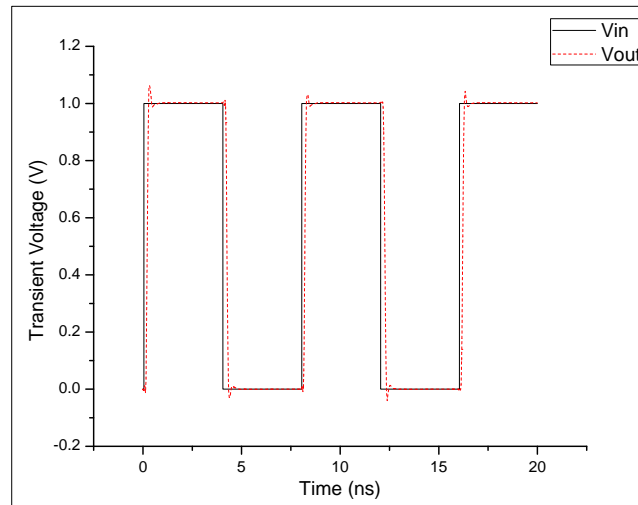


Figure 4.4: Transient voltage waveforms: (a) at port 1 denoted as  $V_{in}$  and at port 2 denoted as  $V_{out}$ .

suggested approach is desirable for a transmission line, high speed interconnects as well on board discontinues such as via holes. A practical test case indicates that the analysis of signal integrity for complicated interconnecting systems can be done efficiently. Ideally, any passive and linear microstrip circuit can be studied and transient simulation can be executed utilizing the proposed approach before its real execution, so the design cost and time will be concentrated. In future, the proposed method can be used to perform the transient simulation of variety of EMC-EMI, Signal Integrity and Power Integrity problems in the high-speed complex hybrid interconnect and lumped circuit systems.

# Chapter 5

## Conclusions and scope of further work

### 5.1 Conclusions

The thesis proposes efficient methodologies for two major issues encountered in design and testing of gigahertz systems having Monolithic Microwave Integrated Circuit (MMIC): package/housing effect and signal integrity problems.

The first part of the thesis discusses packaging/housing effect. Presently there is no CAD tool available to predict active MMIC performance in a cavity. The thesis presents an EM field analysis of active MMIC and packaging/housing effect on active MMIC. An experimental test case is used here to investigate and analyze the package/housing effect. Low Noise Amplifier (LNA) MMIC is used as an experimental test case. In this thesis, the theoretically cavity resonance problem is studied. The cavity resonance problem is investigated for the experimental test case using Eigen mode solver and transient solver. Eigen mode solver technique is very robust and easy to find out the resonance, presence in the enclosed cavity structure. It has been investigated that circuit simulation results, RF on wafer measurement results and test box test data results are not matching because of the package/housing effect. Package/housing effect degrades the performance of the LNA MMIC chip and shows the gain dip at different locations in the desired band. E field and H field distribution are also analyzed using Eigen mode analysis. In the section [3.3.2](#), for investigating the cavity resonance problem for a given test box, active MMIC chip is

replaced by its equivalent scattering parameters(S-parameters) and transient analysis are performed. CPML boundary conditions results can be consider as RF on wafer measurement results which is matching with circuit simulation results. PEC boundary condition results validate the package/housing effect in an experimental test case.Next,active non planar MMIC is modeled, simulated and analyzed the E/H field distribution due to the discontinuity presence in active MMIC. In the section 3.4, modeling of active non planer MMIC and transient analysis of active MMIC with discontinuity in the layout is performed. For modeling the MMIC, directly ADS software to CST MWS imports option is used but due to some missing layers, this option does not work. Then Full layout has been partitioned into 3 parts for reducing the mesh cells and for keeping the simulation time without losing result accuracy. In this debugging approach also simulation time reduces but results are not expected. GDS-II file format option is also used but results are not expected. At last then studying the layer details of MMIC chip, individual components of MMIC are modeled, simulated and compared with results obtained using ADS. Now the results almost matched. And so, once again partition layout has been prepared and intermediate stage results are compared which matched with ADS results. After becoming confident with these results, the full LNA chip is modeled and simulated without package/housing. Results approximately matched with ADS. Deviation in result is because of the limitation of assigning mesh cells more than 1 million in CST MWS. E-Field, H-Field, Surface current, power density and power loss of the MMIC are studied. In post mitigation technique, we modified package dimensions and proposed packaged geometry whose test box test results are matched with circuit simulation and RFOV results. Commercially available RF absorbers are studied and appropriate RF absorber is used to mitigate the package/housing effect.

The second part of dissertation proposes an efficient and uncomplicated access to embed broadband frequency domain responses of passive and linear networks into circuit solver using the vector fitting method. In this thesis, systematic methodology is discussed and details of embedding the macromodel into circuit solver are described. Single ended via connected with two microstrip lines test case is presented which demonstrating that the suggested approach is desirable for a transmission line, high speed interconnects as well on board discontinues such as via holes. A practical test case indicates that the analysis of signal integrity for complicated interconnecting systems can be done efficiently.

Ideally, any passive and linear microstrip circuit can be studied and transient simulation can be executed utilizing the proposed approach before its real execution, so the design cost and time will be concentrated.

## 5.2 Scope of further work

- The full wave simulation is performed on laptop having 2GB RAM and intel 2GHz Processor. Still the simulation time is about 15 days in the CST Microwave Studio (MWS) for analysis of packaging/housing effect with a full active MMIC chip. Hence it is concluded that for this type of huge aspect ratio problem either dedicated supercomputer or special GPU cards are needed to cut back the simulation time.
- True transient co-simulation type method which is supported by CST Microwave Studio can be used to handle active devices with MMIC chip and cavity.
- It is likewise necessary to note down before performing true transient co-simulation, the active device model which is used in MMIC must be usable in commercial 3D software like CST Microwave Studio.
- It is also concluded that to reproduce the accurate layout from one tool to another tool is also the most challenging part of this thesis, hence it is recommended that software package must have both circuit simulation and 3D simulation facility in a single package.
- In future, the second part of the proposed work can be used to perform the transient simulation of variety of EMC-EMI, Signal Integrity and Power Integrity problems in the high-speed complex hybrid interconnect and lumped circuit systems.

# Bibliography

- [1] F. Ishitsuka and N. Sato, “Low-cost, high-performance package for a multi-chip mmic module,” *10th Annual IEEE Gallium Arsenide Integrated Circuit (GaAs IC) Symposium*, pp. 221–224, 1988.
- [2] F. Ishitsuka, “A new multilayer ceramic-frame package for high-frequency mmic modules,” *IEICE Transactions on Electronics*, vol. 74, no. 8, pp. 2344–2348, 1991.
- [3] G. Robinson, “Resonant frequency calculations for microstrip cavities (correspondence),” *Microwave Theory and Techniques, IEEE Transactions on*, vol. 19, no. 7, pp. 665–666, Jul 1971.
- [4] B. Hallford and C. Bach, “Lid interaction protected shield enclosed dielectric mounted microstrip,” *US Patent 3,638,148*, Jan 1972.
- [5] D. Williams, “Damping of the resonant modes of a rectangular metal package [mmics],” *Microwave Theory and Techniques, IEEE Transactions on*, vol. 37, no. 1, pp. 253–256, Jan 1989.
- [6] A. Armstrong and P. Cooper, “Techniques for investigating spurious propagation in enclosed microstrip,” *Radio and Electronic Engineer*, vol. 48, no. 1.2, pp. 64–72, Jan 1978.
- [7] R. Jansen and L. Wiemer, “Full-wave theory based development of mm-wave circuit models for microstrip open end, gap, step, bend and tee,” *IEEE MTT-S International Microwave Symposium Digest*, vol. 2, pp. 779–782, June 1989.
- [8] J. Burke and R. Jackson, “Reduction of parasitic coupling in packaged mmics,” *IEEE MTT-S International Microwave Symposium Digest*, vol. 1, pp. 255–258, May 1990.



- 
- [9] R. Jackson, "The use of side wall images to compute package effects in mom analysis of mmic circuits," *Microwave Theory and Techniques, IEEE Transactions on*, vol. 41, no. 3, pp. 406–414, Mar 1993.
- [10] P. Mezzanotte, M. Mongiardo, L. Roselli, R. Sorrentino, and W. Heinrich, "Analysis of packaged microwave integrated circuits by fdtd," *Microwave Theory and Techniques, IEEE Transactions on*, vol. 42, no. 9, pp. 1796–1801, Sep 1994.
- [11] C.-N. Kuo, B. Houshmand, and T. Itoh, "Full-wave analysis of packaged microwave circuits with active and nonlinear devices: an fdtd approach," *Microwave Theory and Techniques, IEEE Transactions on*, vol. 45, no. 5, pp. 819–826, May 1997.
- [12] R. Faraji-Dana and Y. Chow, "Accurate and efficient cad tool for the design of optimum packaging for (m)mics," *Microwaves, Antennas and Propagation, IEE Proceedings*, vol. 142, no. 2, pp. 81–88, Apr 1995.
- [13] H. Chen and Y.-X. Zhang, "A synthetic design of eliminating crosstalk within mtls," *Progress In Electromagnetics Research*, vol. 76, pp. 211–221, 2007.
- [14] F. Xiao and Y. Kami, "Modeling and analysis of crosstalk between differential lines in high-speed interconnects," *PIERS Online*, vol. 3, no. 8, pp. 1293–1297, 2007.
- [15] P. Bernardi, R. Cicchetti, G. Pelosi, A. Reatti, S. Selleri, and M. Tatini, "An equivalent circuit for emi prediction in printed circuit boards featuring a straight-to-bent microstrip line coupling," *Progress In Electromagnetics Research B*, vol. 5, pp. 107–118, 2008.
- [16] J. Dhar, R. K. Arora, A. Dasgupta, and S. Rana, "Enclosure effect on microwave power amplifier," *Progress In Electromagnetics Research C*, vol. 19, pp. 163–177, 2011.
- [17] S. Chaturvedi, S. V. Bhalke, G. Sai Saravanan, and S. K. Koul, "Electromagnetic simulation and characterization a metal ceramic package for packaging of high isolation switches," *Progress In Electromagnetics Research C*, vol. 16, pp. 111–125, 2010.
- [18] C.-W. Ho, A. E. Ruehli, and P. A. Brennan, "The modified nodal approach to network analysis," *Circuits and Systems, IEEE Transactions on*, vol. 22, no. 6, pp. 504–509, 1975.

- 
- [19] A. F. Peterson, S. L. Ray, R. Mittra, I. of Electrical, and E. Engineers, *Computational methods for electromagnetics*. IEEE press New York, 1998.
- [20] A. E. Ruehli and A. C. Cangellaris, "Progress in the methodologies for the electrical modeling of interconnects and electronic packages," *Proceedings of the IEEE*, vol. 89, no. 5, pp. 740–771, 2001.
- [21] R. Achar and M. Nakhla, "Simulation of high-speed interconnects," *Proceedings of the IEEE*, vol. 89, no. 5, pp. 693–728, May 2001.
- [22] A. Taflove and S. C. Hagness, "Computational electro-dynamics," *Artech house*, 2000.
- [23] M. N. Sadiku, *Numerical techniques in electromagnetics*. CRC press, 2000.
- [24] A. E. Ruehli, "Equivalent circuit models for three-dimensional multiconductor systems," *Microwave Theory and Techniques, IEEE Transactions on*, vol. 22, no. 3, pp. 216–221, 1974.
- [25] L. T. Pillage, R. Rohrer *et al.*, "Asymptotic waveform evaluation for timing analysis," *Computer-Aided Design of Integrated Circuits and Systems, IEEE Transactions on*, vol. 9, no. 4, pp. 352–366, 1990.
- [26] T. K. Tang and M. S. Nakhla, "Analysis of high-speed vlsi interconnects using the asymptotic waveform evaluation technique," *Computer-Aided Design of Integrated Circuits and Systems, IEEE Transactions on*, vol. 11, no. 3, pp. 341–352, 1992.
- [27] J. E. Bracken, V. Raghavan, R. Rohrer *et al.*, "Interconnect simulation with asymptotic waveform evaluation (awe)," *Circuits and Systems I: Fundamental Theory and Applications, IEEE Transactions on*, vol. 39, no. 11, pp. 869–878, 1992.
- [28] D. F. Anastasakis, N. Gopal, S.-Y. Kim, and L. T. Pillage, "Enhancing the stability of asymptotic waveform evaluation for digital interconnect circuit applications," *Computer-Aided Design of Integrated Circuits and Systems, IEEE Transactions on*, vol. 13, no. 6, pp. 729–736, 1994.
- [29] E. Chiprout and M. S. Nakhla, "Analysis of interconnect networks using complex frequency hopping (cfh)," *Computer-Aided Design of Integrated Circuits and Systems, IEEE Transactions on*, vol. 14, no. 2, pp. 186–200, 1995.

- 
- [30] P. Feldmann and R. W. Freund, "Efficient linear circuit analysis by padé approximation via the lanczos process," *Computer-Aided Design of Integrated Circuits and Systems, IEEE Transactions on*, vol. 14, no. 5, pp. 639–649, 1995.
- [31] K. J. Kerns and A. T. Yang, "Preservation of passivity during rlc network reduction via split congruence transformations," *Computer-Aided Design of Integrated Circuits and Systems, IEEE Transactions on*, vol. 17, no. 7, pp. 582–591, 1998.
- [32] A. Odabasioglu, M. Celik, and L. T. Pileggi, "Prima: passive reduced-order interconnect macromodeling algorithm," *Proceedings of the IEEE/ACM international conference on Computer-aided design, IEEE Computer Society*, pp. 58–65, 1997.
- [33] Q. Yu, J. M. L. Wang, and E. S. Kuh, "Passive multipoint moment matching model order reduction algorithm on multiport distributed interconnect networks," *Circuits and Systems I: Fundamental Theory and Applications, IEEE Transactions on*, vol. 46, no. 1, pp. 140–160, 1999.
- [34] R. Achar, P. K. Gunupudi, M. Nakhla, and E. Chiprout, "Passive interconnect reduction algorithm for distributed/measured networks," *Circuits and Systems II: Analog and Digital Signal Processing, IEEE Transactions on*, vol. 47, no. 4, pp. 287–301, 2000.
- [35] W. T. Beyene and J. E. Schutt-Ainé, "Accurate frequency-domain modeling and efficient circuit simulation of high-speed packaging interconnects," *Microwave Theory and Techniques, IEEE Transactions on*, vol. 45, no. 10, pp. 1941–1947, 1997.
- [36] W. T. Beyene and J. E. Schutt-Aine, "Efficient transient simulation of high-speed interconnects characterized by sampled data," *Components, Packaging, and Manufacturing Technology, Part B: Advanced Packaging, IEEE Transactions on*, vol. 21, no. 1, pp. 105–114, 1998.
- [37] K. L. Choi and M. Swaminathan, "Development of model libraries for embedded passives using network synthesis," *Circuits and Systems II: Analog and Digital Signal Processing, IEEE Transactions on*, vol. 47, no. 4, pp. 249–260, 2000.
- [38] M. Elzinga, K. L. Virga, and J. L. Prince, "Improved global rational approximation macromodeling algorithm for networks characterized by frequency-sampled data,"

- Microwave Theory and Techniques, IEEE Transactions on*, vol. 48, no. 9, pp. 1461–1468, 2000.
- [39] W. T. Beyene, “Improving time-domain measurements with a network analyzer using a robust rational interpolation technique,” *Microwave Theory and Techniques, IEEE Transactions on*, vol. 49, no. 3, pp. 500–508, 2001.
- [40] S. Chakravorty, S.-H. Min, and M. Swaminathan, “Comparison between chebyshev and power series expansion functions for interpolating data,” *Electrical Performance of Electronic Packaging, IEEE*, pp. 153–156, 2001.
- [41] S.-H. Min and M. Swaminathan, “Efficient construction of two-port passive macro-models for resonant networks,” *10th Topical Meeting on Electrical Performance of Electronic Packaging, IEEE*, pp. 229–232, 2001.
- [42] B. Gustavsen and A. Semlyen, “Rational approximation of frequency domain responses by vector fitting,” *Power Delivery, IEEE Transactions on*, vol. 14, no. 3, pp. 1052–1061, Jul 1999.
- [43] A. Morched, J. Ottevangers, and L. Marti, “Multi-port frequency dependent network equivalents for the emtp,” *Power Delivery, IEEE Transactions on*, vol. 8, no. 3, pp. 1402–1412, July 1993.
- [44] B. Gustavsen and O. Mo, “Interfacing convolution based linear models to an electromagnetic transients program,” *Proc. Int. Conf. Power Systems Transients*, pp. 4–7, 2007.
- [45] A. C. Lima, B. Gustavsen, and A. B. Fernandes, “Inaccuracies in network realization of rational models due to finite precision of rlc branches,” *Int. conf. on Power Syst. Transients*, pp. 4–7, 2007.
- [46] R. S. J-G. Yook, L.P.B. Katehi and K. Shalkhauser, “Experimental and theoretical study of parasitic leakage/resonance in a k/ka- band mmic package,” *IEEE MTT-S Inter.Microwave Symp. Dig.*, June 1996.
- [47] *GaAs IC ED02AH design manual*. Philips, pp. 10-11 , 2003.
- [48] D. M. Pozar, *Microwave engineering*. John Wiley & Sons, pp. 278-279, 2009.

- 
- [49] G. Antonini, "Spice equivalent circuits of frequency-domain responses," *Electromagnetic Compatibility, IEEE Transactions on*, vol. 45, no. 3, pp. 502–512, Aug 2003.
- [50] E.-X. Liu, E.-P. Li, L.-W. Li, and Z. Shen, "Finite-difference time-domain macro-model for simulation of electromagnetic interference at high-speed interconnects," *Magnetics, IEEE Transactions on*, vol. 41, no. 1, pp. 65–71, Jan 2005.
- [51] B. Gustavsen and H. De Silva, "Inclusion of rational models in an electromagnetic transients program: Y-parameters, z-parameters, s-parameters, transfer functions," *Power Delivery, IEEE Transactions on*, vol. 28, no. 2, pp. 1164–1174, April 2013.
- [52] *Star-HSPICE Manual*. Release 1998.2, pp. 26.4-26.44 , July 1998.

## List of Publications

1. A. Sarvaiya, S. Gupta, and D. Ghodgaonkar, "Interaction of active mmic with package/housing-theory, analysis and measurement," *Advanced Electromagnetics*, vol. 3, no. 1, pp. 26-30, 2014.
2. A. Sarvaiya, S. Gupta, "Inclusion of broadband frequency responses of passive and linear networks into circuit solver: A simple approach using vector fitting," *International journal of microwave and optical technology*, vol. 10, no. 2, pp. 105-110, 2015.
3. A. Sarvaiya, S. Gupta, "An Efficient Macromodeling Methodology for Transient Simulation of Signal Integrity Problems," *3<sup>rd</sup> International Advanced Electromagnetics Symposium (AES-2014)*, Hangzhou-China, pp. 323-326, Decemeber, 2014.
4. A. Sarvaiya, S. Gupta, D. Ghodgaonakar, A. Bhattacharya "Analysis of radiation from multidevice high gain amplifier and interaction of active MMIC with package/housing- Theory, Analysis and Measurement," *A compedium of research papers during year 2013, Space Application Centre, Ahmedabad*, pp. 179-183, January, 2014.
5. A. Sarvaiya, S. Gupta, D. Ghodgaonakar, "A full wave analysis of antenna using 3D FDTD with CPML and near to far field transformation algorithm," *4<sup>th</sup> International Conference, Antenna Test and Measurement Society (ATMS-2011)*, Ahmedabad-India, pp. 33-37, February 2011.